# LUND UNIVERSITY

**PET-CT imaging of neuroendocrine tumours - Beyond diagnostics**

Gålne, Anni

2024

*Document Version:*
Publisher's PDF, also known as Version of record

[Link to publication](#)

Total number of authors:
1

*Creative Commons License:*
CC BY-NC-ND

# PET-CT imaging of neuroendocrine tumours

## Beyond diagnostics

**ANNI GÅLNE**
**DEPARTMENT OF TRANSLATIONAL MEDICINE | FACULTY OF MEDICINE | LUND UNIVERSITY**

PET-CT imaging of neuroendocrine tumours
Beyond diagnostics

# PET-CT imaging of neuroendocrine tumours

## Beyond diagnostics

Anni Gålne

LUND
UNIVERSITY

DOCTORAL DISSERTATION

Doctoral dissertation for the degree of Doctor of Philosophy (PhD) at the Faculty of Medicine at Lund University to be publicly defended on 10th of October 2024 at 09.00 in Lecture Hall F2, Skåne University Hospital, Lund

*Faculty opponent*
Professor Frederik A. Verburg
Erasmus Medical Center, Rotterdam, The Netherlands

**Author:** Anni Gålne

**Title and subtitle:** PET-CT imaging of neuroendocrine tumours – Beyond diagnostics

**Abstract:**

**Background:** Neuroendocrine tumours (NETs) typically overexpress somatostatin receptors. By radiolabelling somatostatin analogues with a positron-emitting radionuclide ($^{68}$Ga-DOTATOC or $^{68}$Ga-DOTATATE), these tumours can be detected with high sensitivity and specificity using somatostatin receptor positron emission tomography-computed tomography (PET-CT).

**Aim:** To enhance knowledge about NETs imaged with PET-CT, beyond the diagnostic work-up.

**Methods:** Paper I, based on a clinical trial (Gapetto), evaluated whether treatment with long-acting somatostatin analogues affected the uptake of $^{68}$Ga-DOTATATE in the normal liver or tumours. Changes in uptake, measured as SUVmax, were assessed in patients before and after treatment initiation. Paper II, based on a cohort study, explored whether the total somatostatin receptor-expressing tumour volume measured by PET-CT imaging, correlated with health-related quality of life or specific NET symptoms in patients with metastatic gastroenteropancreatic NET (GEP-NET). Paper III was a developmental study aimed at constructing an Artificial intelligence (AI) model to automatically detect and quantify somatostatin receptor-expressing tumour volume using a UNet3D convolutional neural network. The AI model's tumour segmentation was compared with that of two reference physicians. Paper IV, a retrospective study, assessed whether the total somatostatin receptor-expressing tumour volume at baseline PET-CT could predict treatment outcomes in GEP-NET patients post $^{177}$Lu-DOTATATE treatment. Tumour volumes were quantified from baseline and follow-up PET-CT images for these patients.

**Results:** Paper I revealed that treatment with long-acting somatostatin analogues significantly reduced the uptake of $^{68}$Ga-DOTATATE in normal liver tissue, while the tumour uptake remained unchanged. Paper II did not find a correlation between total tumour volume and health-related quality of life, although a weak positive correlation was observed between specific NET-associated symptoms (such as dyspnoea, diarrhoea, and flushing) and larger tumour volume. Paper III demonstrated that an AI model for tumour segmentation could be developed, displaying a strong correlation with the physicians' reference segmentation. Paper IV indicated that baseline tumour volume did not predict treatment outcomes, but an increase in tumour volume at the first follow-up predicted worse outcomes.

**Conclusions:** Evaluating NETs with somatostatin receptor PET-CT is feasible after initiating treatment with long-acting somatostatin analogues. Factors other than tumour volume likely have a greater impact on the health-related quality of life in patients with metastasised GEP-NET. AI models can be developed to segment tumour volume from somatostatin receptor PET-CT. Baseline tumour volume was not a predictive factor for outcomes following treatment with $^{177}$Lu-DOTATATE.

**Key words:** PET-CT, neuroendocrine tumours, quantification, treatment, AI, quality of life

Signature

Date 2024-08-21

# PET-CT imaging of neuroendocrine tumours

## Beyond diagnostics

Anni Gålne

*To my beloved family,*
*Olof, Ingrid, Kerstin, and Lisen,*

*and in loving memory of my ever-supportive father,*
*who was taken from us too soon by*
*neuroendocrine tumour disease*

# Table of Contents

# Abstract

**Background:** Neuroendocrine tumours (NETs) typically overexpress somatostatin receptors. By radiolabelling somatostatin analogues with a positron-emitting radionuclide ($^{68}$Ga-DOTATOC or $^{68}$Ga-DOTATATE), these tumours can be detected with high sensitivity and specificity using somatostatin receptor positron emission tomography-computed tomography (PET-CT).

**Aim:** To enhance knowledge about NETs imaged with PET-CT, beyond the diagnostic work-up.

**Methods:** Paper I, based on a clinical trial (Gapetto), evaluated whether treatment with long-acting somatostatin analogues affected the uptake of $^{68}$Ga-DOTATATE in the normal liver or tumours. Changes in uptake, measured as SUVmax, were assessed in patients before and after treatment initiation. Paper II, based on a cohort study, explored whether the total somatostatin receptor-expressing tumour volume measured by PET-CT imaging, correlated with health-related quality of life or specific NET symptoms in patients with metastatic gastroenteropancreatic NET (GEP-NET). Paper III was a developmental study aimed at constructing an Artificial intelligence (AI) model to automatically detect and quantify somatostatin receptor-expressing tumour volume using a UNet3D convolutional neural network. The AI model's tumour segmentation was compared with that of two reference physicians. Paper IV, a retrospective study, assessed whether the total somatostatin receptor-expressing tumour volume at baseline PET-CT could predict treatment outcomes in GEP-NET patients post $^{177}$Lu-DOTATATE treatment. Tumour volumes were quantified from baseline and follow-up PET-CT images for these patients.

**Results:** Paper I revealed that treatment with long-acting somatostatin analogues significantly reduced the uptake of $^{68}$Ga-DOTATATE in normal liver tissue, while the tumour uptake remained unchanged. Paper II did not find a correlation between total tumour volume and health-related quality of life, although a weak positive correlation was observed between specific NET-associated symptoms (such as dyspnoea, diarrhoea, and flushing) and larger tumour volume. Paper III demonstrated that an AI model for tumour segmentation could be developed, displaying a strong correlation with the physicians' reference segmentation. Paper IV indicated that baseline tumour volume did not predict treatment outcomes, but an increase in tumour volume at the first follow-up predicted worse outcomes.

**Conclusions:** Evaluating NETs with somatostatin receptor PET-CT is feasible after initiating treatment with long-acting somatostatin analogues. Factors other than tumour volume likely have a greater impact on the health-related quality of life in patients with metastasised GEP-NET. AI models can be developed to segment tumour volume from somatostatin receptor PET-CT. Baseline tumour volume was not a predictive factor for outcomes following treatment with $^{177}$Lu-DOTATATE.

# Thesis at a glance

| Paper | Aims | Patients | Methods | Findings |
|-------|------|----------|---------|----------|
| I | To evaluate the effect of long-acting somatostatin analogues on the uptake of the radiolabelled somatostatin analogue $^{68}$Ga-DOTATATE in tumours and normal liver parenchyma, as assessed by PET-CT imaging. | In the Gapetto-study, 262 patients underwent 495 PET-CT examinations with complete data, providing statistics for specific subgroup analyses. | This prospective observational study evaluated SUVmax in tumours and normal liver parenchyma before and after initation of treatment with long-acting somatostatin analogues. The interval since last injection of treatment to imaging was recorded. | The uptake of $^{68}$Ga-DOTATATE in tumours was not affected by long-acting somatostatin analogues but the uptake decreased in normal liver parenchyma. No significant effects were observed based on the interval since the last injection. |
| II | To evaluate the correlation between whole-body somatostatin receptor-expressing tumour volume (SRETVwb) and health-related quality of life. | A total of 71 patients with metastatic gastroentero-pancreatic neuroendocrine tumour (GEP-NET) were included. | Health-related quality of life and neuroendocrine tumour symptoms were assessed with standardised questionnaires. SRETVwb was retrospectivly quantified from a PET-CT aquired within a year of completing the questionnaires. | No correlation was found between SRETVwb and the summary score of health-related quality of life. However, a weak positive correlation was found between neuroendocrine tumour symptoms and larger SRETVwb. |
| III | To develop an artificial intelligence (AI) model to detect and quantify SRETVwb and whole-body total lesion somatostatin receptor expression (TLSREwb) from $^{68}$Ga-DOTATOC/TATE PET-CT images. | A total of 148 patients constituted the training set, of which 108 had PET-positive tumours. The test group consisted of 30 patients, of which 25 had PET-positive tumours. | All tumours were segmented from PET-CT images. A UNet3D convolutional neural network was used to train an AI model. Two physicians segmented tumours in the test group for comparison with the AI model. | An AI model was successfully developed to segment SRETVwb and TLSREwb. There was a good correlation between the segmented SRETVwb and TLSREwb by the AI model and those by the physicians. |
| IV | To evaluate whether tumour burden at baseline PET-CT can predict treatment outcomes in patients with GEP-NET following treatment with $^{177}$Lu-DOTATATE. | A total of 31 patients who were treated with $^{177}$Lu-DOTATATE and had a <6 months old baseline $^{68}$Ga-DOTATOC/TATE PET-CT was included in this retrospective study. | Tumour burden was quantified from baseline and first follow-up PET-CT and expressed as; SRETVwb, TLSREwb, largest tumour lesion diameter and SUVmax. Progression-free survival was defiend from start of treatment to radiological or clinical progression. | No predictive value was found for baseline tumour burden. An increase in tumour burden at follow-up was predictive of shorter progression-free survival. |

# Populärvetenskaplig sammanfattning

Neuroendokrina tumörer är ett samlingsbegrepp för en grupp av tumörer som uppstår från neuroendokrina celler. Neuroendokrina tumörer kan förekomma på många ställen i kroppen, men vanligast är i magtarmkanalen, bukspottkörteln och lungorna. Den här sortens tumörer skiljer sig ofta från "vanlig cancer", då tumörerna oftast är mer långsamväxande och ibland kan producera hormoner. Patienter med denna sjukdom lever ofta lång tid, även om de har spridd sjukdom. Oftast har neuroendokrina tumörer ett mycket större antal somatostatinreceptorer på sin yta än vad det finns i normal vävnad i kroppen. En somatostatinreceptor är en molekyl på cellytan som kan fånga upp och överföra signaler från signalämnet somatostatin. Eftersom somatostatin bryts ner snabbt i kroppen har man utvecklat ämnen som liknar somatostatin men som kan stanna längre i kroppen. Dessa kallas för somatostatinanaloger. Somatostatinanaloger kan användas som behandling vid neuroendokrin tumörsjukdom genom att de hämmar tumörernas tillväxt samt genom att de kan lindra hormonella symtom.

Genom att märka somatostatinanaloger med ett radioaktivt spårämne ($^{68}$Ga eller Gallium-68), kan man även avbilda neuroendokrina tumörer genom att följa upptaget av det radioaktiva spårämnet med en PET-DT-kamera. PET-DT står för positronemissionstomografi – datortomografi och är en kombinerad bilddiagnostisk metod. En timme före undersökningen får patienten en spruta med den radioaktivt märkta somatostatinanalogen. Vid PET-undersökningen fångar man upp de radioaktiva strålarna från $^{68}$Ga som fastnat i tumörerna och samtidigt görs också en DT (skiktröntgen) av kroppen. PET-undersökningen gör att man kan upptäcka om det finns neuroendokrina tumörer någonstans i kroppen och DT-undersökningen gör att man kan se exakt var i kroppen tumörerna finns.

**Somatostatinreceptor PET-DT** är en ny metod som har funnits i Lund sedan Gapetto-studien startade år 2013. Huvudsyftet med den här avhandlingen är att fördjupa kunskapen om värdet av olika mätvärden från somatostatinreceptor PET-DT vid avbildning av neuroendokrina tumörer och om det finns mer värde i bilderna än att bara hitta eventuella tumörer och var i kroppen de finns.

I **den första studien** undersökte vi patienter som gjorde somatostatinreceptor PET-DT både före och efter insatt behandling med somatostatinanalog. Det har funnits en oro att man kan missa tumörer eftersom både somatostatinanalogen från behandlingen och den radioaktivt märkta som används vid bilddiagnostiken, binder in till samma receptor. Teoretiskt skulle de därför kunna konkurrera ut varandra. Våra resultat visade dock att det bara var normal levervävnad som fick lägre upptag efter insatt behandling. Upptaget i tumörerna var väsentligen oförändrat även efter behandlingsstart. Detta leder till att tumörer som sitter i levern i stället kan bli lättare att upptäcka. Eftersom behandling med somatostatinanalog kan hjälpa både vid

symptom och genom att hindra tumörtillväxt, är detta ett viktigt resultat som innebär att patienterna inte behöver vänta i onödan på sin behandling.

I **den andra studien** undersökte vi livskvalitet och tumörbörda hos patienter med spridd neuroendokrin tumörsjukdom från magtarmkanalen och bukspottkörteln. Vi studerade om den totala tumörvolymen uppmätt på PET-DT undersökningen hängde ihop med patienternas livskvalitet. Vi kunde dock inte hitta något samband mellan livskvalitet och total tumörvolym. Om det hade funnits starka samband hade detta varit intressant att studera vidare, och man hade i så fall kunnat fundera på om tumörminskande kirurgi, även när sjukdomen inte är botbar, skulle kunna öka patienternas livskvalitet. Däremot såg vi ett svagt samband mellan total tumörvolym och specifika neuroendokrina symptom, såsom andfåddhet, diarré och blodvallningar vilket bekräftar tidigare studier.

I **den tredje studien** utvecklade vi en metod som använder artificiell intelligens (AI) för att automatiskt mäta total tumörbörda hos patienterna. För en människa tar volymmätningar väldigt lång tid att utföra och används därför inte i kliniskt arbete. Om en AI-modell blev bra på detta så skulle det kunna användas vid uppföljning av cancer, för att mäta om tumörvolymen har ökat eller minskat, och kanske också för att förutsäga hur en patient kommer svara på en behandling. AI-modellens mätningar jämfördes med två läkares tumörmätningar (läkare A och B) och överenstämmelsen mellan AI-modellen och de två läkarna var god men inte perfekt. AI-modellen missade fler tumörer än vad läkare B gjorde, när läkare A användes som facit.

I **den fjärde studien** utvärderade vi om det fanns något värde i att mäta total tumörvolym från PET-DT utförd före behandling med radioaktiv somatostatinanalog. Genom att märka somatostatinanaloger med ett radioaktivt ämne, $^{177}$Lu (Lutetium-177), får man en intern målsökande strålbehandling där det radioaktiva läkemedlet framför allt fastnar i de neuroendokrina tumörerna. Där avger $^{177}$Lu radioaktiv strålning som leder till celldöd. Vi kunde inte hitta någon skillnad i hur det gick för patienterna beroende på om tumörvolymen uppmättes som stor eller liten innan behandlingen startade. Vi utvärderade också eventuell förändring i tumörvolym vid en uppföljande PET-DT efter behandlingen och fann, som förväntat, att det gick sämre för patienter som hade ökat i tumörvolym. Slutligen utvärderade vi också AI-modellen från studie 3, för att se om den kunde mäta tumörvolymen på dessa patienter. Tyvärr missade AI-modellen stora tumörer i levern hos 7 av 31 patienter och detta visar på vikten av att noggrant utvärdera AI-modeller innan de kan tas i bruk i kliniskt arbete.

# List of Papers

This thesis is based on the following papers, which will be referred to in the thesis by their Roman numerals (I-IV). The papers are appended at the end of the thesis.

*Paper I*

**Gålne A.**, Almquist H., Almquist M., Hindorf C., Ohlsson T., Nordenström E., Sundlöv A., Trägårdh E. A Prospective Observational Study to Evaluate the Effects of Long-Acting Somatostatin Analogs on $^{68}$Ga-DOTATATE Uptake in Patients with Neuroendocrine Tumors. Journal of Nuclear Medicine Dec 2019, 60 (12) 1717-1723; doi: 10.2967/jnumed.119.226332

*Paper II*

Ohlsson H.,* **Gålne A.**,* Trägårdh E., Malmström M., Sundlöv A., Almquist M. Relationship between somatostatin receptor expressing tumour volume and health-related quality of life in patients with metastatic GEP-NET. J Neuroendocrinol. 2022 Apr 15:e 13139. doi: 10.1111/jne.13139, *shared first authorship

*Paper III*

**Gålne A.**, Enqvist O., Sundlöv A., Valind K., Minarik D., Trägårdh E. AI-based quantification of whole-body tumour burden on somatostatin receptor PET/CT. Eur J Hybrid Imaging. 2023 Aug 7;7(1):14. doi: 10.1186/s41824-023-00172-7

*Paper IV*

**Gålne, A.**, Sundlöv, A., Enqvist, O., Sjögreen-Gleisner K, Larsson E, Trägårdh E. Retrospective evaluation of the predictive value of tumour burden at baseline [$^{68}$Ga]Ga-DOTA-TOC or -TATE PET/CT and tumour dosimetry in GEP-NET patients treated with PRRT. EJNMMI Rep. 8, 24 (2024). https://doi.org/10.1186/s41824-024-00210-y

# Author's contribution to the Papers

*Paper I*

In this project my contribution encompassed compiling data, conducting statistical analyses, creating figures and tables, interpreting results, drafting the manuscript, revising it, and addressing reviewers' comments. Throughout these tasks, I received guidance and support from my supervisors and co-authors, whose expertise was invaluable in ensuring the accuracy and quality of my first paper.

*Paper II*

This research project was a collaborative effort between another PhD student and me, where we synergistically combined our respective areas of research to conduct comprehensive analyses. The quality of life data was collected by Håkan Ohlsson et al., while I collected the PET-CT data under supervision. The other parts of the study were conducted jointly.

*Paper III*

In this paper my contribution included study design, data collection, statistical analysis, figures and tables, interpretation of the results, preparation of manuscripts, revision of manuscripts and response to reviewers. My contributions were limited regarding ethical approval and the training of the AI model.

*Paper IV*

My contribution to this paper included all aspects of study design, ethical application, data collection, data analysis, statistical analysis, figures and tables, interpretation of the results, preparation of the manuscript, revision of the manuscript and response to reviewers.

# Abbreviations (and glossary)

| | |
|---|---|
| $^{18}$F-FDG | Fluorodeoxyglucose is a glucose analogue labelled with radioactive fluorine ($^{18}$F) with a half-life of about 110 minutes. |
| $^{68}$Ga | Gallium-68 is one of the unstable isotopes of Gallium, which is a silvery, soft metal with atomic number 31. Only two of the 31 known isotopes are stable. $^{68}$Ga will go through β+ decay. $^{68}$Ga is used for imaging with PET, with a half-life of about 68 minutes. |
| $^{68}$Ge | Germanium-68, half-life 271 days, decays primarily to $^{68}$Ga |
| $^{177}$Lu | Lutetium-177 is a radioactive isotope with atomic number 71. It is unstable and will go through β- decay. It also emits γ-radiation. The half-life is about 6.5 days. $^{177}$Lu is used for treatment (PRRT). |
| $^{90}$Y | Yttrium-90, is unstable and will go through β- decay with a half-life of about 64 hours. $^{90}$Y is used for treatment (PRRT). |
| 5-HIAA | 5-hydroxyindole acetic acid, a metabolite from serotonin |
| AI | Artificial intelligence |
| Bq | Becquerel, the SI unit of radioactivity, 1 Bq = 1 decay per second |
| BSREM | Block-sequential regularised expectation maximisation algorithm |
| CNN | Convolutional neural network |
| CT | Computed tomography, a radiological imaging technique that uses x-rays to create detailed cross-sectional images of the body |
| DOTATATE or DOTATOC | DOTA is a chelator or linker molecule which allows for binding of radionuclides such as $^{68}$Ga, or $^{177}$Lu to somatostatin analogues shortened as -TOC or -TATE. Small differences in the molecular structure of the somatostatin analogues gives the ending -TATE or TOC. |
| EANM | European Association of Nuclear Medicine |
| ECOG/WHO -performance status | Eastern Cooperative Oncology Group evaluation of functional status, adopted by WHO. Usually named ECOG/WHO performance status |
| EM | Expectation maximisation |
| EORTC | European Organisation for Research and Treatment of Cancer |
| G1, G2, G3 | Grading of NETs according to the WHO, based on the grade of differentiation and proliferation |
| GEP-NET | Gastroenteropancreatic neuroendocrine tumour |

| | |
|---|---|
| Gy | Gray, the SI unit of absorbed radiation dose. It measures the amount of ionizing radiation energy absorbed per unit mass of tissue. 1 Gy = 1 joule/kg |
| IQR | Interquartile range |
| Ki-67 | Nuclear protein associated with tumour cell proliferation |
| LAR | Long-acting release |
| LA SSA | Long-acting somatostatin analogue |
| MIP | Maximum intensity projection |
| MRI | Magnetic resonance imaging |
| NEC | Neuroendocrine carcinoma |
| NEN | Neuroendocrine neoplasia both NET and NEC |
| NET | Neuroendocrine tumour |
| OS | Overall survival |
| PERCIST | PET response criteria in solid tumours |
| PET | Positron emitting tomography, a nuclear medicine imaging technique. A radiopharmaceutical is injected into the body and undergoes β+ decay. The positron interacts with an electron resulting in the emission of two γ-ray photons which are detected to create cross-sectional images of the radiopharmaceutical distribution in the body. |
| PET-CT | An advanced hybrid imaging technique that combines the functional imaging capabilities of PET with the anatomical details provided by CT |
| PFS | Progression-free survival |
| PRRT | Peptide receptor radionuclide therapy, usually with the radiopharmaceutical $^{177}$Lu-DOTATATE |
| QLQ-C30 | Questionnaire from EORTC with 30 questions, for evaluating health-related quality of life |
| QLQ-GI.NET21 | A complimentary questionnaire to EORTC QLQ-C30 for evaluating specific NET symptoms |
| OSEM | Ordered-subset acceleration of the expectation maximisation algorithms |
| RADS | Reporting and data systems |
| RECIST 1.1 | Response evaluation criteria in solid tumours version 1.1 |
| ROI | Region of interest |
| SIRT | Selective internal radiation therapy |
| SD | Standard deviation |
| SPECT | Single-photon emission computed tomography |
| SRETV | Somatostatin receptor-expressing tumour volume |
| SRETVwb | Whole-body somatostatin receptor-expressing tumour volume |
| SSTR | Somatostatin receptor, five different subtypes exist, often named SSTR1-5 |

| | |
|---|---|
| SUL | Standardised uptake value for lean body mass |
| SUV | Standardised uptake value, can be measured as maximum (max), mean or peak value |
| TNM-stage | Staging of tumours according to T (tumour), N (nearby lymph nodes) and M (metastases) |
| TLSRE | Total lesion somatostatin receptor expression |
| TLSREwb | Whole-body total lesion somatostatin receptor expression |
| VOI | Volume of interest |
| WHO | World Health Organization |
| X-rays | X-rays are a form of electromagnetic radiation with high energy and short wavelength, commonly used in medical imaging during conventional radiography or CT. |
| β- decay | During beta minus decay a high-energy electron is emitted from a neutron, transforming the neutron into a proton and increasing the atomic number of the nucleus. The process also creates an electron antineutrino. |
| β+ decay | During beta plus decay, a high-energy positron is emitted from a proton, transforming the proton into a neutron and decreasing the atomic number of the nucleus. The process also creates and electron neutrino. β+ decay is also known as positron emission, and is the process used for imaging with PET. |
| γ-rays | Gamma rays are high-energy electromagnetic radiation, with higher energy than x-rays, emitted during decay from radioactive isotopes. |

# Beyond diagnostics

Over the past decade, and throughout my years as a research student, there has been a rapid evolution in the diagnostic landscape of neuroendocrine tumours (NETs). Positron emission tomography-computed tomography (PET-CT) has gained status as a fundamental imaging method for the initial diagnostic work-up, re-staging, and follow-up of various cancers. Older, less sensitive methods for detecting tumours have often been replaced or augmented with PET scans.

From 2013 to 2019, ^{68}Ga-DOTATATE was the radiopharmaceutical used in the Gapetto-study for imaging of NETs with somatostatin receptor PET-CT at Skåne University Hospital, Lund. In 2019, there was a shift in production to ^{68}Ga-DOTATOC, due to the approval of SomaKit TOC by the European Medicines Agency. Consequently, both radiopharmaceuticals are studied in the papers of this thesis.

The utilisation of somatostatin receptor PET-CT at Skåne University Hospital has increased since 2013, with approximately 450 patients now being examined annually. Despite being a relatively novel technique, numerous unanswered questions have sparked clinical investigations. Consequently, the number of published papers on somatostatin receptor PET-CT has surged since 2010, exploring the method's potential in various aspects. Some of the research questions addressed in this thesis have also been investigated by other researchers, yielding both conflicting and corroborative findings. Given the rarity and heterogeneity of this disease, the common obstacles include small-scale studies and inconsistent results, potentially due in part to variations in study populations.

We have been able to answer some questions through our research contributions, but new ones have emerged. In the future, this scattered knowledge landscape could benefit from multicentric prospective studies. These can help to overcome some of the challenges associated with this heterogeneous and somewhat uncommon disease.

# Introduction

## Characteristics of neuroendocrine neoplasia

Neuroendocrine neoplasia originates from cells in the diffuse neuroendocrine system. The diffuse neuroendocrine system is widespread throughout the body, forming a heterogeneous group of tumours.[1] Neuroendocrine neoplasia can appear in almost every epithelial organ, including the gastrointestinal tract, respiratory tract, urogenital tract, breast, thyroid, skin, and central nervous system.[2] Depending on the primary origin, these tumours show significant differences in clinical features, pathological findings, and prognosis.[1, 3]

### History

These unique types of tumours were initially detailed by German pathologist Oberndorfer, who termed them "karzinoide tumoren" or **carcinoid tumours**.[4] Such tumours resembled carcinomas but were believed to be more benign.[4] In 1907, he presented six cases of submucosal lesions in the small intestine and summarized the features of carcinoids as typically multiple, small, slow-growing tumours.[5] These were well-defined, showed no inclination to infiltrate surroundings areas, and did not metastasise.[5] Although his colleagues initially contested his findings, arguing these tumours resembled adenomyomas or pancreatic tissue, his work was eventually published in the 1907 Frankfurt Journal of Pathology under the title "Carcinoid Tumours of the Small Intestine".[6]

Oberndorfer later reviewed additional cases. In 1929, twenty-two years from the original description, he revised his characterisation from benign behaviour to potentially more malignant, and added that they could metastasise.[5] However, Oberndorfer did not describe the endocrine features and symptoms of these tumour types. Interestingly, similar tumours in the small intestine had been detailed by several physicians during the late 19th century, before Oberndorfer gave them a name.[5] It is widely accepted that the first report of carcinoid syndrome was made by Ransom in 1890 in The Lancet publication.[7] Ransom reported Dr. Ringer's treatment of a 50-year old married woman at the University College Hospital in London in 1887. The patient complained of two egg-sized masses in her lower abdomen, along with pain and frequent diarrhoea following meals. Years later the same woman returned to Dr. Ringer, displaying cachexia and an abdomen

seemingly filled with tumour masses, especially in the liver. Her symptoms had worsened considerably, accompanied by severe dyspnoea after eating food. Following her death a few months later, Ransom documented the necropsy, which revealed a liver riddled with tumours and a walnut-sized tumour in the ileum. He also provided a detailed description of the microscopic features of the tumour.[7]

## Epidemiology

Neuroendocrine neoplasia is relatively rare, but its incidence and prevalence have significantly increased over the last few decades. The annual age-adjusted incidence is estimated at approximately 7 per 100000 individuals, while the 20-year limited duration prevalence is roughly 0.05% in the United States.[8] The rise in incidence and prevalence is possibly partly due to improved diagnostics and treatment.[8] Men and women are almost equally affected, but the location of the primary tumour varies significantly depending on age, sex, and race. The gastrointestinal canal is most frequently involved, specifically the small bowel or rectum, followed by the lungs and pancreas (Figure 1).[8, 9]
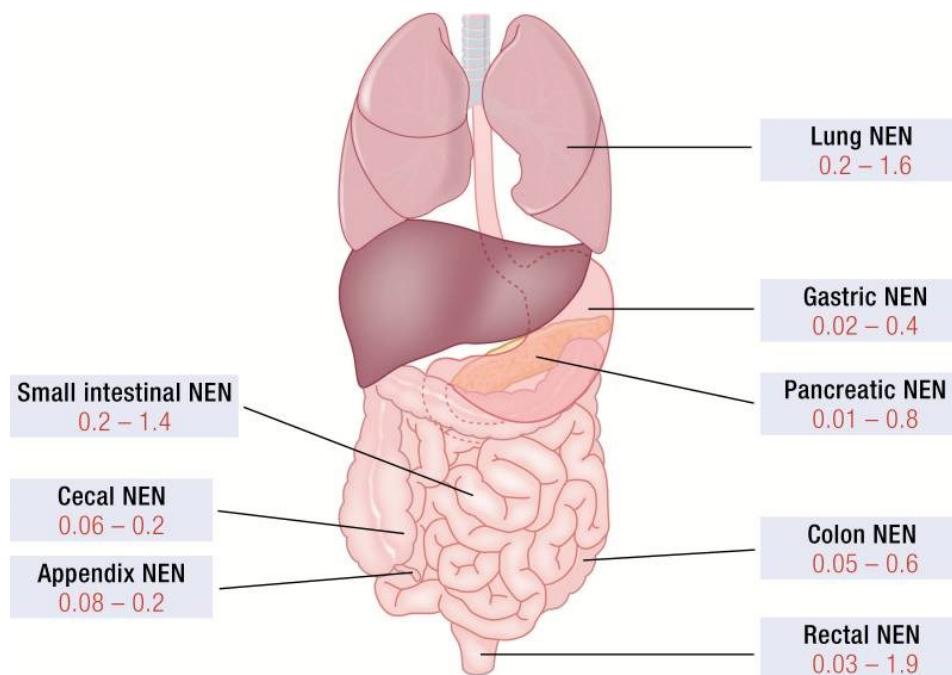


**Figure 1. The most common primary tumour sites and incidence rates**
Illustration of the most common primary neuroendocrine neoplasia (NEN) sites with incidence rates from Dasari et al [8] and Fraenkel et al.[9] © Endocrine Society 2020. Original image from Advances in the Diagnosis and Management of Well-Differentiated Neuroendocrine Neoplasms, Hofland et al.,[10] article distributed under the CC BY 4.0 http://creativecommons.org/licenses/by/4.0

The aetiology of the majority of these tumours remains unknown, and most cases are sporadic.[11] However, sometimes, neuroendocrine neoplasia is a part of an inherited syndrome with an increased risk for developing tumours, such as Multiple Endocrine Neoplasia type 1 (MEN1), Von Hippel-Lindau syndrome, Neurofibromatosis type 1, Tuberous Sclerosis Complex and Multiple Endocrine Neoplasia type 2 (MEN2).[12] A family history of cancer, high body mass index and diabetes are potentially relevant risk factors unrelated to the primary tumour site. Meanwhile, smoking and alcohol consumption might be risk factors for tumours at specific sites.[13, 14]

## Classification

To standardise terminology and diminish complexity, the World Health Organization (WHO) recently proposed a universal classification system for neuroendocrine neoplasms. This system is based on differentiation and proliferative grading, and described in the 2022 WHO Classification of Endocrine and Neuroendocrine Tumours (Table 1).[15]

**Table 1. WHO definition system for epithelial neuroendocrine neoplasia (NEN)**
A universal definition system proposed by WHO 2022 for NEN based on differentation and grading.[15]

| Tumour category definition | Neuroendocrine neoplasia (NEN) | |
|---|---|---|
| Tumour class | Well-differentiated NEN | Poorly differentiated NEN |
| Tumour type | NET | NEC |
| Tumour subtype | Depending on location | Large cell or small cell NEC |
| Tumour grade | G1, G2, G3 | High grade (by definition) |

Neuroendocrine neoplasms are characterised by their expression of biomarkers from the secretion pathways of normal neuroendocrine cells, particularly large dense core vesicles and small synaptic-like vesicles.[15] These well-differentiated epithelial neoplasms, which maintain characteristics of normal neuroendocrine cells are classified as NETs. NETs can metastasise, and they can be further divided into NET grade 1 (G1), grade 2 (G2), or grade 3 (G3), based on the speed at which malignant cells divide (mitotic rate) and Ki-67 proliferation index, a nuclear protein and an indicator of cell proliferation.[3, 16]

Poorly differentiated epithelial neoplasms, featuring pronounced cellular atypia and little resemblance to ordinary neuroendocrine cells, are known as neuroendocrine carcinomas (NECs). NECs are by definition high-grade tumours and are furthermore classified as either small cell NEC or large cell NEC.[3, 16] Certain neuroendocrine neoplasms may encompass other tumour elements, often adenocarcinoma. When each of these tumours is represented in at least 30% of the tumour mass, they are referred to as mixed neuro-endocrine neoplasms (MiNENs).[3, 17] Emerging genomic evidence suggests that NETs and NECs are unrelated

neoplasms, with genomic differences especially observed in neuroendocrine neoplasia of the pancreas.[17] Non-epithelial neuroendocrine neoplasms are recognised as paragangliomas.[18]

The 2019 WHO classification of neuroendocrine neoplasia in the gastrointestinal tract and hepatopancreatobiliary organs, is presented in Table 2.

**Table 2. WHO classification and grading for neuroendocrine neoplasia of the gastrointestinal tract and hepatopancreatobiliary organs**
Neuroendocrine tumour (NET), neuroendocrine carcinoma (NEC); mixed neuroendocrine-non-neuroendocrine neoplasm (MiNEN). *Mitotic rates expressed as the number of mitoses/2 mm$^2$ as determined by counting in 50 fields of 0.2 mm$^2$, the Ki-67 proliferation index value is determined by counting at least 500 cells in the regions with highest labelling. The final grade of the neoplasm is based on the highest category from either mitotic rate or Ki-67 index. **Poorly differentiated NEC are not formally graded but are, by definition, considered high-grade.[3]

| Terminology | Differentiation | Grade | Mitotic rate* | Ki-67 index* |
|---|---|---|---|---|
| NET, G1 | Well-differentiated | Low | <2 | <3 % |
| NET, G2 | | Intermediate | 2-20 | 3-20 % |
| NET, G3 | | High | >20 | >20 % |
| NEC, small cell type | Poorly differentiated | High** | >20 | >20 % |
| NEC, large cell type | | High** | >20 | >20 % |
| MiNEN | Well or poorly differentiated | Variable | Variable | Variable |

Neuroendocrine neoplasms from the lung are classified as either well-differentiated NETs or poorly differentiated NECs. The lung NETs are further graded as typical carcinoid (grade 1), and atypical carcinoid (grade 2), whereas the lung NECs are further graded as small cell lung carcinoma and large cell NEC.[15, 19] The mitosis count and necrosis serve as the most valuable morphological criteria when evaluating neuroendocrine neoplasia of the lung, distinguishing between NET and NEC, as well as between typical-atypical carcinoid and small cell lung carcinoma and large cell NEC.[19] It is worth noting, though, that even though these subgroups are classified under one category (neuroendocrine neoplasms of the lung), typical and atypical carcinoid tumour differ significantly from small cell lung carcinoma and large cell NEC in clinical, epidemiological, histological, immunohistochemical, and genetical aspects.[19]

Microscopically, NETs are well-differentiated epithelial neoplasms exhibiting neuroendocrine differentiation, often characterised by an organoid architecture, uniform nuclei, and coarsely granular chromatin sometimes described as "salt and pepper chromatin". Necrosis is an infrequent occurrence but can manifest as punctate in higher-grade NETs.[3] Most NETs display a low Ki-67 proliferation index, however, some – notably pancreatic NETs – can express a very high index, which alone is not a distinctive marker between NETs and NECs.

NECs are considerably aggressive neoplasms, that are poorly differentiated, characterised by extensive necrosis, high mitotic rates and a high Ki-67 proliferation index.[3]

Immunohistochemical markers, typically used for identifying neuroendocrine neoplasms, include antibodies towards chromogranin A and synaptophysin.[10] In certain tumours, the sensitivity of chromogranin A may be limited, necessitating additional neuroendocrine markers such as those targeting different hormones or peptides, to determine neuroendocrine differentiation.[10, 20]


## Tumour staging and prognosis

Tumour staging is a system that describes whether tumour growth is local or if the tumour has spread to regional lymph nodes or resulted in distant metastases, usually described as the tumour, nodes and metastases (TNM) stage. The T-category (tumour) evaluates local tumour growth, the N-category (nodes) evaluates pathological regional lymph nodes near the tumour are and the M-category (metastases) evaluates distant metastases.[21]

Well-differentiated NETs not only differ from poorly differentiated NECs in terms of tumour characteristics, but also in survival rates. Generally, well-differentiated NETs grow indolently, and patients with localised NET have a median overall survival ranging between 14 years for primary tumours in the small intestine and more than 30 years for primary tumour in the appendix.[8]

Patients with regional NET have a median overall survival of 10.2 years ranging from 33 months for patients with a tumour of an unknown primary to more than 30 years for patients with a primary tumour in the appendix.[8] Even patients with well-differentiated NETs (G1/G2) presenting with distant metastases have a relatively good prognosis, with a 5-year survival rate of 61–69% for primary tumours in the cecum or small intestine, a 5-year survival rate of 50% for pancreatic primary tumours, and a 5-year survival rate of 30% for primary tumours in the stomach, rectum, lung, or colon.[8]

In contrast, patients with NEC have a significantly less hopeful prognosis. Even when only presented with localised or regional NEC, the 5-year survival ranges between 25–50%.[22] For patients with metastatic NEC, the median overall survival is less than a year.[23, 24]

Data on survival rates for patients with well-differentiated, metastasised NET G3 are scarce but are believed to be intermediate between NET G2 and NEC. A small single-centre study found an estimated median survival of 19 months.[25]

## Symptoms and syndromes

Throughout the gastrointestinal tract and the pancreas, at least 15 known cell-types exist that produce hormonal peptides and biogenic amines.[26] Consequently, well-differentiated NETs, originating from these cells, can sometimes produce and secrete bioactive substances such as serotonin, insulin, gastrin, bradykinins, prostaglandins, histamine, substance P, and tachykinins.[27] When the hormone production causes clinical manifestations, these tumours are sometimes called "functioning" NETs whereas "non-functioning" NETs are tumours without biologically active hormone production.[28] These substances can cause a variety of hormonal syndromes, usually named after the specific hormone causing the syndrome (Table 3).

**Table 3. Functioning NETs and their clinical features**
An overview of some functioning NETs is presented in the table. Other rare functioning NETs are calcitoninoma, CRHoma, GRFoma, PET causing hypercalcemia (PTHRp-oma), ghrelinoma, or pancreatic NET secreting renin, luteinizing hormone, erythropoietin, or IF-II.[3, 28-30]

| Examples of functioning NETs | Location | Clinical features | Complimentary name |
|---|---|---|---|
| ACTHoma | Lung, pancreas | High levels of ACTH leading to hypokalaemia, diabetes mellitus, hypertension, moon face, muscle weakness, oedema | Ectopic Cushing's syndrome |
| Carcinoid syndrome | Small intestine, rarely lung (5%) and pancreas (1%) | High levels of bioactive substances such as serotonin, histamine, tachykinins and prostaglandins leading to diarrhoea, flushing, bronchospasm, tricuspid heart valve fibrosis | |
| Gastrinoma | Duodenum (70%), pancreas (25%), other (5%) | High gastrin levels leading to reflux, dyspepsia, gastric ulcers, PPI-responsive diarrhoea | Zollinger-Ellison syndrome |
| GHRHoma | Pancreas, lung, jejunum, other | High levels of growth hormone releasing hormone leading to acral overgrowth and cardiomegaly | Ectopic acromegaly |
| Glucagonoma | Pancreas | High glucagon levels leading to diabetes mellitus, deep venous thrombosis, depression, dermatitis (necrolytic migratory erythema) | 4 D syndrome |
| Insulinoma | Pancreas | High levels of insulin leading to fasting hypoglycaemia | Endogenous hyperinsulinemia hypoglycaemia or Whipple triad |
| Somatostatinoma | Pancreas (55%), duodenum - jejunum (45%) | High somatostatin leading to diabetes mellitus, diarrhoea, steatorrhea, gallstones, achlorhydria, weight loss, central hypothyroidism | |
| VIPoma | Pancreas (75%) | High levels of VIP leading to secretory diarrhoea, hypokalaemia, achlorhydria hypercalcemia | Verner-Morrison syndrome |

The classic syndrome, known as **"carcinoid syndrome"**, involves episodic flushing, diarrhoea, hypotension, heart-valve dysfunction, or wheezing due to bronchospasm. This syndrome typically requires metastases to the liver, and symptoms vary, depending on the combination of bioactive substances secreted. These may include serotonin, histamine, tachykinins, and prostaglandins.[31, 32] The interpretation of symptoms is challenging due to their variability, intensity, and exacerbation by different triggers.[31] The release of carcinoid related bioactive substances can be triggered by certain foods (e.g., alcoholic beverages, coffee, tomatoes, bananas, nuts) or by exercise.[33]

Enterochromaffin cells synthesise around 95% of the body's serotonin from dietary tryptophan. These cells are part of the diffuse neuroendocrine system in the gastrointestinal tract. Thus, NETs occurring in the intestine, especially those in the small intestine, may produce large amounts of serotonin.[3, 34]

Generally, serotonin is metabolised in the liver and is only present in low amounts in the circulation. However, if liver metastases are present, the serotonin produced by these metastases escapes degradation in the liver. Consequently, it causes symptoms and impacts the heart and lungs, by vasoconstriction, bronchoconstriction, and endocardial fibrosis.[32]

However, most NETs are non-functioning, and symptoms unrelated to hormone production might be present for all types of tumours. Presenting symptoms may include abdominal pain, bowel obstruction, gastrointestinal bleeding, cough, recurrent bronchopulmonary infections, or haemoptysis, with symptoms dependent on the location of the primary tumour or metastases.[28] Incidental findings account for between 10–40 % of diagnosed tumours,[28] and metastatic disease, especially liver metastases, is often present when the mass effects of tumours or symptoms appear.[34]

## Somatostatin and the receptor

Somatostatin, an inhibitory neuroendocrine peptide, consists of either 14 or 28 amino acids.[35] It plays a significant role in neurotransmission, various endocrine functions, cell proliferation and angiogenesis.[35] Cells that produce somatostatin are prevalent in both the central and peripheral nervous systems, the gastrointestinal tract, as well as the endocrine and exocrine pancreas. These cells are also found, albeit to a lesser extent, in the thyroid, adrenals, submandibular glands, kidneys, prostate, and placenta.[35]

For example, the wide range of effects of somatostatin includes the inhibition of exocrine secretions such as gastric acid production, pancreatic enzyme or bile secretion, in addition to inhibition of endocrine secretions in the pituitary, such as growth hormone, thyroid stimulating hormone and prolactin, as well as in the pancreas and gastrointestinal tract (e.g. insulin, glucagon, gastrin, cholecystokinin,

and vasoactive intestinal peptide).[36] The anti-secretory effects are generally mediated through the cAMP-dependent pathway and through the activation of protein phosphatases which result from a decline in $Ca^{2+}$. The antitumoural effects of somatostatin are mainly mediated through the activation of intracellular tyrosine phosphatase, which operates through different pathways, resulting in decreased proliferation, migration, invasion and inducing apoptosis.[37]

Somatostatin exercises its effects through neurotransmission, locally via auto- or paracrine methods, or through the bloodstream as a true hormone through interaction with a G-protein coupled **somatostatin receptor**.[38, 39] Humans are known to have five different somatostatin receptors (subtype 1–5), and somatostatin elicits varying effects hinged on the somatostatin receptor subtype expressed on the cell membrane.[39] The effects mediated through somatostatin receptor subtype 1, 2 and 5, are primarily anti-secretory, whereas the main effects of somatostatin receptor subtype 3 are diminished cell proliferation and the induction of cell apoptosis. The functions of the somatostatin receptor subtype 4 are yet to be fully understood.[40]

The biodistribution of somatostatin receptors depends on the subtype (Figure 2).
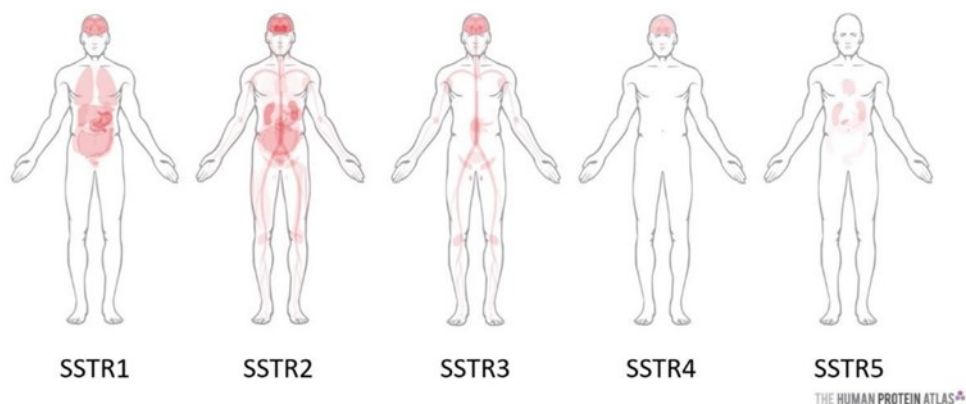


**Figure 2. Anatomogram with biodistribution of somatostatin receptors subtype 1-5**
Somatostatin receptors (SSTR, subtype 1-5) Original images from the Human Protein Atlas, proteinatlas.org. Adapted by Eychenne et al. in Overview of Radiolabeled Somatostatin Analogs for Cancer Imaging and Therapy, Molecules 2020, doi: 10.3390/molecules25174012
Distributed under CC BY 4.0; https://creativecommons.org/licenses/by/4.0/

Most NETs exhibit **overexpression of somatostatin receptors**, as shown in Figure 3. The somatostatin receptor subtype 2 is most frequently overexpressed, while subtypes 1, 3 and 5 are also often overexpressed in NETs to varying extents.[39, 41-44] The least expressed subtype is somatostatin receptor subtype 4.[39] A particularly high incidence and density of somatostatin receptors have been found in growth hormone-secreting pituitary adenomas, gastroenteropancreatic tumours, pheochromocytomas and neuroblastomas. They are overexpressed to a lesser extent

in medullary thyroid cancers and small cell lung cancer.[39] The overexpression of somatostatin receptors forms the basis for the concept of **theranostics** in NETs, which can be used for both imaging and treatment of tumours.
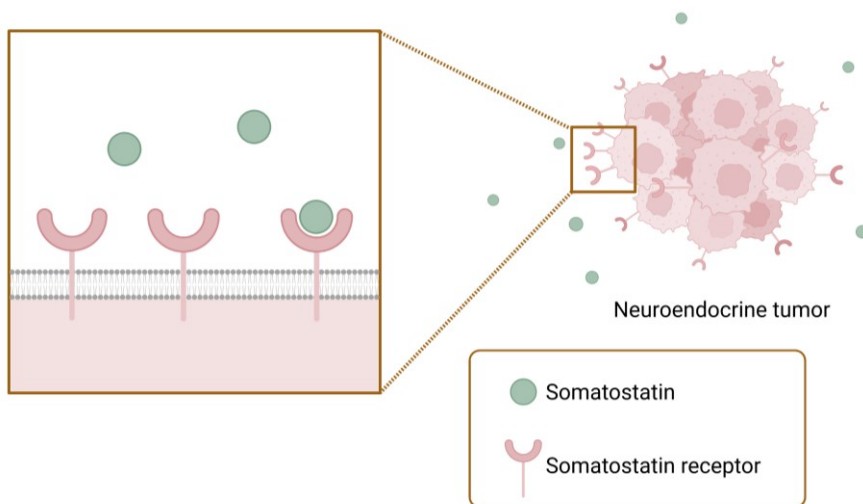


**Figure 3. Neuroendocrine tumour with somatostatin receptors**
Schematic image of a neuroendocrine tumour overexpressing somatostatin receptors. Image created with biorender.com

## Theranostics

Theranostics or theragnostics is a term derived from the Greek words "therapeuein" meaning to treat medically or referring to therapy, and "gnosis" meaning knowledge or referring to diagnostics.[45] Theranostics is a treatment approach that combines diagnostics with therapy. The method uses precise diagnostic tools, such as imaging, to accurately pinpoint the overexpression of somatostatin receptors in NET. These same somatostatin receptors can later be targeted for therapy (Figure 4).

Modern imaging procedures use radiolabelled somatostatin analogues (such as $^{68}$Ga-DOTATOC or $^{68}$Ga-DOTATATE) which target the somatostatin receptors that are then visualised with a PET-CT examination. The treatment procedure is often termed **peptide receptor radionuclide therapy (PRRT)**, commonly employing the radiopharmaceutical $^{177}$Lu-DOTATATE, which also targets the somatostatin receptors.[46]

The essence of theranostics lies in identifying the correct patient for the appropriate treatment and tracking the response, often characterised as personalised or individualised medicine. Nuclear medicine has been practising theranostics for over

80 years, one of its earliest examples being the imaging of thyroid diseases using various iodine isotopes and targeted treatments with radioactive iodine.[47]
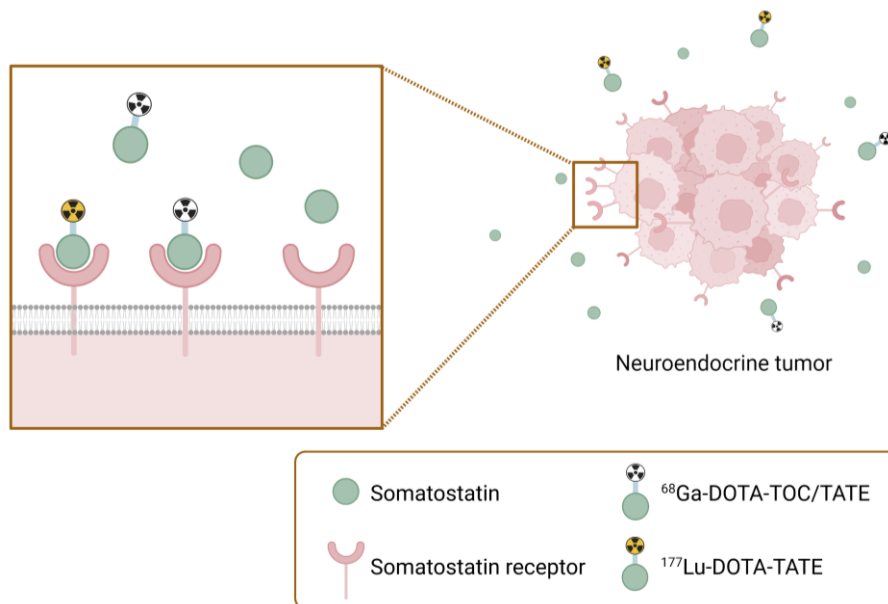


**Figure 4. Theranostic principles**
Schematic image of a neuroendocrine tumour overexpressing somatostatin receptors which can be imaged with the radiopharmaceutical ^{68}Ga-DOTATOC or ^{68}Ga-DOTATATE or targeted with drugs such as somatostatin analogues or ^{177}Lu-DOTATATE. Image created with biorender.com

# Diagnosis of NET

NET may be suspected due to typical symptoms or as incidental findings during radiological imaging or surgery. The diagnosis and treatment require a multidisciplinary team involving oncology, radiology, nuclear medicine, surgery, and pathology/laboratory medicine. The diagnosis and staging are based on histopathology, biochemical findings and imaging.[48]

The histopathological diagnosis of NET, including immunohistochemistry, is achieved through microscopic examination of a needle biopsy from the tumour, or surgical removal of the tumour. Biochemical testing of blood and sometimes urine comprises a significant element of the diagnostic work-up. General tumour markers such as chromogranin A are measured during diagnostic work-up and follow-ups to identify recurrences. Chromogranin A is often produced in neuroendocrine (tumour) cells, correlating to the tumour burden, particularly before treatment.[49] For functional or hormone-producing tumours, specific tumour markers such as 5-

hydroxyindole acetic acid (5-HIAA), a serotonin metabolite, gastrin, insulin or other hormones could be obtained.[50] Endoscopy is commonly employed for diagnosing NETs in the stomach or duodenum. Endoscopic ultrasound could also feature in the examination of pancreas, providing detailed images, and aiding in the diagnosis of pancreatic NET.[48] The NETest, a liquid biopsy that examines the genetic expression of 51 NET genes in the blood, has been developed.[51] The NETest demonstrates high diagnostic accuracy, and shows potential for assessing disease response or recurrence.[52-54] However, its incorporation into clinical routine has been limited by high cost and restricted availability.

Morphological imaging of NETs is a crucial component of the diagnostic process. Typically, a CT scan is performed on the thorax and abdomen to assess the primary tumour and any metastases. Extended imaging of the limbs or head and neck is conducted if there is suspicion of disease involvement in these areas. Magnetic resonance imaging (MRI) and ultrasound may also be performed as part of the diagnostic work-up for enhanced tumour characterisation, particularly with liver metastases and when ultrasound-guided biopsies are required. However, these methods have limitations in detecting small tumours and tumours situated outside the examination area. A comparison between preoperative morphologic imaging and thin slice pathological examination concluded that less than 50% of neuroendocrine liver metastases were preoperatively identified.[55]

Historically, **somatostatin receptor imaging** through scintigraphy with ^{111}In-labelled somatostatin analogues (octreotide), commonly known as OctreoScan® has been the prevalent method for functionally visualising NETs.[56, 57] However, scintigraphy has notable limitations, such as inability to identify small lesions, deficient image quality, and drawn-out imaging protocols. This spurred the development of radiopharmaceuticals that target somatostatin receptors for imaging with PET-CT.[58, 59]

Today, the most widely used radiolabelled somatostatin analogues are ^{68}Ga-DOTA-conjugated peptides, including **[68]Ga-DOTATATE**, **[68]Ga-DOTATOC**, but also radiolabelling with ^{64}Cu exists such as ^{64}Cu-DOTATOC.[59, 60]

For this thesis, such somatostatin receptor imaging with PET-CT, is referred to as **somatostatin receptor PET-CT**, an exceedingly valuable imaging method for NETs. This technique ranges in use from the diagnostic work-up, and staging, to re-staging suspected recurrences, assessment during follow-up after treatment, and selecting patients for PRRT with ^{177}Lu-DOTATATE.[46]

# Imaging with PET-CT

PET-CT is a hybrid imaging method that combines the nuclear medicine technique of PET with x-rays generated by the CT. These two examinations are integrated through a single-unit PET-CT scanner and are performed in the same session, illustrated in Figure 5.
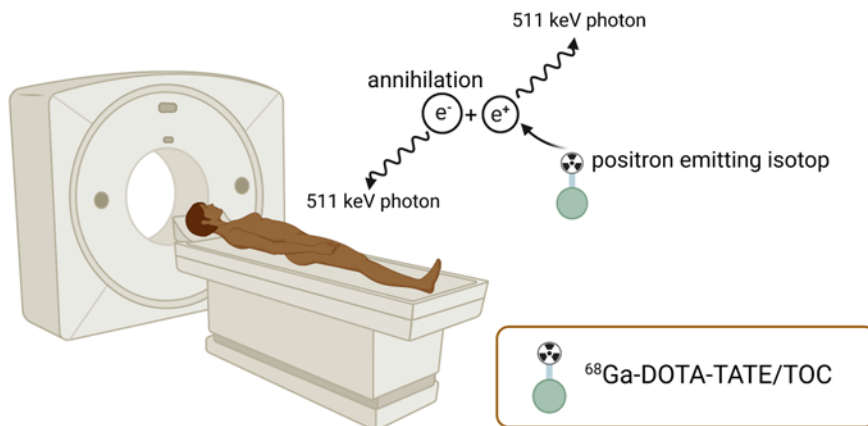


**Figure 5. Illustration of a PET-CT scanner**
Usually, one hour before the PET-CT scan, the patient is injected with a radiopharmaceutical, such as $^{68}$Ga-DOTATOC, intravenously. During the examination both the PET scan and the CT scan are acquired. Image created with biorender.com

To perform the PET scan, the patient receives an intravenous injection of a radiopharmaceutical, which is a drug containing a radioactive isotope.[61] **$^{18}$F-FDG**, a radiolabelled analogue of glucose (fluorodeoxyglucose), is the most commonly used radiopharmaceutical for functionally visualising malignancy with PET-CT.[62] Generally, cancer cells possess increased glucose metabolism compared to normal tissues, which is why an accumulation of $^{18}$F-FDG can often be observed in many tumours.[63] However, well-differentiated NETs are slow-growing and rarely exhibit increased metabolism.[10] Therefore, **somatostatin receptor PET-CT** is often more appropriate for imaging suspected or known NETs. Conversely, for aggressive tumours, such as NEC, and occasionally NET G3, a complementary examination with $^{18}$F-FDG PET-CT proves valuable, sometimes referred to as **dual-imaging**.[64] Depending on the chosen radiopharmaceutical, the PET images provide functional information, such as somatostatin receptor expression or glucose metabolism. The CT images offer anatomical and morphological information and are also used for attenuation correction of the PET images.

## The request

To conduct a radiological and/or nuclear medicine exam, a study requisition containing pertinent clinical information about the patient is essential. Each examination must be justified according to the Swedish Radiation Safety Authority's Regulations concerning Safety in Nuclear Facilities (SSMFS 2018:5). These regulations require the radiation exposure for each patient to be compared against the potential benefit from the examination. Relevant clinical information in the requisition is also crucial in designing the PET-study with the appropriate radiopharmaceutical and creating a suitable CT-examination. This information helps manage proper examination scheduling and planning of the study with relevant patient preparations. The request is also important for ensuring a correct interpretation of the images and properly responding to the exam.

## Preparation and administration of $^{68}$Ga-DOTATOC

The radiopharmaceutical $^{68}$Ga-DOTATOC is currently used for somatostatin receptor PET-CT at Skåne University Hospital, following the approval of SomaKit TOC by the European Medicines Agency.[65] The preparation of $^{68}$Ga-DOTATOC involves radiolabelling SomaKit TOC with a $^{68}$Ga-chloride solution. The kit contains 40 micrograms of edotreotide (DOTATOC) and a reaction buffer.[65]

$^{68}$Ga is produced by a generator, which is a standalone system that holds $^{68}$Ge (Germanium-68) with a physical half-life of 271 days. $^{68}$Ge decays spontaneously to $^{68}$Ga, which is then extracted using an eluent, most commonly a chloride solution.[66] The production of $^{68}$Ga is highly reproducible and robust, making it suitable for remote locations where a cyclotron is not available for radionuclide production or as a convenient supplement for radionuclide production even at sites with a cyclotron.[66] However, generator production presents issues such as higher costs and a lower daily capacity for patient examinations, as compared to compared to radionuclide production with PET cyclotrons.

The PET radiopharmaceutical is administered as an intravenous bolus injection. The EMA SomaKit TOC product information for $^{68}$Ga-DOTATOC states that the prescribed activity per 70 kg patient is between 100–200 MBq.[65] The effective dose after administration of 100 MBq is estimated at 2.1 mSv, similar to the natural background radiation in Sweden over one year.[65, 67] After intravenous injection, $^{68}$Ga-DOTATOC is rapidly cleared from the blood. Approximately 50 min post-injection, the accumulation of the radiopharmaceutical in the organs has reached a plateau.[65] The physical half-life of $^{68}$Ga is 68 min and the body slowly excretes it through urine. That is why patients are advised to drink water following radiopharmaceutical administration, and to void frequently to decrease radiation exposure to the bladder.[60, 65]

After an uptake interval for $^{68}$Ga-DOTATOC, the PET-CT images are typically collected 40–90 minutes post-administration of the injection.[65]

## Acquisition of the PET images

The injected radiopharmaceutical distributes throughout the body and accumulation occurs in both tumours and normal tissues, depending on the tracer. The radioactive isotope undergoes beta plus **(β+) decay**, emitting **positrons**. These positrons, after reducing to thermal velocity, combine with an electron to form an electron-positron pair. This pair then annihilates, releasing two **photons** (with energy of 511 keV) in opposing directions.[63]

The PET camera is constructed as a full ring or cylindrical system. It offers 360-degree detection of photons around the patient. Each pair of photons travels in opposing directions, interacting with the detectors within a very brief time frame. This interaction is termed a **coincidence event**. Once a coincidence event is registered, a line can be calculated between the detectors, where the annihilation photons were registered.[61]

Coincidence events are accumulated in large numbers to reconstruct cross-sectional images. The volume of events corresponding to a line indicates the quantity of accumulated radioactivity between the opposing detectors. Three types of coincidences can occur. The first is a **true coincidence** event, as described above, which forms the true image. The second, a **random coincidence**, occurs when two unrelated photons are registered as a coincidence event. This contributes to an overestimation of true activity and a heightened level of background noise. The third type of coincidence is **scatter coincidence**, which transpires when photons alter their original direction and continue within the patient due to a Compton interaction. This leads to decreased contrast, degraded image quality by introducing noise and inaccuracies, making corrections necessary.[61]

True events are often lost due to photon interaction within the body, resulting in both scattering and absorption – a phenomenon known as attenuation. For instance, the chances of detecting photons originating from deep within the body are diminished compared to those near the surface. The data obtained from a CT scan is utilised to correct this attenuation, thus enhancing the PET image. However, there are still limitations due to factors such as patient movement and breathing patterns.[61]

Directly after the CT images are obtained, PET data are collected ranging from mid-thigh to the base of the skull. PET-data are acquired either for a bed position of approximately 20 cm over a few minutes (the time depends on the administered activity), after which the patient bed is moved through the gantry for the collection of PET data at the next bed position. Alternatively, a flow system gradually moves the patient through the gantry. Overall, the PET-acquisition process takes about 15–

20 min. Images from both techniques are merged to create PET-CT images. An example of a patient's image is shown in Figure 6.
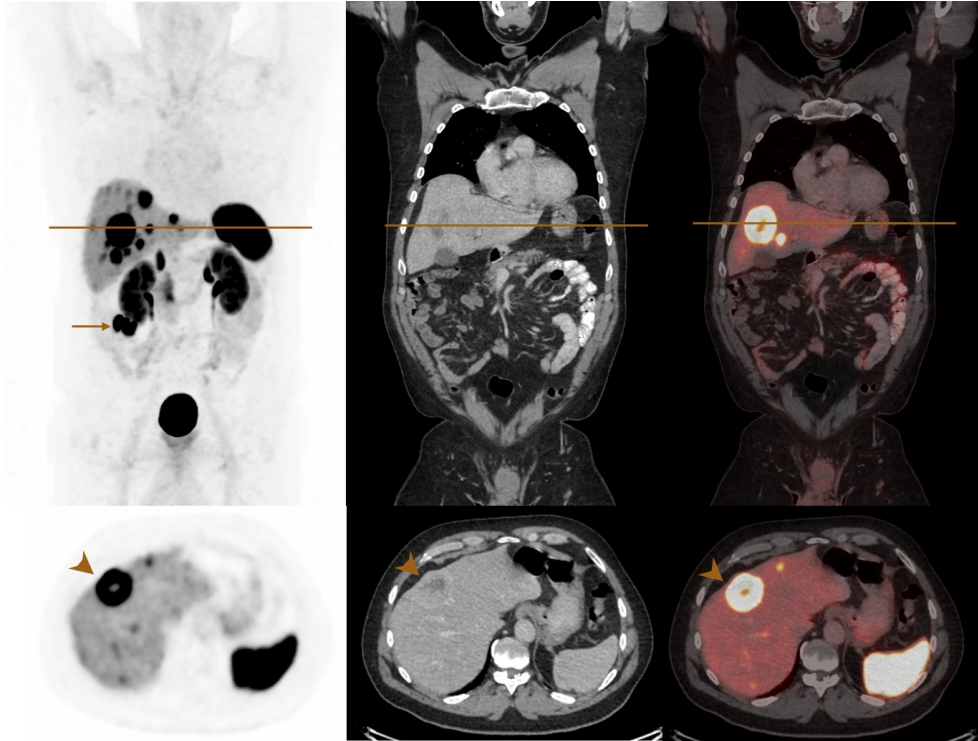


**Figure 6. Example of a somatostatin receptor PET-CT examination of a patient with NET**
Top row shows coronal images, and bottom row shows axial images. The brown line illustrates the level of the axial image. To the left are the PET-images with the top image showing maximum intensity projection (MIP). In the middle are the CT-images and on the right are the combined PET-CT images. The arrow points to primary tumour in small intestine while the arrowheads points to liver metastases.

An illustration comparing the non-attenuation-corrected images (B) to the attenuation-corrected images (A) is provided in Figure 7. Attenuation-corrected images are primarily used in the interpretation of PET-CT scans. However, images without attenuation correction are beneficial for interpreting or verifying small superficial findings, or in cases where motion or metal artefacts affect the corrected images.
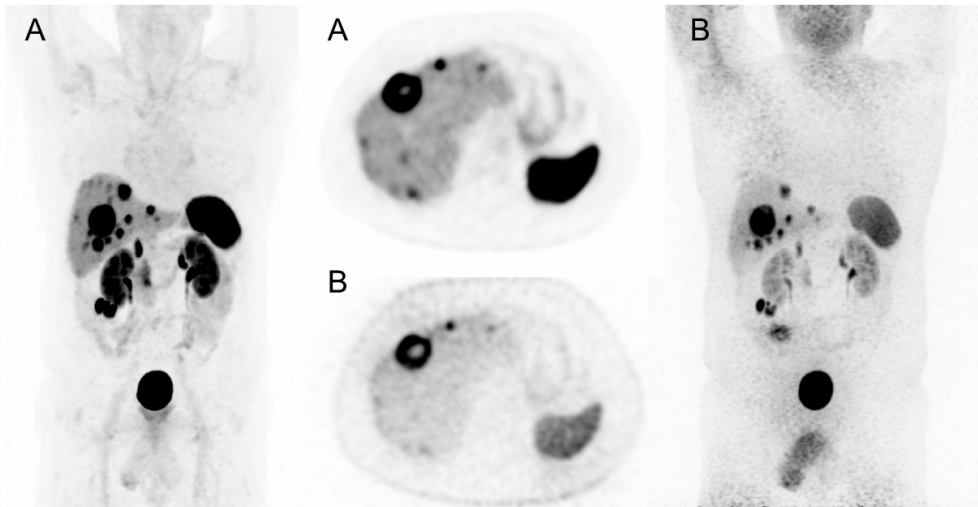
**Figure 7. Illustration of PET images with attenuation-correction and non-attenuation-correction**
(A) shows PET images with attenuation-correction, and (B) displays the same examination with non-attenuation-corrected images. Coronal MIP images are shown tho the right and left, with axial images over the liver presented in the middle (same level).

## Acquisition of the CT images

The CT-scanner employs **x-rays**, a kind of electromagnetic radiation with very high energy. These x-rays are produced inside an x-ray tube, which uses high voltage between the cathode and anode, resulting in the emission of electrons from the cathode that accelerates towards the anode. The typical tube voltage ranges between 70 and 140 kV. The number of electrons accelerated towards the anode decides the tube current (mA). Upon hitting the anode, the electrons release their energy as x-ray photons and heat.[68] Both the x-ray tube and the detector array rotate around the patient within the cylindrical PET-CT camera.[69] As the x-rays penetrate the body they are attenuated differently depending on the density and composition of the tissue inside the body.[69] The x-rays that pass through the body are detected by scintillators in the detector array which subsequently emit light photons through fluorescence after being excited by the x-ray photons. These light photons are transformed into electrical signals, thereby collecting raw projection data.[68] By consistently moving the patient through the gantry, data for the entire volume of interest (e.g., head, thorax, or abdomen) is assembled.[69]

Typically, barring any contraindications, intravenous iodinated contrast media is administered to the patient just before obtaining the CT scan.[70] The intravenous contrast enhances both organs and vascular structures, thereby increasing the detection rate of cancers and metastases.[71, 72]

### Image reconstruction

After the PET data is acquired and corrected for attenuation, the next step involves a complex, mathematically process known as image reconstruction.[73] Commonly utilised methods for CT image reconstruction include filtered back-projection (FBP) and iterative reconstruction (IR) algorithms.[68] In contrast to the relatively noiseless CT data, the high noise and limited spatial resolution that characterise PET data necessitates more advanced methods than FBP for image reconstruction. These techniques can involve iterative processes, such as expectation maximisation (EM), ordered-subset acceleration of the EM-algorithms (OSEM), and block-sequential regularised expectation maximisation algorithm (BSREM, Q.Clear).[73, 74] The need to further process images with large amounts of noise may lead to post-filtering, where the images are smoothed by averaging adjacent pixels. However, this approach also runs the risk of blurring the edges.[75]

# PET-CT quantification of NETs

To distinguish between normal and abnormal levels of activity in PET images, the standardised uptake value (SUV) was developed. This dimensionless ratio measures uptake in different tissues, normalised to the distribution volume. It is calculated within a specific region of interest inside the body. The SUV is determined from the injected dose in becquerels (Bq), the decay-corrected activity concentration in tissue in Bq per millilitre (Bq/ml) and the body weight, using the formula below. The SUV is considered as a **semi-quantitative** parameter and can be influenced by various parameters.[76]

$$SUV = \frac{Activity\ concentration\ in\ tissue\ (Bq/ml)}{Injected\ dose\ (Bq)\ /\ Body\ weight\ (g)}$$

Maximum SUV (**SUVmax**) refers to the highest voxel value within a region of interest (ROI). Conversely, mean SUV (SUVmean) signifies the average uptake within a ROI.[76] Sometimes, SUVpeak is also utilised, defined as the mean SUV within a small volume of interest (VOI) of a fixed size, typically 1 cm$^3$, concentrating on a high-uptake area of the tumour.[77] Occasionally, instead of normalising the uptake relative to the patient's weight, it is preferred to normalise the uptake by the patient's lean body mass (weight minus fat) to prevent overestimated glucose uptake in obese patients.[78] SUL stands for SUV normalised by lean body mass, rather than body weight.

In clinical practice, SUVmax is the parameter most commonly used to quantify tumour uptake in PET images. Measuring SUVmax is observer-independent and fast. However, there are disadvantages with SUVmax, as it only represents one voxel within a ROI, implying that the whole tumour burden is not represented.

Numerous factors can influence the SUV, such as body composition, blood glucose levels during $^{18}$F-FDG PET-CT imaging, somatostatin analogue treatment during somatostatin receptor PET-CT imaging, uptake time, respiratory motions, acquisition time, and reconstruction parameters. Additionally, the SUV in tumours can change over time, and there can be a partial volume effect where small lesions are underestimated. Several different methods attempt to correct and standardise for some of these aspects.[79]

As the fastest method for measuring uptake, many studies report using SUVmax. High tumour uptake (SUVmax) of $^{68}$Ga-DOTA-conjugated peptides have demonstrated a correlation with well-differentiated NETs, longer progression-free survival, and improved response to PRRT.[80-82] It has also been shown that the lowest SUVmean in a tumour lesion > 1 ml holds prognostic value assessing progression-free survival or overall survival, with lower values indicating a worse prognosis.[83] Conversely, NETs with high tumour uptake of $^{18}$F-FDG, signify increased tumour metabolism, a higher Ki-67 index, and poorer overall survival.[84, 85]

Image segmentation can be divided into two distinct but interconnected tasks – recognition and delineation.[86] Recognition in clinical practice refers to the identification of pathologies or abnormal radiopharmaceutical uptake in images by a nuclear medicine physician or radiologist. In contrast, tumour delineation in clinical practice tends to be more descriptive, usually appearing in the radiology report supplemented by specific measurements – such as the largest tumour diameter. Precise delineation in research requires each abnormal uptake in every voxel to be differentiated from the background and non-significant uptakes.[79]


**Tumour burden**

In $^{18}$F-FDG PET-CT scans, various tumour segmentation techniques like metabolic tumour volume (high metabolism tumour volume) and total lesion glycolysis (the product of SUVmean and metabolic tumour volume) have been examined.[87] Numerous studies have evaluated both metabolic tumour volume and total lesion glycolysis as significant predictors for overall survival in $^{18}$F-FDG PET-CT, though an optimal tumour segmentation method is still undefined.[87, 88] **Tumour segmentation** can be conducted through several methods, like semi-automatic methods involving threshold-based strategies using fixed absolute, fixed relative, background and adaptive approaches.[87] Manually outlining the tumour volume has multiple drawbacks such as time restrictions and significant inter-and intra-observer variance.[79] Semi-automatic methods typically exhibit good inter-and intra-observer agreement.[89]

Recently, similar methods were introduced for measuring neuroendocrine tumour burden at somatostatin receptor PET-CT. The volume of the tumours expressing

somatostatin receptors were segmented in ^{68}Ga-DOTATATE PET-CT images. This was defined as the tumour volume with more than 50% uptake of SUVmax (fixed relative threshold) for each lesion. These volumes were then combined to calculate the **whole-body somatostatin receptor-expressing tumour volume (SRETVwb)**.[90, 91] The total lesion somatostatin receptor expression was then determined by multiplying the SUVmean of each lesion by its volume. The results for all lesions were then totalled to determine the **whole-body total lesion somatostatin receptor expression (TLSREwb)**.[90, 91]
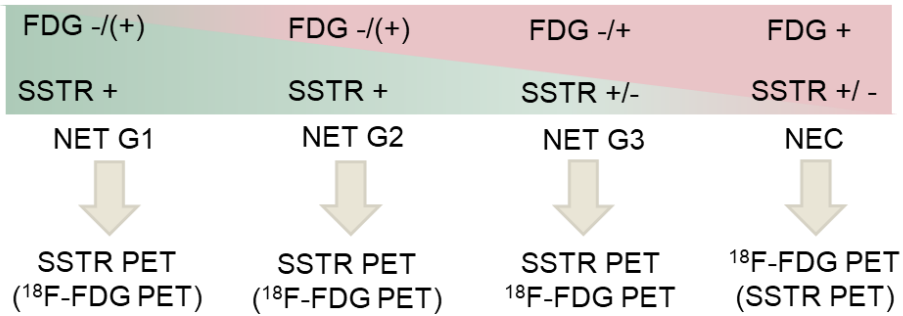
Only a limited number of studies have evaluated the relationship between SRETVwb and progression-free survival or overall survival across different clinical settings. These studies used fixed relative thresholds ranging from 30% to 50%, depending on the study.[91-94] Notably, a larger tumour volume (measured as SRETVwb) was associated with significantly shorter progression-free survival or overall survival, suggesting that this measurement may have prognostic value.[91-94] However, measurements of TLSREwb using similar methods have not shown independent prognostic value in several studies.[91-93, 95, 96]

Additionally, some studies have investigated the prognostic value of neuroendocrine metabolic tumour volume by ^{18}F-FDG PET-CT. The results indicated that this could be an independent prognostic factor for poorer overall survival and progression-free survival.[97-99]


## Dual imaging

^{18}F-FDG and somatostatin receptor PET-CT have demonstrated complimentary value concerning the imaging of NET using PET-CT. Mainly used for tumour staging, evaluating the feasibility of PRRT, and detecting recurrent disease somatostatin receptor PET-CT plays a vital role. Conversely, ^{18}F-FDG PET provides significant prognostic value, with a generally worse prognosis associated with FDG-avid tumours.[100-102] Performing ^{18}F-FDG PET is advised in cases with NEC before radical surgery for localised disease, in NET G3 cases before radical surgery and when PRRT is anticipated.[103] It is also occasionally valuable for prognostication and therapy planning in cases with NET G1-G2.[103] The complementary value of ^{18}F-FDG PET and somatostatin receptor PET is depicted in Figure 8.

In recent years, reporting systems for somatostatin receptor PET-CT, either alone or in combination with ^{18}F-FDG PET-CT, have been developed for structured image interpretation, treatment planning and prognostication.[104, 105]

| FDG -/(+) | FDG -/(+) | FDG -/+ | FDG + |
|---|---|---|---|
| SSTR + | SSTR + | SSTR +/- | SSTR +/ - |
| NET G1 | NET G2 | NET G3 | NEC |
| ↓ | ↓ | ↓ | ↓ |
| SSTR PET (18F-FDG PET) | SSTR PET (18F-FDG PET) | SSTR PET 18F-FDG PET | 18F-FDG PET (SSTR PET) |

**Figure 8. Choice of PET depending on aggressiveness of disease**
Illustration of the use of 18F-FDG PET or somatostatin receptor (SSTR) PET depending on the grade of disease. + or – demonstrates if the tumour is FDG or SSTR avid. The figure is build opon the Nordic guidelines (2021) for diagnosis and treatment of gastroenteropancreatic NET.[103]

*SSTR-RADS 1.0*

Several reporting and data systems (RADS) have been developed for different organs such as the prostate (PI-RADS), breast (BI-RADS), and thyroid (EU-TIRADS). The typical goal of these systems is to standardise reporting and stratify risk related to lesions.[106-108] The use of RADS enhances communication by improving clarity and providing consistency in radiology reports, as compared to the commonly used free-form text. Both referring clinicians and radiologists prefer this system.[109]

SSTR-RADS 1.0 was developed as a standardised evaluation and reporting tool for somatostatin receptor PET-CT images, utilised for diagnosis and treatment planning.[105] It relies on a 3-point qualitative assessment scoring system to define the uptake in somatostatin receptor-avid lesions. Level 1 denotes uptake ≤ that of the blood pool, level 2 denotes uptake greater than the blood pool but ≤ physiological uptake in normal liver parenchyma, and level 3 is defined as uptake > the physiological uptake in the liver.[105] Since its introduction, SSTR-RADS 1.0 has proven to be a highly reproducible scoring system, demonstrating high intra- and inter-reader agreement.[110]

The system has the potential to standardise diagnosis and treatment planning for NET patients.[110] SSTR-RADS 1.0 is not currently used in the clinical setting at our hospital, but might be included in future reports, correlating to the implementation of other RADS in different radiological settings aimed at improving structured reporting. An overview of SSTR-RADS 1.0 is provided in Table 4.

**Table 4. SSTR-RADS 1.0**
An overview of SSTR-RADS 1.0, adopted and condensed from original paper by Rudolf et al.[105]

| SSTR-RADS category | Definition |
|---|---|
| SSTR-RADS-1 | 1A - Benign findings, e.g. only well-known normal physiological uptake in organs <br> 1B - Benign but abnormal uptake, e.g. known thyroid adenoma. |
| SSTR-RADS-2 | Level 1 uptake in sites atypical for metastatic NET. Those lesions are almost certainly benign, e.g. axillary lymph nodes |
| SSTR-RADS-3 | Findings that need further work-up e.g. biopsy, other imaging methods or follow-up imaging. <br> 3A - Level 1-2 uptake in soft-tissues <br> 3B - Level 1-2 uptake in bone lesions <br> 3C - Level 3 uptake in a site atypical for a NET-lesion, suggesting another non-NET malignancy. <br> 3D – High likelihood for malignancy at morphological imaging (or uptake of $^{18}$F-FDG if dual imaging is performed) but no uptake at SSTR PET. This could either be dedifferentiation of a NET-lesion or another malignancy. |
| SSTR-RADS-4 | Findings with level 3 uptake in sites typical for NET lesions but without morphological correlate at CT. Highly likelihood of being NET. PRRT can be considered. |
| SSTR-RADS-5 | Findings with level 3 uptake and anatomic correlate. Confirmation with biopsy is generally not necessary (but might be needed for other purposes as defining primary tumour and the tumour grade). PRRT can be considered. |

*NETPET score*

While both somatostatin receptor PET-CT and $^{18}$F-FDG PET-CT provide different aspects of NET disease, a system was developed to interpret and report varying findings from these two examinations.[104] This scoring system was recently validated as an independent prognostic biomarker in a multicentric retrospective evaluation of patients with gastroenteropancreatic NET (GEP-NET).[111] However, it remains unknown whether the NETPET score shows predictive value for the response to PRRT, chemotherapy, or other treatments.

The grading of uptake between the two PET examinations is subjectively assessed with preset window settings for SUV, ranging from 0–15 for somatostatin receptor PET and 0-7 for $^{18}$F-FDG PET. The $^{18}$F-FDG-avidity is evaluated in the single lesion exhibiting the highest uptake relative to the uptake at the somatostatin receptor PET-CT ("the most discordant lesion").[104] An overview of the NETPET score is provided in Table 5.

**Table 5. NETPET score**

An overview of the NETPET score, summarised from the original by Chan et al [104]. The groups P1 and P2-P4a represents predominant somatostatin receptor (SSTR) avid disease likely to responde to PRRT, P4b is regarded as a group where there might be a role for PRRT but perhaps in combination with other treatments. P5 is regarded as unlikely to gain from PRRT.

| NETPET score category | $^{18}$F-FDG avid lesions | SSTR avid lesions | Comment |
|---|---|---|---|
| P0 | - | - | |
| P1 | - | + | |
| P2 | | | FDG avidity < SSTR avidity |
|    a | + | + | 1-2 lesions |
|    b | + | + | ≥ 3 lesions |
| P3 | | | FDG avidity = SSTR avidity |
|    a | + | + | 1-2 lesions |
|    b | + | + | ≥ 3 lesions |
| P4 | | | FDG avidity > SSTR avidity |
|    a | + | + | A 1-2 lesions |
|    b | + | + | B ≥ 3 lesions |
|    b | + | +/- | FDG avidity > SSTR avidity in ≤1 lesion and ≤ 1 lesion with FDG avidity and SSTR negative |
| P5 | + | +/- | FDG avidity > SSTR avidity in ≥2 lesions |
| | + | +/- | ≥2 lesions with FDG aviditiy and SSTR negative |
| | + | - | All lesions FDG avid and SSTR negative |

# Therapy

Surgical removal of NETs is the only treatment that aims at achieving a cure.[112] Surgery can also provide symptom relief, and may sometimes be indicated even for a disease that has metastasised.[113] Given that a substantial number of patients with NET present with metastatic disease, other treatment options are of great interest. While many treatment possibilities exist, a definite treatment algorithm does not exist due to the multi-dimensional nature of this disease. Factors such as proliferation rate, somatostatin receptor expression, tumour avidity at $^{18}$F-FDG PET, original tumour location, hormonal secretion, the patient's overall health, and individual preferences must all be considered in crafting an individualised treatment plan.

In general, an inverse relationship exists between the expression of somatostatin receptors in tumours and the rate of proliferation. Tumours with a low proliferation rate are ideally imaged with somatostatin receptor PET-CT, while tumours with a high proliferation rate or a high Ki-67 index are best imaged with $^{18}$F-FDG PET-CT. These factors also influence prognosis and the choice of treatment. Well-differentiated tumours, such as NET G1 or G2, are more suitable for treatment with somatostatin analogues, PRRT, or occasionally other antiproliferative targeting therapies. Tumours with a high proliferation rate, like NET G3 or NEC, are more

suitable for traditional chemotherapy and external radiotherapy, though the treatments mentioned above might also be considered, albeit potentially less effective. A watch-and-wait-approach may be adopted for patients with NET G1 and a low tumour burden, as these patients can exhibit stable disease for a prolonged period.[20]

## Somatostatin analogues

Somatostatin analogues are typically one of the first-line treatments for patients with advanced GEP-NETs, contributing to symptom control, tumour growth suppression and prolonged progression-free survival.[114-116] Given that the *in vivo* somatostatin half-life is quite short, long-acting somatostatin analogues were developed to better accommodate patient administration.[117] Two long-acting somatostatin analogues Sandostatin®-LAR® (octreotide long-acting release (LAR)), and Somatuline® Autogel® (lanreotide) are approved for this use. The recommended dose for an antiproliferative effect is 30 mg octreotide-LAR every 4 weeks or 120 mg lanreotide every 4 weeks, based on two placebo-controlled studies that demonstrated prolonged progression-free survival in patients with GEP-NET or enteropancreatic-NET.[114, 115] If symptom control is not achieved, the treatment dosage may be increased or the dosage interval shortened. Up to 80% of patients with functioning NETs show symptom improvements following this treatment, including reduced flushing and diarrhoea.[20] Long-acting somatostatin analogues demonstrate good tolerability and are recommended as an antiproliferative treatment for slow-growing, advanced somatostatin receptor-avid, GEP-NET with a Ki-67 ≤10 %.[20] Many patients require additional treatment with pancreatic enzymes while undergoing this treatment, as the somatostatin hormone and the analogue treatment inhibit the excretion of pancreatic enzymes.[48]

There is a prevailing fear that use of long-acting somatostatin analogues may lead to misinterpretation during somatostatin receptor PET-CT imaging due to the theoretical risk of the analogue interfering with the radiopharmaceutical binding of the receptor.[118, 119] The latest European Association of Nuclear Medicine (EANM) procedure guidelines for somatostatin receptor PET-CT from 2023 still recommend a time interval of 3-4 weeks after administration of long-acting somatostatin analogues to prevent a possible receptor blockade.[60] Despite this, substantial evidence supporting a significant blockade during PET-CT imaging is currently lacking.

## Chemotherapy

Chemotherapy is a systemic antiproliferative cytotoxic treatment designed to interfere with cell division.[120] Rapidly dividing cells, including aggressive tumours,

normal organs with rapid cell division, such as the gastrointestinal tract, hair follicles and bone marrow, are typically the most susceptible to chemotherapy. These are also the regions where side effects are most common.[120] Traditional chemotherapy treatments such as cisplatin/carboplatin plus etopside, temozolomide with or without capecitabine, or streptozocin plus 5-fluorouracil are principally considered for patients with metastatic diseases and intermediate to high-grade tumours (NET G2-G3 and NEC).[48] Occasionally chemotherapy is indicated before surgery for down-staging of tumours.[48]

## Other antiproliferative targeting therapies

Everolimus, a mammalian target of rapamycin (mTOR) inhibitor, demonstrates an antiproliferative effect, providing disease control for pancreatic NET, lung NET and non-functioning intestinal NET.[20] However, side effects are frequent leading to a majority of patients necessitating dose reduction.[20] Interferon alpha (IFN-α) a previously used treatment for NET, combines improved symptom control with an antiproliferative effect. Its side effects are less favourable than those of long-acting somatostatin analogues, thus IFN-α is typically deployed as a second-line treatment.[121] Sunitinib, a multiple tyrosine kinase inhibitor exhibits marginally longer progression-free survival compared to a placebo for patients with pancreatic NET. Despite this, it fails to improve the quality of life, and often leads to common side effects, including a worsening of diarrhoea.[20]

## Liver directed therapies

In patients with metastasised NET, the liver is the most common site of metastasis, with about 80% of patients in the Swedish Cancer Registry exhibiting liver involvement.[122] If liver metastases are present, potential treatment regimens include liver surgery, local liver ablation, embolization or trans arterial locoregional ablation with selective internal radiation therapy (SIRT), PRRT and liver transplantation depending on the patient and the availability of treatment options.[123, 124] Liver surgery is exclusively performed in subspecialized hospitals in Sweden.[125] Possible ablation therapies directed towards smaller metastases are typically carried out with microwave ablation or radiofrequency ablation.[20] If liver metastases provoke hormonal or local symptoms, trans-arterial liver artery embolization with particles that lead to ischemia can serve as a possible locoregional therapy. Occasionally, this embolization is combined with chemotherapy in the particles (TACE). SIRT is achieved through the selective embolization of liver arteries with microspheres radiolabelled with $^{90}Y$, causing local ischemia and local radiotherapy.[20]

## Other treatment options

External radiation therapy could be considered for brain metastases or symptomatic bone metastases.[48] It may potentially be viewed as curative in instances where only an isolated metastasis is present, and surgery is not an option.[48]

Telotristat ethyl is a relatively new symptomatic treatment that inhibits the synthesis of serotonin, leading to an improvement in the number of bowel movements for patients with carcinoid diarrhoea.[126]

## Peptide receptor radionuclide therapy

If metastatic disease is present and disease progression occurs, treatment with radiolabelled somatostatin analogues, known as PRRT, has been developed, using components such as $^{177}$Lu-DOTATATE or $^{90}$Y-DOTATOC.[127] This therapy targets the overexpression of somatostatin receptors in NETs and subsequently these receptors can be used for both imaging and distinctive therapies. The radiolabelled somatostatin analogues, once bound to the somatostatin receptors, cause the receptor to internalise, and the radiolabelled peptides are stored in lysosomes. This process allows the radioactivity to remain inside the tumour cell. [127, 128]

The unstable radionuclide $^{177}$Lu has a half-life of 6.65 days and undergoes beta minus **(β⁻) decay** by emitting a high-energy electron. These electrons have a short penetration range in tissue, averaging 0.67 mm, resulting in both single and double-strand DNA breaks.[129] $^{177}$Lu also emits **γ-rays**, which makes it possible to image the radiopharmaceutical within the patient, quantify the uptake in tumours or normal organs, perform dosimetry, and monitor the tumour response. This can be accomplished using a planar gamma camera or its tomographic counterpart, known as single photon emission computed tomography (SPECT). [127, 130, 131]

$^{90}$Y emits β- particles, with a penetration length of about 10 mm in the body. This feature provides a somewhat different therapeutic potential. However, post therapy imaging is less straightforward due to lack of γ-rays.[127]

Since the introduction of PRRT in the 1990s, significant advancements in progression-free survival have been observed, with the selection of appropriate patients through somatostatin receptor imaging.[131] The first prospective, randomised study with PRRT, NETTER-1, showed longer progression-free survival for patients given a regimen of four cycles of 7.4 GBq **$^{177}$Lu-DOTATATE**, in combination with long-acting somatostatin analogues (30 mg octreotide), compared to the group receiving only 60 mg of octreotide monthly. Based on these results, Lutathera® was approved by the EMA and FDA.[129, 131]

An illustration of PRRT treatment is provided in Figure 9 and examples of post PRRT imaging are provided in Figure 10.
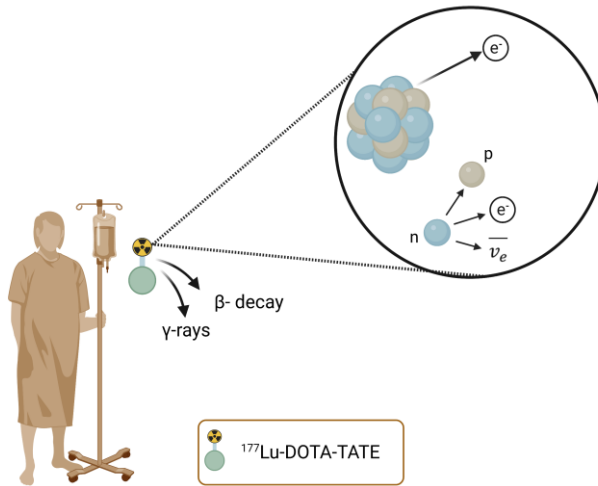
**Figure 9. Treatment with PRRT**
Illustration of the decay of $^{177}$Lu during treatment with $^{177}$Lu-DOTATATE. Neutron (n), proton (p), electron (e$^-$) and antineutrino ($v_e$). Created with biorender.com
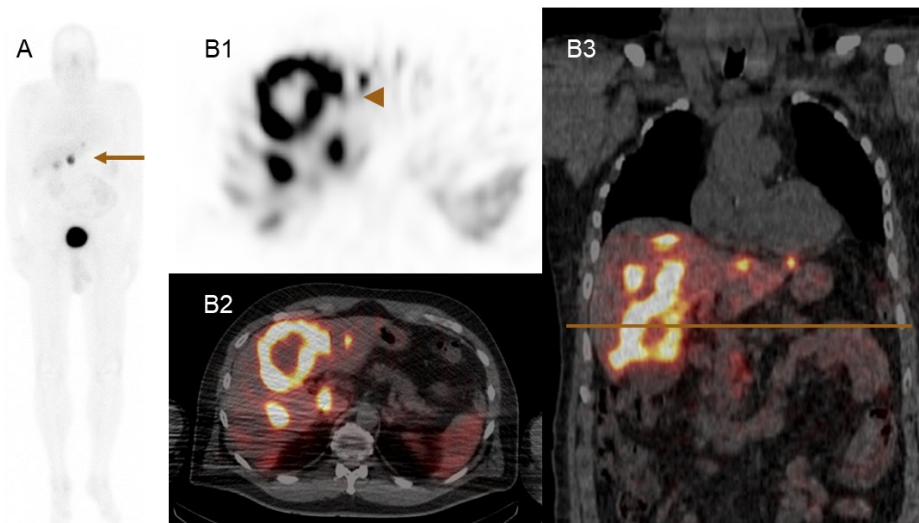


**Figure 10. Post PRRT imaging**
Patient A: Planar whole-body imaging after PRRT. The arrow points to uptake in liver metastases.
Patient B: SPECT-CT imaging of the uptake of 177Lu-DOTATATE post therapy. Axial SPECT image over the liver, with arrowhead pointing to uptake in liver metastases (B1). Combined SPECT-CT image at the same level as B1 (B2). Coronal image showing uptake in liver metastases, with a line illustrating the level of the axial images (B3).

High uptake in tumours is necessary for treatment with PRRT, requiring at least a relative Krenning score of 2, as previously evaluated with ^{111}In-labelled octreotide scintigraphy. An overview of the Krenning score is presented in Table 6.[132] The ^{111}In-labelled octreotide scintigraphy has been largely replaced by somatostatin receptor PET-CT due to its lower radiation dose, superior sensitivity, and simpler imaging acquisition process.[133] However, there is still no definitive translation of patient selection criteria from scintigraphy to somatostatin receptor PET-CT. This is mainly because small lesions visualised by somatostatin receptor PET-CT may not meet earlier selection criteria, and the use of a somatostatin receptor PET tends to result in higher Krenning scores.[134]

**Table 6. Overview of the Krenning score**
Initially developed for assessment of the uptake on planar imaging.[57, 132]

| Relative uptake score | Comment |
| --- | --- |
| 0 | No uptake |
| 1 | Much lower than liver |
| 2 | Equal to liver |
| 3 | Greater than liver |
| 4 | Greater than spleen |

To achieve the clinical benefits of PRRT, careful selection of suitable patients and accurate evaluation of treatment response are integral. Side effects can be partly managed by selecting appropriate patients for treatment, early identification of risk factors for toxicity, and closely monitoring patients post-treatment and before each new cycle of PRRT. Common side effects include mild hair loss (60%) and nausea (25%), while vomiting and abdominal pain affect about 10% of the patients.[127] Nephrotoxicity is also a potential later side effect as the kidneys are regarded as the dose-limiting organ together with the red-marrow.[135] More rare but potentially fatal side effects such as myelodysplastic syndrome and hormonal crises also exist.[127] The nephrotoxicity of ^{177}Lu-DOTATATE can be mitigated by administering an infusion of amino acids (L-lysine and L-arginine) before, during and after the infusion of ^{177}Lu-DOTATATE.[127] Administering antiemetic drugs alongside treatment is recommended to decrease nausea and vomiting.[127]

PRRT is an effective treatment, demonstrating tumour shrinkage or stabilization for a significant number of patients with advanced NETs.[131, 136, 137] However, it should be noted that disease progression occurs in up to 20% of patients during treatment, or within 6 months to 1 year after completing treatment.[119, 131]

Since the approval of ^{177}Lu-DOTATATE its use has been limited to four cycles of 7.4 GBq. However, other treatment protocols, like image-based dosimetry-guided treatment[138, 139] and combinations of chemotherapy and PRRT[140] are being explored. The fixed treatment regimen does not take into account the total tumour volume that needs treatment, nor the patient's size. Hence, personalised treatment may

potentially yield better results compared to a one-size-fits-all regime. Sundlöv et al. demonstrated that individualised treatment with ^{177}Lu-DOTATATE based on kidney dosimetry was feasible, with 73% of patients able to receive more than four cycles.[139] Similarly, Garske-Roman et al. carried out a prospective study with kidney dosimetry where patients underwent between 3 to 9 treatment cycles.[138] The study showed that patients who reached the dose limit of 23 Gy had longer overall survival than those who did not.[138]

*Dosimetry*

Dosimetry involves estimating the absorbed dose delivered by ionising radiation to tissue, which can be applied in PRRT. Post-therapy imaging during PRRT allows for the verification of uptake and quantification of the radiation dose to tumours and non-target volumes.[141] Dosimetry during PRRT can be achieved through multiple SPECT-CT acquisitions after the administration of a treatment cycle. By defining ROIs or VOIs in the images, such as those over the kidneys or tumours, the activity concentration can be measured, typically expressed in Bq/ml. The construction of a time-activity curve for each VOI, allows for the calculation of the area under the curve, which is used to determine the total time-integrated activity.[142] The absorbed dose to tissue can then be estimated using the Medical Internal Radiation Dose (MIRD) formalism, measured in gray (Gy).[142] 1 Gy is defined as the absorption of 1 joule of radiation energy per kilogram of tissue.[143]

*Predictors of poorer survival when treated with PRRT*

Biomarkers are essential for cancer screening in healthy individuals, estimating prognosis, predicting treatment outcomes, and disease monitoring during follow-up. The FDA-NIH Biomarker Working Group defines a biomarker as:

> "A defined characteristic that is measured as an indicator of normal biological processes, pathogenic processes, or biological responses to an exposure or intervention, including therapeutic interventions. Biomarkers may include molecular, histologic, radiographic, or physiologic characteristics. A biomarker is not a measure of how an individual feels, functions, or survives."[144]

A biomarker can also be used to gauge how well the body responds to a treatment for a disease or condition.[145] Imaging biomarkers, a subset of biomarkers, are measurements derived from medical images such as mammography, CT, MRI or PET-CT.[146]

In general, a **prognostic biomarker** is used to predict the likelihood of a certain clinical event, such as the recurrence of a disease or death. On the other hand, a **predictive biomarker** is commonly used to identify patients who are more likely to encounter a positive or negative effect from a treatment.[147] Predictive biomarkers are typically derived from clinical trials that compare treated patients with a control group, while prognostic biomarkers mostly originate from observational data.[82]

Figure 11 provides an overview of potentially relevant biomarkers throughout the disease continuum.
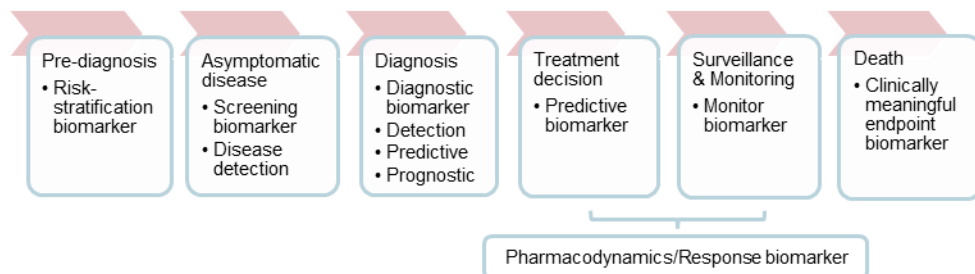


**Figure 11. Disease timeline with potential relevant biomarkers**
Biomarker categories on the continuum of a disease
Image inspired by the original by Chiu et al [148] Imaging biomarkers for clinical applications in neuro-oncology: current status ant future perspectives. Biomark Res 11, 35 (2023)
Distributed under CC BY 4.0; https://creativecommons.org/licenses/by/4.0/

Biomarkers for predicting responses to PRRT in the context of NET can be categorised into the following categories[82]:

- Clinical biomarkers such as health-related quality of life scales and specific symptom scales for NET.

- Tissue biomarkers obtained from pathology, such as Ki-67.

- Biomarkers found in blood, such as chromogranin A and 5-HIAA.

- Genomic multianalyte biomarkers (e.g., the NETest).

- Imaging biomarkers derived from contrast-enhanced CT, multiphase contrast MRI, somatostatin receptor PET-CT, ^{18}F-FDG PET-CT.

- Dosimetry with SPECT imaging performed after treatment with PRRT.

All of these biomarkers exhibit some value in various clinical contexts, but not all have an established role as predictive biomarkers for PRRT response. Morphological and functional imaging of NET, primarily with somatostatin receptor PET-CT, which is currently the gold standard for functional imaging, is indispensable as a biomarker source for predicting response to PRRT. The challenges of evaluating response to PRRT were recently reviewed by Liberini et al.[82] They asserted that morphological and functional imaging continue to play an essential role in the NET work-up and that imaging biomarkers, possibly in combination with circulating biomarkers and genomic biomarkers, will influence the future care of PRRT patients by individualising their treatment.[82]

*The role of tumour burden for prediction of response to PRRT*

The current literature extensively covers the topic of the diagnostic performance of somatostatin receptor PET-CT. A systematic review and meta-analysis of studies evaluating pre-treatment staging with somatostatin receptor PET-CT found that 23 of the 24 studies concluded that this examination was important in guiding treatment decisions for patients with NET.[149] However, the literature is more scattered concerning the impact of measurements from somatostatin receptor PET-CT in predicting response to treatment with PRRT. Presently, there are yet no definitive predictive imaging biomarkers. A high uptake at the somatostatin receptor PET-CT is an inclusion criterion for treatment with PRRT and is associated with a favourable response, but no clear evidence indicates to what extent a higher cut-off value of SUVmax, SUVmean, SUVmax-to-liver ratio, or total tumour volume correlates with the response to treatment for individual patients.[149]

# Assessment of response to treatment with imaging

Imaging in oncologic care is a crucial part of the diagnosis and staging of the disease, treatment planning, evaluating the response to treatment and when there is suspicion of complications or disease progression. Imaging biomarkers are characteristics present in a patient's image. In oncology, imaging biomarkers are used for disease identification, prognostication, prediction of therapeutic outcome, and to assess the response following therapy. Examples of imaging biomarkers used in medical and scientific practices include; the assessment of objective response by the standardised response evaluation in solid tumours criteria (RECIST) – which serves as a response biomarker,[150] the TNM classification of malignant tumours for staging the extent of cancer spread – typically used as a prognostic biomarker,[21] and somatostatin receptor-avid lesions at somatostatin receptor PET-CT to identify neuroendocrine tumour lesions and to guide decision-making about PRRT.[146]

The RECIST 1.1 is one of the most common response assessment tools used, in both research and clinical work. When evaluating response using the RECIST 1.1 criteria, both target lesions and non-target lesions are defined at the baseline examination. The sum of the longest diameters of up to five target lesions (maximum two target lesions per organ) at baseline are compared during follow-up examinations. This process also involves the evaluation of potential new lesions and a re-evaluation of non-target lesions. Outcomes at follow-up are categorised in to four groups: complete response, partial response, stable disease, or progressive disease.[150] Table 7 provides more details about RECIST 1.1.

**Table 7. RECIST 1.1**
Summary of the response evaluation with RECIST 1.1.[150] Sum of the longest diameters (SLD)

| Complete response (CR) | Partial response (PR) | Stable disease (SD) | Progressive disease (PD) |
|---|---|---|---|
| Disappearance of all lesions and pathological lymph nodes | ≥ 30% decrease of SLD | Does not meet criteria for either PR or PD | ≥ 20% increase of SLD compared to smallest SLD in study or* or** |
| | No new lesions | No new lesions | *new lesions |
| | No progression of non-target lesions | No progression of non-target lesions | **unequivocal progression of non-target lesions |

Evaluating response based purely on morphological imaging, utilising RECIST 1.1, may not always be sufficient. RECIST 1.1 encounters difficulties when analysing tumours with irregular boundaries, skeletal metastases, and necrotic or partially cystic lesions. Therapy-induced tumour necrosis could cause inflammation and swelling of a lesion, which can masquerade as stable disease or even progressive disease.[151, 152] A retrospective study of 354 patients with GEP-NET treated with PRRT found that, among the 206 patients with stable disease at the 3-month follow-up, 9% initially experienced an increase in tumour diameter of more than 10% at the first follow-up, 6 weeks after the last cycle of PRRT.[151] The median increase was 18% with a range of 10–71%, suggesting caution when utilising RECIST 1.1 to categorise progressive disease at 6-week follow-ups following PRRT.[151] According to RECIST 1.1, progressive disease is defined by a ≥20% increase in the sum of the longest diameters and an absolute increase of at least 5 mm, which corresponds roughly to a 70% increase in tumour volume – a substantial increment in the tumour burden. Consequently, other response criteria have been proposed, some of which are applicable to specific types of cancer. For instance, the Choi criteria, which were developed for gastrointestinal stromal tumours (GIST), take into account tumour density when evaluating a response, as well as the change in size of tumours.[153] A recent study compared RECIST1.1 to Choi criteria in patients with GEP-NET, finding that RECIST 1.1 had greater clinical utility and prognostic value than Choi, despite still having limitations that highlight the need for novel prediction tools for treatment outcomes.[154]

In comparison to morphological response evaluations such as RECIST 1.1 criteria, there is also a need for response evaluation that assesses the biological function or response to treatment, such as the metabolic response. Various response criteria have been developed for ^{18}F-FDG PET imaging.[155] Several tumours such as lymphomas, gastrointestinal stromal tumours, and sarcomas can metabolically respond well to treatment but may show very subtle shrinkage at initial follow-ups, resulting in stable disease by RECIST 1.1 criteria, yet metabolically showing partial or complete response.[78] The European Organization for Research and Treatment of

Cancer (EORTC) developed a PET-based response assessment,[156] and later a similar refined PET response criteria in solid tumours (PERCIST) was developed as a standardised way to assess the metabolic response with ^{18}F-FDG PET imaging.[78] These criteria use four similar categories for response assessment as RECIST 1.1, namely, complete metabolic response, partial metabolic response, stable metabolic disease and progressive metabolic disease.[78] The different response criteria have shown equal performance, but PERCIST might be preferred for simpler use.[157] Using PERCIST criteria, SUL is preferred over SUV to reduce variability in the uptake among individuals due to differing weights.[78]

Other response evaluations for ^{18}F-FDG PET imaging include the Deauville score, and the Lugano criteria, which are commonly used during lymphoma treatments. The Deauville five-point scale assesses the lesion uptake relative to the background tissue, mediastinal blood pool and the liver.[155] The Deauville score is sometimes integrated and interpreted following the Lugano classification and used alongside other evaluated parameters in four response categories, complete response, partial response, stable disease and progressive disease.[155]

Somatostatin receptor PET-CT has a well-established role in diagnostics and restaging when recurrence is suspected. However, its value during routine follow-up for stable disease remains more uncertain.[158] Furthermore, no established criteria currently exist for assessing treatment response with somatostatin receptor PET-CT.

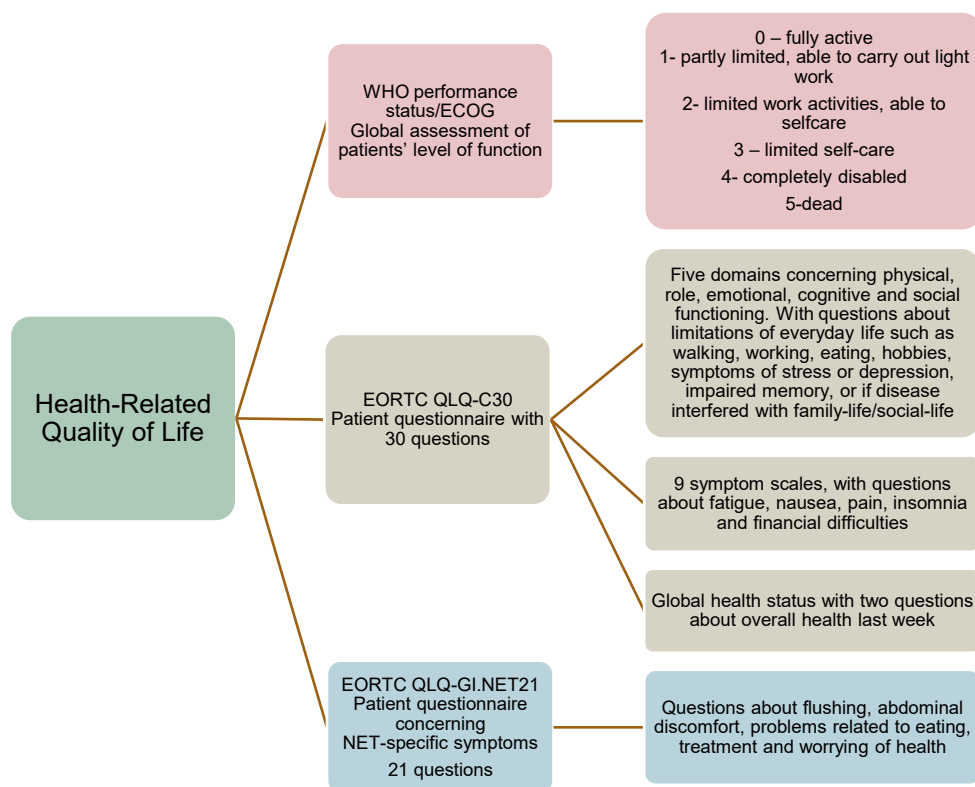
# Health-related quality of life

Quality of life, or the somewhat narrower concept of health-related quality of life, represents a multi-dimensional perspective on health that includes both physical and mental health aspects related to overall well-being. Health-related quality of life can be assessed in several ways. Nevertheless, in cancer patients, the most frequently used questionnaire is the cancer-specific European Organisation for Research and Treatment of Cancer questionnaire (EORTC QLQ-C30).[159] This questionnaire evaluates different functioning domains such as physical, role, emotional, cognitive, and social functioning as well as common cancer symptoms such as like nausea, fatigue and pain. A composite score (QLQ-C30 summary score) can be calculated from the average of all functioning domains and symptoms. This summary score could potentially reduce the risk of type-I errors resulting from multiple tests.[160] Husson et al. determined that the QLQ-C30 summary score possesses robust prognostic value concerning overall survival, evaluated across different cancer populations in a "real-world" setting.[161]

Patients with NETs frequently exhibit varying symptoms, often due to tumour hormone production. To address these symptoms, a specific questionnaire, EORTC

QLQ-GI.NET21 has been developed.[162, 163] The supplemental QLQ-GI.NET21 module concentrates on disease-specific symptoms related to the gastrointestinal system, endocrine system, pain, and disease associated concerns.[162, 163]

For clinical or research purposes, a patient's overall health and level of function can be estimated using the Eastern Cooperative Oncology Group (ECOG) functional status scale, which ranges from 0 to 5, and has been adopted by the WHO.[164] Figure 12 illustrates the concept of health-related quality of life, which can be evaluated using various tools such as ECOG/WHO performance status, EORTC QLQ-C30, and EORTC QLQ-GI.NET21.



**Figure 12. Health-related quality of life**
Overview of tools for assessment of health-related quality of life.[159, 162-164]

NETs can significantly affect a patient's health-related quality of life, causing general symptoms such as fatigue, weakness, and weight loss, as well as symptoms from functioning NETs, such as flushing, diarrhoea, and bronchospasm (previously outlined in Table 3).[165] A Swedish study by Ohlsson et al. discovered that specific

NET-associated symptoms, such as sensitivity to certain foods, soiling, and the sensation of incomplete bowel emptying, most strongly correlated with a decrease in health-related quality of life.[166]

There is an increasing trend in the use of tools for assessing health-related quality of life in treatment studies. A new treatment not only needs to prove itself as safe and able to improve outcomes, but it should preferably enhance health-related quality of life, or at the very least, not diminish the patients' quality of life during long-term follow-up.

### Tumour burden in correlation to health-related quality of life

It is not yet fully understood whether tumour burden is correlated with health-related quality of life. Only a few studies have explored the relationship between tumour burden and health-related quality of life.[167, 168] Debulking surgery of hepatic metastases, aimed at reducing tumour burden, is sometimes indicated when uncontrolled carcinoid symptoms persist despite other treatments.[169, 170] However, these studies do not specifically assess the association with health-related quality of life. Instead, health-related quality of life has been evaluated in several treatment studies for NET-patients undergoing treatment with PRRT. It has been demonstrated that PRRT is associated with improvements in health-related quality of life and extended time to symptom worsening.[171, 172] Also, the NETTER-1 study revealed noteworthy enhancements in health-related quality of life encompassing global health status, physical abilities and relief from symptoms like fatigue, pain and diarrhoea in patients treated with PRRT.[173]

# Artificial intelligence

Artificial Intelligence (AI) broadly refers to the capacity of computers, machines, or software to execute tasks that typically necessitate human intelligence. The AI field is evolving swiftly, applying its technology across various domains such as industry, science, and an expansive market of applications. Renowned applications include web search tools, autonomous vehicles, human speech recognition incorporated in modern mobile phones, and creative apps that generate text or images.

AI has emerged as a prominent topic in the field of medical imaging in recent years. The low threshold for developing AI algorithms in radiology, primarily due to the digitisation of data such as images and outputs like imaging reports, has facilitated significant advancements in the creation of radiological AI tools. A recent randomised prospective study by Lång et al. contrasted the standard double reading of mammography with that of an AI-assisted single reading. It was found that while

the cancer detection rate was comparable between the two groups, AI notably reduced the workload.[174]

## Background

In the early stages of the AI development, the problems AI was designed to solve were usually straightforward for computers, but time-intensive or too complex for humans, often expressed as a list of mathematical rules.[175] A famous early example occurred in 1997 when world chess champion Garry Kasparov was defeated by a computer for the first time.[176] This type of early AI did not require extensive knowledge about the world, as a chessboard only provides a limited number of potential combinations. However, tasks such as speech recognition or image interpretation, which are more intuitive for humans, have proven to be much more challenging for AI to master.

Such knowledge is harder to express in systematic manner, and thus, AI systems need to develop their understanding by observing patterns from raw data.[175] This branch of AI, often called machine learning, typically involves humans experts identifying distinct features in data, like edges and applying mathematical techniques to categorise the data based on these features. A further subfield within machine learning is deep learning, which can manage more complex tasks such as image interpretation. In image interpretation, not only are distinct features like edges valuable but also other complex features.[175] The favoured method for most image analysis applications today is the use of convolutional neural networks (CNN).[175] An overview of AI is provided in Figure 13.
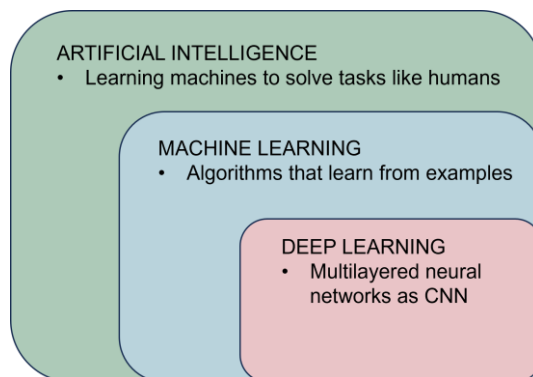


**Figure 13. Overview of AI**
Schematic overview of the broad term AI and its subfields. Convolution neural networks (CNN)

CNNs were initially inspired by the visual cortex in animals and humans. They replicate the processing of visual information through the brain, where neurons are

arranged in hierarchical layers from the primary visual cortex, and secondary visual cortex to the inferotemporal cortex in the posterior and anterior layers.[177] The brain's initial layers detect basic object features, such as edges, while the deeper layers detect more complex combinations. Towards the end of this process, the brain identifies and recognises entire objects, before finally forming a more abstract or semantic understanding of the information.[177]

In a CNN, information is processed similarly through multiple layers with deep learning techniques, activating different "neurons" at each layer. The CNN is a mathematical structure usually composed of three types of layers (or building blocks): convolutional layers, pooling layers, and fully connected layers.[178] Each convolution involves a matrix of weights that analyses the image features through mathematical processing to create feature maps of the original image.[177] The next steps involve working on these feature maps at each layer to extract further information. Pooling layers are applied between convolutional layers to reduce the spatial resolution. Ultimately, the output, such as the segmentation of tumour volume, is produced.[179] If the task pertains to classification, the output layer becomes a set of classifiers, for instance classification of organ or tumour lesion yes/no, as depicted in Figure 14. During the training process, feedback is provided to the various convolutional layers to optimise the output, a process sometimes referred to as backpropagation.[178] CNNs are typically trained with labelled data (the ground truth), also known as supervised learning.[180] In medical applications, CNNs are primarily used for classification (e.g. cancer yes/no), segmentation (e.g., organs, tumour volume), and detection (e.g., identifying lung nodules).[177, 181]
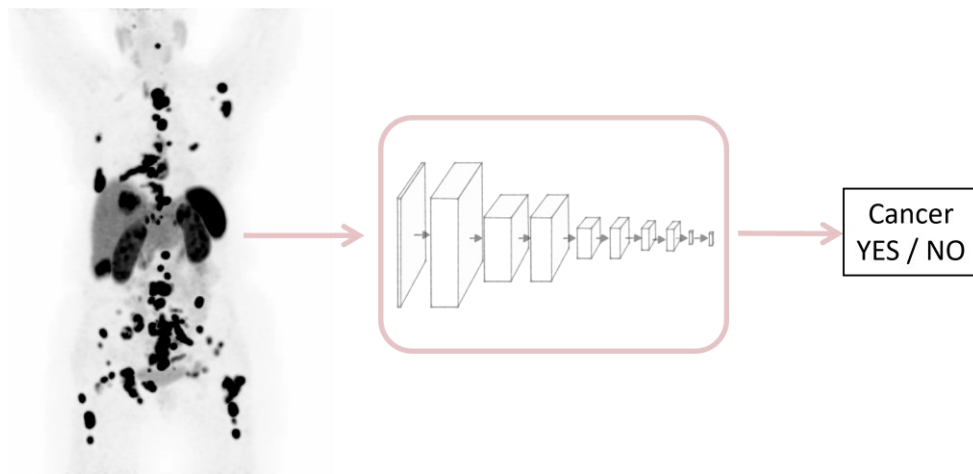


**Figure 14. Schematic of CNN**
Image of a PET scan (MIP) with cancer as input. The boxes represent the different layers of convolution neural networks (CNN). The output, in this case is cancer, or no cancer.

## Datasets and ground truth for training an AI model

Deep learning requires datasets, such as medical images, for training. In the context of deep learning for medical imaging, the training or 'ground truth' data is a dataset of medical images with labels. These labels are often added by a human, indicating aspects like segmented tumours.[182] It could be of value if the training data contains both images with tumours and images without tumours.[182] Accuracy of the training data chosen for training is of utmost importance, as the model will learn from the provided data. Additionally, the training data must contain a variety of examples. If the training data lacks diversity, the AI model develop biases. However, acquiring high-quality training data can be both expensive and time-consuming.[178]

The dataset used for developing an AI model is typically divided into training, validation and test sets.[178] The training set data are used for training the actual parameters of the network, while the validation set is used to monitor the model's performance during the training process and to fine-tune hyperparameters.[178] Consequently, the term "validation" is used differently in machine learning compared to its use in medicine, where "validation" usually refers to the process of verifying a prediction model.[178] An overview of the dataset partitioning is illustrated in Figure 15.
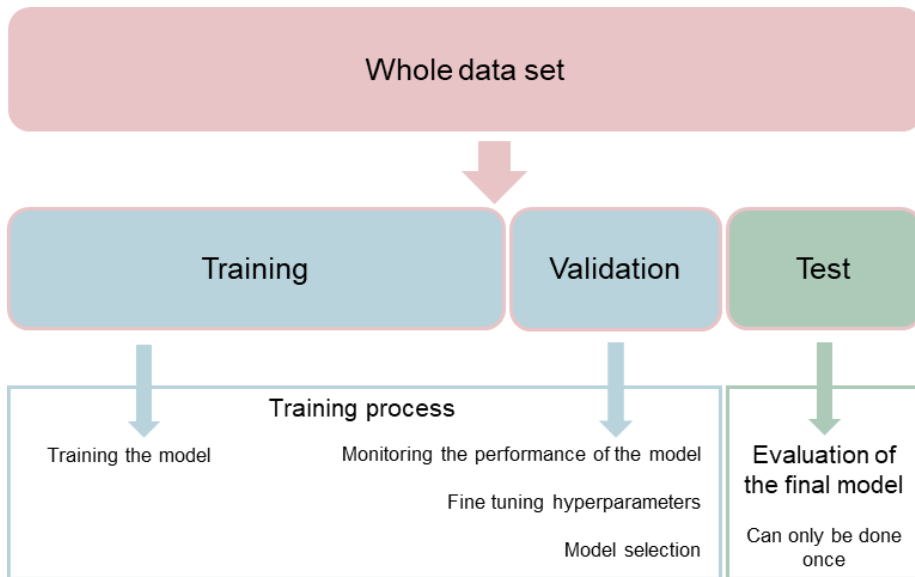


**Figure 15. Dataset partitioning**
Image illustrating the partitioning of the entire data set into training, validation and test sets. Image adapted from the original by Yamashita et al.[178] Convolutional neural networks: an overview and application in radiology. Insights in imaging 9, 2018. Distributed under CC BY 4.0; https://creativecommons.org/licenses/by/4.0/

The final step in the development of an AI model is the evaluation of the final model with the test set. This step should be performed only once, and it is a prerequisite that the cases are completely unseen by the developed AI model to accurately predict its generalisability.[178] However, before an AI model can be introduced to the market, it is crucial to validate its performance and effectiveness in various settings. This process involves several approaches where the AI model is exposed to new datasets and diverse populations to examine how well it performs and ensure it can adapt to different settings.

## Human versus AI in medical imaging

During the human interpretation of medical images, clinicians search for life-threatening findings and details relevant to the patient's condition, such as the primary tumour location and the presence of metastases. This process of detecting pathology in images is occasionally referred to as pattern recognition. Once a potential concern is detected, it needs to be evaluated and interpreted in the light of the patient's medical history and other variables. This data is then compared with probabilities of differential diagnosis.

In addition to this, other findings relevant to the diagnostic work-up, prognostication, and treatment such as ascites, pleural effusion, or a thrombosis, must also be evaluated and interpreted. Finally, identification, evaluation and interpretation of incidental findings, those not explicitly requested, are addressed. These sometimes necessitate further investigation or follow-up.

During this process, humans excel at determining whether an image is normal or abnormal, but struggle with quantifying findings numerically. For instance, a tumour's measurement might be estimated by its diameter, but an exact assessment of its volume is significantly more challenging and time-consuming. Grading often uses a three-step scale, identified by adjectives such as mild/moderate/severe or possible/probable/definite. Conversely, AI models are adept at quantifying data and numerically reporting findings.[183] Thus, AI might prove a useful tool in future medical image interpretation. AI is also being developed to optimise radiation levels to patients, improve radiology reports, and enhance image quality.[183, 184] The following are some examples of future (or already available) AI tools in the field of medical image (radiology) interpretation:

*Detection*
- Improving prioritisation by identifying life-threatening disease in images waiting for interpretation, and by then sorting the list accordingly, or flagging cases with acute findings, so that the interpreting radiologist has the opportunity to return result in an optimised order.[185]

- Finding and marking all small lung nodules, which are easy to overlook during image interpretation.[186]
- Detection of suspicious lesions in mammography, reducing the need for two radiologists to interpret all screening images.[174]

*Segmentation*
- Segmentation of tumour volume (e.g., neuroendocrine tumour volume).[187]
- Radiation treatment planning by segmentation of tumours for optimising radiation dose.[188]

*Classification*
- Detection and classification of prostate cancer.[189]

## Authorisation

Medical devices that impact health, including AI models or AI software sold in the European Union (EU), need the CE mark to indicate product compliance with EU regulations and standards for safety, health, and environmental protection.[190] Recently, the EU Parliament adopted the EU AI Act, which is the world's first comprehensive AI law.[191] The EU AI Act is part of the EU's digital strategy to balance innovation and technological advancements with fundamental rights and ethical standards.[191] Depending on the risk an AI system poses, varying degrees of regulation may be required, ultimately resulting in different CE mark classes.[191]

All commercially available, CE-marked AI models for medical radiological imaging are listed in a database, "Health AI Register".[192] Their efficacy has been evaluated according to an adapted hierarchical model, designed specifically to assess AI models.[193, 194] This is presented in Table 8.

Since the introduction of AI models in medical imaging, there has been anticipation for enhancements of healthcare and reduction in costs. However, according to a recent publication, little is yet understood about the AI's contribution to clinical practice, although the field continues to evolve.[195] The Health AI Register only lists one registered CE marked AI software product designed for whole-body PET-CT, which is used to detect, quantify and segment FDG-avid lesions.[192] In 2020, the effectiveness of 100 CE-marked AI software products was evaluated in 237 peer-reviewed articles related to these products.[194] Each paper was classified based on the hierarchical model of efficacy (as outlined in Table 8). Only six products were classified with level 4 efficacy, while just two products achieved level 5 and/or 6 efficacy.[194] Even though all these products have received CE marking and are commercially available, the clinical impact of the majority is yet to be announced.

**Table 8. A system to assess the efficacy of an AI model**
Hierarchical model of efficacy to assess the contribution of AI software to the diagnostic imaging process, adapted from Fryback and Thornbury[193] by van Leeuwen et al.[194]

| Level | Explanation | Typical measures |
|---|---|---|
| Level 1 t (technical) | Technical efficacy<br>Article demonstrates the technical feasibility of the software | Reproducibility, inter-software agreement, error rate |
| Level 1 c (clinical) | Potential clinical efficacy<br>Article demonstrates the feasibility of the software to bli clinically applied | Correlation to alternative methods, potential predictive value, biomarker studies |
| Level 2 | Diagnostic accuracy efficacy<br>Article demonstrates stand-alone performance of the AI model | Standalone sensitivity, specificity, area under the ROC curve or Dice score |
| Level 3 | Diagnostic thinking efficacy<br>Article demonstrates the added value to the diagnosis | Radiologist performance with/without AI, change in radiological judgement |
| Level 4 | Therapeutic efficacy<br>Article demonstrates the impact of the software on patient outcomes | Effect on treatment or follow-up examinations |
| Level 5 | Patient outcome efficacy<br>Article demonstrates the impact of the software on patient outcomes | Effect on quality of life, morbidity, or survival |
| Level 6 | Societal efficacy<br>Article demonstrates the impact of the software on society by performing an economic analysis | Effect on costs and quality-adjusted life years |

# Background summary

The use of somatostatin receptor PET-CT for imaging neuroendocrine tumours (NETs) is a highly sensitive and specific method for identifying these tumours, as they typically overexpress somatostatin receptors.

The theranostic principle in NET involves the targeting of somatostatin receptors during both imaging and treatment. Radiolabelled somatostatin analogues such as $^{68}$Ga-DOTATOC and $^{68}$Ga-DOTATATE target somatostatin receptors during PET-CT imaging. Long-acting somatostatin analogues bind to somatostatin receptors and provide symptom control and some antiproliferative effect. PRRT with $^{177}$Lu-DOTATATE also targets the somatostatin receptors, delivering internal radiotherapy to tumours, and producing significantly improved outcomes for a substantial number of patients.

As these tumours typically grow slowly, and NET patients can survive for extended periods even with widespread metastatic disease, it is crucial to assess their health-related quality of life throughout the disease's progression.

Although PET-CT is a vital tool in the diagnostic work-up, imaging data are not quantified in clinical practice due to the time-consuming nature of the process. Moreover, no quantitative imaging biomarkers have been established for somatostatin receptor PET-CT in terms of prognostication, predicting treatment outcomes, or response assessment.

Several questions are still awaiting answers, but a few have been addressed in this thesis:

- Can treatment with long-acting somatostatin analogues interfere with the detection of NETs during treatment?

- Is total tumour burden linked to health-related quality of life?

- Is it possible to develop an AI model to quantify total tumour burden?

- Is baseline tumour burden correlated with treatment outcomes following treatment with PRRT?

Beyond the diagnostic work-up for detecting NETs using somatostatin receptor PET-CT imaging, several areas are ripe for improvement and advancement concerning the information contained in patient images. The goal of these efforts is to enhance patient care and outcomes in the future.

# Aims

The overall aim of this thesis is to enhance our understanding of NETs, extending beyond the diagnostic process when imaged with somatostatin receptor PET-CT. We explore various aspects, such as the impact of treatment on the uptake of the radiopharmaceutical at the somatostatin receptor PET-CT, if tumour burden correlates with health-related quality of life, the creation of an AI model to measure tumour burden, and the possibility of baseline PET-CT parameters predicting treatment outcomes following $^{177}$Lu-DOTATATE therapy.

## Paper I

The primary aim was to assess whether treatment with long-acting somatostatin analogues impacted the uptake of $^{68}$Ga-DOTATATE during somatostatin receptor PET-CT imaging in patients with NETs. This was evaluated in two distinct situations:

1. if there was a difference in the uptake in normal liver tissue and tumours in patients after the start of treatment with long-acting somatostatin analogues compared to imaging before treatment.

2. if the interval from the last dose of long-acting somatostatin analogue to imaging with somatostatin receptor PET-CT affected the uptake in normal liver tissue and tumours.

The exploratory aim was to evaluate whether the clinical assessment of the disease, classified as either progression, regression, or stable disease, corresponded with changes in the uptake of $^{68}$Ga-DOTATATE.

## Paper II

The primary aim was to determine whether there was a correlation between the total tumour burden at somatostatin receptor PET-CT and the health-related quality of life evaluated with the EORTC QLQ-C30 summary score.

The secondary aim was to ascertain whether the total tumour burden or the distribution of tumours in the body influenced the patients' symptoms, as assessed with the specific questionnaire QLQ-GI.NET21.

# Paper III

This paper aimed to develop an AI model to detect and quantify tumours and metastases from somatostatin receptor PET-CT images.

# Paper IV

The primary aim was to evaluate whether the tumour burden, as observed on baseline somatostatin receptor PET-CT, could predict progression-free survival or overall survival after treatment with ^{177}Lu-DOTATATE.

The secondary aims were to ascertain whether there was a correlation between the tumour burden at baseline PET-CT and the mean tumour absorbed dose, or if the mean tumour absorbed dose at the first treatment cycle, or a change in tumour burden at follow-up, could forecast treatment outcomes.

The exploratory aim was to assess whether the tumour burden in patients undergoing ^{177}Lu-DOTATATE therapy could be accurately evaluated using the AI model presented in Paper III.

# Patients and methods

The PET-CT examinations in Papers I–IV were all conducted at Skåne University Hospital in Lund. The PET-CT protocols for Papers I–IV, along with image analyses for Papers II–IV are detailed below. They are fundamentally the same for all studies. The image analysis in Paper I is separately described in the methods for Paper I.

## PET-CT protocol Paper I–IV

The scans in these studies were conducted using a Discovery MI or D690 (GE Healthcare, Milwaukee, WI, USA) PET-CT system. $^{68}$Ga-DOTATATE and $^{68}$Ga-DOTATOC were prepared according to established techniques.[59, 196, 197]

Approximately 60 min after intravenous injection of activity of 2-2.5 MBq/kg (minimum administered activity 100 MBq and maximum 300 MBq), a PET-CT scan from the mid-thigh to the base of the skull was performed. The PET acquisition time varied from 3.0 to 3.25 min per bed position. In 2019, with the approval of SomaKit TOC[65] by European Medicines Agency there was a shift in production from $^{68}$Ga-DOTATATE to $^{68}$Ga-DOTATOC. Hence, both tracers are included in Papers II–IV.

Images were initially reconstructed using BSREM (Q.Clear) with a beta value of 700, which later was changed to 900 during 2020 (Discovery MI) or OSEM with three iterations, 12 subsets, and a 5-mm Gaussian post-processing filter (Discovery 690). Time-of-flight and point-spread function correction were applied for both PET-CT systems.

If there were no contraindications for intravenous contrast, most examinations included a diagnostic CT with oral and intravenous contrast. According to our protocol, a low-dose CT was performed instead of a diagnostic CT if this had been administered 4-6 weeks before the PET-CT examination, provided that no major treatments, such as surgery, had been applied in the interim. For the diagnostic CT, the acquisition was executed in helical mode using 100 kV, 120–240 mA, and a noise index of 14 for the liver series, whereas 100 kV, 80–450 mA, and a noise index of 40 were used for the neck-thorax-abdomen series.

# Image analyses Paper II–IV

Images were analysed by an experienced nuclear medicine physician and a radiologist in the clinical setting. A PhD student in nuclear medicine/senior radiology resident (AG) and an experienced nuclear medicine physician (ET) carried out the retrospective segmentation of tumours in consensus using the Hermes software (Hermes Medical Solutions, Stockholm, Sweden) in Paper II. In Paper III, segmentation was performed separately by two physicians (AG as Reader A and ground truth, and KV as Reader B). In Paper IV, AG (by then a radiologist and resident in nuclear medicine) performed the segmentation.

^{68}Ga-DOTATATE or ^{68}Ga-DOTATOC uptake was considered significant for tumour segmentation if it did not correspond to physiological uptake. All lesions with ^{68}Ga-DOTATATE or ^{68}Ga-DOTATOC uptake were registered with measurements of SUVmax, SUVmean, and two volumetric parameters: somatostatin receptor-expressing tumour volume (SRETV), measured in ml, and total lesion somatostatin receptor expression (TLSRE). Specifically, SRETV was defined as the tumour volume having uptake exceeding 50% of SUVmax within a VOI. TLSRE, on the other hand, was defined as the product of SRETV and the SUVmean of the tumour volume. Manually drawn VOIs were sometimes necessary to circumvent the high normal background uptake in the liver.[91] These VOIs were rendered in axial, coronal and sagittal projections, as shown in Figure 16.
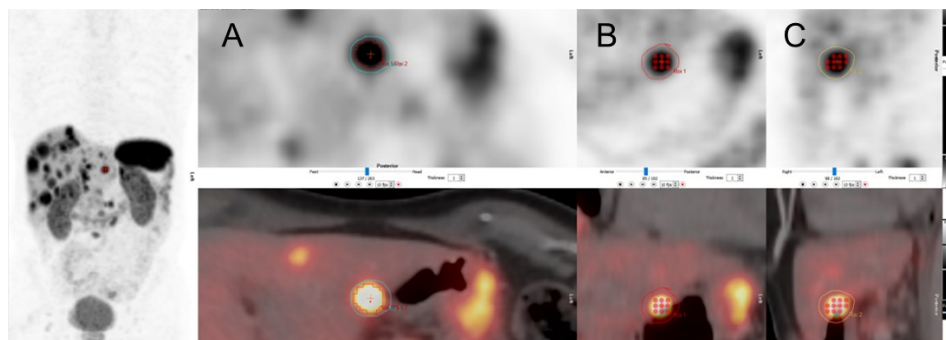


**Figure 16. Illustration of the segmentation in three planes**
Illustration of manually drawn VOIs around a liver metastasis in three planes – axial (A), coronal (B) and sagittal (C). The volume obtained using the semiautomatic method of delineating 50% of SUVmax is illustrated with a red ring in (A) and dots in (B) and (C).

Overlapping tumour volumes were avoided. In the case of confluent uptake from closely related lesions or very complex lesions with irregular uptake, manually drawn VOIs were required to exclude adjacent lesions' uptake or increase the accuracy of the volumes obtained. Within the VOI an irregular tumour volume with voxels higher than 50% of SUVmax was automatically generated. The sum of all

SRTEV and TLSRE were calculated and defined as whole-body SRETV (**SRETVwb**), and whole-body TLSRE (**TLSREwb**) respectively.

# Paper I

## Patients

The Gapetto-trial was a prospective, observational study, with all patients coming from the departments of Surgery and Oncology at Skåne University Hospital. The inclusion criteria were:

- Age $\geq$ 18 years.

- Written informed consent.

- Fulfilled at least one of the following criteria from imaging with ^{68}Ga-DOTATATE PET-CT:

    o Re-evaluation of a previously diagnosed, histologically verified NET, with ongoing treatment with a long-acting somatostatin analogue.

    o Under evaluation for suspected NET and probable to initiate long-acting somatostatin analogue treatment within a year.

The only exclusion criteria were pregnancy or breastfeeding.

## Methods

The initial ^{68}Ga-DOTATATE PET-CT scan was scheduled shortly after the patient was included in the trial. Upon inclusion, the location of the primary tumour, the tumour grade, and whether the patient had received treatment with a long-acting somatostatin analogue (including dosage and interval), were all recorded. On the same day that the patients arrived for their PET-CT imaging, they reported whether they had been treated with the long-acting somatostatin analogue and the number of days since their last injection. As this was an observational study, no specific interval was established between the PET-CT examinations or between the last dose of long-acting somatostatin analogue and the imaging.

A clinical evaluation was completed by the responsible physician after the ^{68}Ga-DOTATATE PET-CT examination, with medication and treatment plan details recorded. For patients undergoing multiple PET-CT examinations, a new clinical evaluation was performed after each PET-CT. The disease status was then categorised as regressing, progressing, or stable. This comprehensive evaluation

was based on the clinical examination, tumour markers, and morphology. Information on changes in the extent of uptake in the PET images was not used in determining the disease status.

*Image analyses*

Images were analysed by a qualified nuclear medicine physician. In all scans, the SUVmax of the normal liver was measured in a ROI, where normal liver parenchyma could be measured, avoiding large blood vessels. If multiple tumour lesions were present, the SUVmax of the five lesions with the highest SUVmax were recorded. During each examination, the general location of the tumours was noted, but the specific tumour size and precise location of the measured tumours were not registered.

To assess the primary objectives of the Gapetto trial, the SUVmax values in both the tumours and the normal liver tissue, in addition to the tumour-to-liver ratio, were compared:

- Before and after initiation of treatment with long-acting somatostatin analogue

- In relationship to the interval between the last dose of long-acting somatostatin analogue and imaging

An exploratory analysis was also conducted to determine if the clinical evaluation of disease status, defined as regression, progression, or stable disease, correlated with changes in the SUVmax in tumours. Median changes in SUVmax were compared across groups based on disease status at the second evaluation.

*Statistical analyses*

Descriptive statistics were used to describe the cohort. For the first aim, a Wilcoxon related-samples rank test was used, while for the additional analyses, Kruskal–Wallis tests were applied. A *p*-value less than 0.05 was deemed significant.

# Paper II

## Patients

All patients included in this study were part of a larger cohort of patients with GEP-NET who were sampled in 2019 and answered four different questionnaires concerning health-related quality of life and specific symptoms associated with NET. A total of 165 patients were incorporated in 2019.

All patients, who were alive on the 1st of September 2019, in the southern healthcare region of Sweden, with a histopathological diagnosis of well-differentiated NET (G1 and G2) originating from the gastrointestinal tract, including the pancreas (GEP-NET), were eligible for inclusion.

The exclusion criteria were:

- Non-metastasised NET

- Appendiceal NET where appendectomy was enough treatment

- Incidentally found NET during resection of an additional cancer

- Inoperable colorectal cancer with no GEP-NET origin

- Coexistent inflammatory bowel disease

Eligible patients were invited via regular mail. They received questionnaires and provided informed consent. If there was no response, a reminder letter was dispatched after a month. Patients who indicated they did not wish to participate, or those who did not respond within 2 months, were classified as non-responders.

In addition to the inclusion and exclusion criteria, patients featured in this subgroup analysis of Paper II had also participated in our ongoing validation of the PET-CT study and had given informed consent to take part. Patients were accepted if a somatostatin receptor PET-CT was conducted within a year before or after completing the questionnaires. If the PET-CT scan was performed after the questionnaires were completed and the patient began tumoral treatments, such as chemotherapy in this timeframe, they were excluded.

## Methods

*Questionnaires*

Patient health-related quality of life and symptoms was evaluated through the cancer-specific European Organisation for Research and Treatment of Cancer questionnaire (EORTC) QLQ-30 and QLQ-GI.NET21.[159] The submitted questionnaires were analysed as per the EORTC reference manual, which transforms the answers into linear scales; 100 represents optimal function or high quality of life.[198] A summary score for health-related quality of life was calculated using the EORTC QLQ-30.[160]

*Medical information*

Medical information, including primary tumour site, presence of distant metastasis/residual tumour, Ki-67 index at diagnosis, and tumour grade were recorded. Additionally, details about pre-existing diseases, prior tumour resections, treatments with somatostatin analogues, interventions for bowel symptoms (such as

diarrhoea or obstipation), levels of urine 5-HIAA, chromogranin A levels, the time elapsed since diagnosis, along with ongoing or previous treatments with PRRT or chemotherapy, were also documented.

*Statistical analyses*

Simple linear regression analyses were conducted to explore the relationship between the QLQ-C30 summary score and SRETVwb and TLSREwb, respectively. Given that the dispersal of SRETVwb and TLSREwb was skewed, these variables were transformed into their natural logarithms recorded as logSRETVwb and logTLSREwb. To accommodate potential confounders, multiple regression analyses were carried out, adjusting for patient and disease-related factors like age, Charlson Comorbidity Index score, and somatostatin analogue treatment.

The secondary aim was evaluated using a Pearson correlation table, associating tumour volume, both total and at specific sites, with typical NET-associated symptoms (QLQ-C30: fatigue, nausea/vomiting, pain, appetite loss, diarrhoea, and QLQ-GI.NET21: endocrine symptoms, gastrointestinal symptoms, weight loss, muscle/bone pain). A cut-off of r > 0.2 was selected to distinguish weak correlation from no correlation.[199]

# Paper III

## Patients

Patients aged 18 years and older who underwent a clinically indicated somatostatin receptor PET-CT between August 2017 and December 2021 and were included in our PET-CT validation study, were eligible for retrospective image analysis. Out of 848 participants, a subset of 200 were randomly selected for further analysis. Predetermined exclusion criteria included inclusion in Paper IV, incomplete examination, or large extravasation or radiopharmaceuticals outside the patient, such as urine. As segmenting tumours is a time-consuming process, it was not feasible to include all patients. For the test group, clinical data on histopathological diagnosis, Ki-67, type of previous or ongoing treatment, and TNM stage were verified by reviewing the patient's digital medical record.

## Methods

The training dataset for the AI model consisted of PET-CT images, annotated with labels in the form of segmented tumours, which are detailed in the "Image Analyses Paper II–IV" chapter.

The AI model was based on a UNet3D CNN architecture, equipped to process four types of input:

- CT patch

- SUV patch

- Organ mask patch

- SUV ratio patch represents the pixel SUV ratio to the nearest local maximum.

The latest patch was designed to facilitate thresholding at 50% of the lesion SUVmax, as applied during the segmentation of the tumours.

The dataset was randomly divided into training, validation, and test sets (Figure 15). The number of patients was set at 17% for testing, 17% for validation, and the remaining percentage for training. Figure 17 illustrates the UNet3D CNN architecture used in the study.
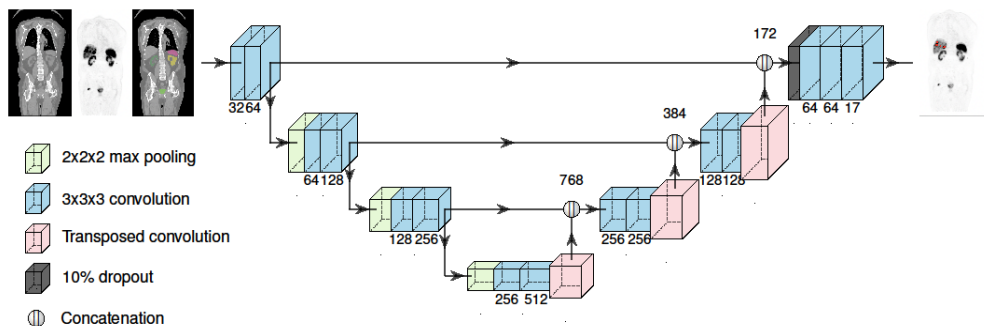


**Figure 17. Illustration of the UNet3D architecture**

The UNet3D CNN was trained using the programming and coding languages Python and C++, in conjunction with TensorFlow, a platform for developing and implementing machine learning algorithms. Training a CNN necessitates providing the network with a sequence of image patches; in this study, these patches were 25x25x25 cm in size. The input patches underwent augmentation via rotations of −0.15 to 0.15 radians, scaling of -10 to 10%, and intensity shifts of -100 to +100 HU for the CT images. Given that tumours constitute a much smaller portion of all pixels in the images than non-tumours pixels, it is crucial to supply the network with patches containing tumours more frequently than by pure chance. The only executed post-processing technique involved the automatic removal of lesions less than 0.05 ml in volume, as these were often identified as false positives in the validation group.

Reader A segmented the ground truth dataset with annotated tumours and the test set. For comparison, another physician, Reader B, also segmented tumours in the test group. We referred to connected components as lesions. We evaluated total tumour burden as SRETVwb and TLSREwb.

*Statistical analyses*

A lesion that partially or fully overlapped with the reference segmentation (AI model or Reader A or Reader B) was classified as a **true positive lesion**. Conversely, a lesion segmented with no overlap with the reference segmentation was categorised as a **false-positive lesion**. Finally, a lesion present in the reference segmentation but not segmented by the AI model (or by the other reader) was labelled as a **false negative lesion**. It is impossible to define true negative lesions not segmented and not detected, which is why they were excluded from the analysis. Sensitivity was computed at the lesion detection level, representing the percentage of detected lesions compared to reference segmentation. The **positive predictive value** was determined as the percentage of true positive lesions divided by the sum of true positive and false-positive lesions, relative to the reference.

The calculations for true positives, false positives, and false negatives, as well as SRETVwb and TLSREwb, were compared between the readers and the AI model. The correlation was evaluated using Spearman rank correlation. A Bland-Altman plot was used to visually assess the levels of agreement.

# Paper IV

## Patients

All adults aged 18 and over who began treatment with ^{177}Lu-DOTATATE at Skåne University Hospital between December 1, 2018, and October 22, 2021, were retrospectively assessed for inclusion. Patients were excluded if they did not have a PET-CT conducted less than 6 months before treatment, if they had a tumour other than GEP-NET, or if ^{177}Lu-DOTATATE therapy other than the standard four cycles with 7.4 GBq was planned. Two additional patients were excluded, one due to surgery between the PET-CT and PRRT, and one due to non-compliance with treatment. Follow-up visits, as well as PET-CT and CT examinations, were performed in a clinical setting, customised based on patient needs. Patient characteristics were gathered by examining the patient's digital medical records.

## Methods

$^{177}$Lu-DOTATATE was administered according to institutional guidelines, with four planned cycles at 8-week intervals. On day four after the first treatment cycle, a SPECT-CT was acquired for kidney dosimetry and evaluation of tumour uptake. Each patient's tumour burden was manually quantified at baseline using a somatostatin receptor PET-CT and the semi-automatic method described earlier. For a subgroup of 25 patients who underwent a follow-up PET-CT, changes in tumour burden were assessed. Tumour burden was defined by measures including SRETVwb, TLSREwb, the diameter of the largest tumour lesion, and the tumour lesion with the highest SUVmax. The mean tumour absorbed dose was calculated from the SPECT-CT images taken after the first treatment cycle. As part of the exploratory aim, the AI model developed in Paper III was used to compare tumour burden segmentation with manual tumour segmentation.

Post-treatment outcomes were evaluated using progression-free survival and overall survival. Progression-free survival was defined as the duration from the start of PRRT to radiological or clinical progression. We evaluated overall survival as the time to death for any reason. Patients were observed until the date of disease progression, death, or until March 30, 2023.

### Statistical analyses

Kaplan-Meier survival curves and the log-rank test were employed to compare progression-free survival and overall survival among the different groups. Univariate Cox regression analyses were performed to examine the relationship between manual measurements of tumour burden, mean tumour absorbed dose, and their correlation with progression-free survival and overall survival. The correlation between tumour burden and mean tumour absorbed dose was evaluated using a scatter plot and a Spearman rank correlation 2-tailed test. The relative change in tumour burden from the first follow-up PET-CT was assessed in three subgroups: a decrease of $\geq 30\%$, stable or an increase of $\geq 20\%$. The correlation between manual measurements and AI model measurements of tumour burden was analysed with a scatterplot and a Spearman rank correlation 2-tailed test. Bland-Altman plots were used to visually represent the levels of agreement.

# Ethical considerations

**Paper I** was conducted as a prospective, single-centre, observational study, preregistered at the EU Clinical Trials Register (2012-004313-13). The study was approved by the Institutional Review Board at Lund University (2012/657), as well as the Swedish Medical Products Agency. All patients provided written informed consent before inclusion.

**Paper II** was prospective in terms of quality of life data, and was approved by the Swedish Ethical Review Authority (2019–02378). The patients included for image analyses in **Papers II and III** were adults (≥18 years) with a clinical indication for somatostatin receptor PET-CT, and they were part of a larger observational study validating PET-CT. These images had already been analysed by an experienced nuclear medicine physician and a radiologist in a clinical setting. Retrospective image analyses were conducted for the subgroups of patients included in **Papers II and III**. The study received approval from the Swedish Ethical Review Authority (2016/417, 2018/753, and 2021-05734-02). All patients gave their written informed consent.

**Paper IV** was a retrospective study, approved by the Swedish Ethical Review Authority (2019-00411 and 2021-04197). As the study was retrospective, informed consent was not required per the ethical approval.

All studies were conducted following the Helsinki Declaration.

The development of medical AI models requires meticulous ethical considerations. The imaging data was carefully pseudo-anonymized before training the AI models, following current guidelines for the management of pseudo-anonymized data.

# Results

## Paper I

The Gapetto trial, conducted between 2013 and 2016, involved 296 patients. Within this trial, a total of 530 PET-CT examinations were performed utilising ^{68}Ga-DOTATATE. Complete PET-CT measurement data were available for 262 patients, who collectively underwent a total of 495 examinations. However, specific requirements such as examinations conducted both before and after the initiation of treatment with long-acting somatostatin analogues, as well as missing clinical data for several patients led to considerable smaller numbers for subgroup analyses.
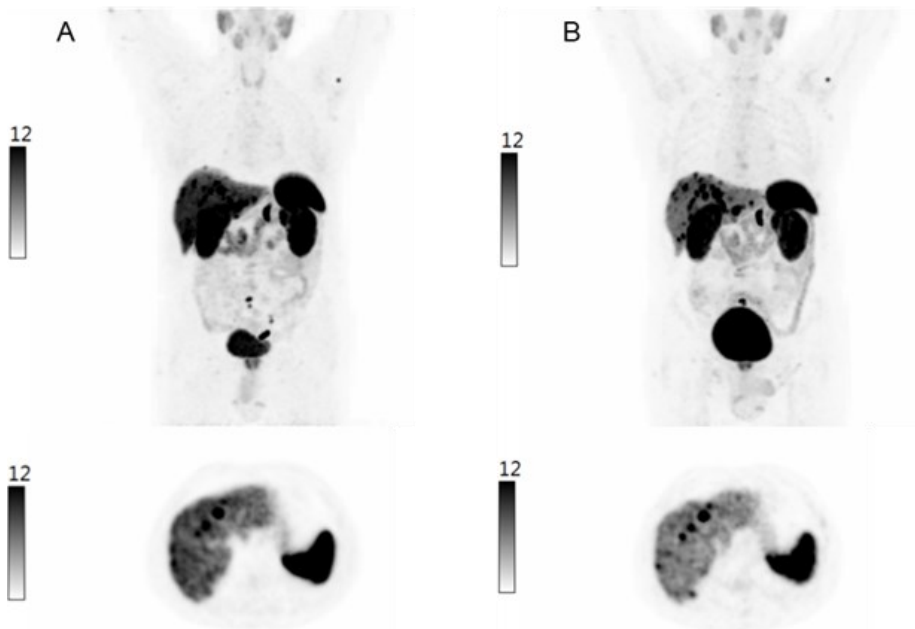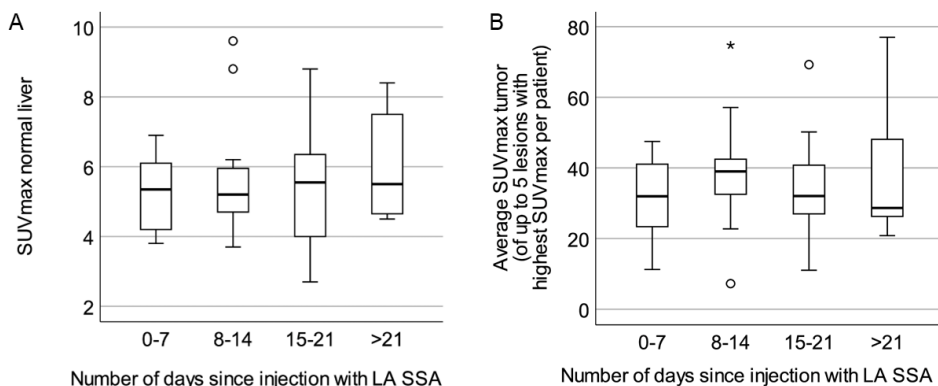


**Figure 18. Illustration of the increased tumour-to-liver ratio**
MIP-images from somatostatin receptor PET of a patient before treatment (A) and after treatment initiation with long-acting somatostatin analogue (B). This image was originally published in JNM. Gålne et al.[200] © SNMMI.

No significant change in the uptake of ^{68}Ga-DOTATATE in tumours was observed in a subgroup of 19 patients who were examined both before and after treatment commencement with a long-acting somatostatin analogue. Rather, a notable reduction in the uptake of normal liver parenchyma was recorded. This diminished uptake in normal liver parenchyma resulted in an increased tumour-to-liver ratio, which ultimately may improve the visualisation of lesions in the liver (Figure 18).

In a subset of 37 patients with stable disease undergoing treatment with long-acting somatostatin analogues, the uptake of ^{68}Ga-DOTATATE in tumours and normal liver tissues was evaluated in relation to the interval between the last treatment injection and PET-CT imaging. No significant differences were observed in tumour or liver uptakes regardless of the length of the interval (Figure 19).



**Figure 19. The uptake depending on the interval since last injection**
Illustration of the uptake in normal liver (A) and in tumours (B) depending on the interval since last injection of long-acting somatostatin analogue (LA SSA). No signifcant differences were seen. This image was originally published in JNM. Gålne et al.[200] © SNMMI.

In a subset of 41 patients, the exploratory analysis suggested significant differences in the changes in ^{68}Ga-DOTATATE uptake within tumours. These changes differed depending on whether the disease status was evaluated as a progressive, stable disease, or regressive. However, there was a wide distribution among the different groups with some overlapping changes in SUVmax (Figure 20).
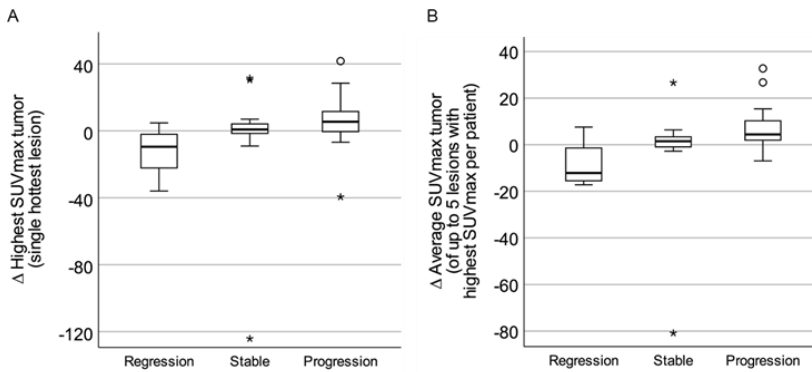
**Figure 20. Differences in the uptake in relation to disease status**
The differences in in the uptake between two examinations is presented in relation to clinical disease status. This image was originally published in JNM. Gålne et al.[200] © SNMMI.

# Paper II

In September 2019, invitations were sent to 245 patients with a histopathological diagnosis of well-differentiated GEP-NET (G1 and G2) to participate in a study on quality of life. Of these, three patients declined, ten were excluded due to an unknown address and 67 did not respond. Ultimately, 165 patients responded yielding a response rate of 67%. Among these 165 patients, 73 had confirmed metastatic disease and had undergone a PET-CT scan within a year of the questionnaires. However, one patient was excluded due to starting new chemotherapy treatment between the questionnaires and the PET-CT scan, and another patient declined to participate in the PET-CT study.

A total of 71 patients were included to evaluate their health-related quality of life relative to tumour burden, assessed via somatostatin receptor PET-CT.

The mean age in the cohort was 69.8 years, with 60% being male. On average, patients had been diagnosed 5.5 years prior, with 82% currently undergoing somatostatin analogue treatment. The majority, 79% were in stage IV of the disease, with distant metastases. The cohort's mean summary score for health-related quality of life was rather high, at 82.3 (standard deviation 14.4). However, 18 patients (25%) rated their global quality of life as less than or equal to 50. In the areas of social, emotional, and role functions, 13, 10 and 10 patients respectively rated their score as less than or equal to 50.

The summary scores for health-related quality of life across different patient tumour volumes are depicted in Figure 21.
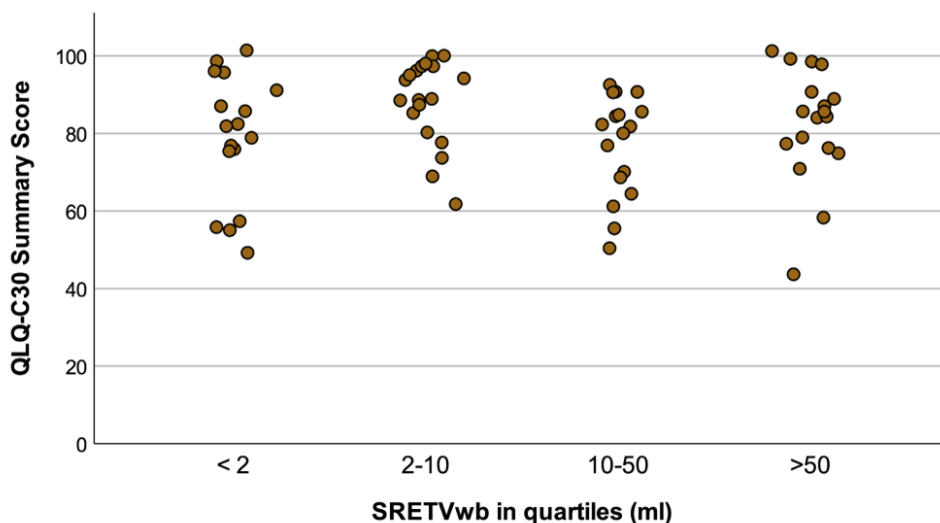
**Figure 21. Scatterplot of the quality of life summary score for different tumour volumes**
Somatostatin receptor-expressing tumour volume (SRETVwb) for all patients categorised in quartiles

The most severe symptoms, rated as scores below 50, were diarrhoea (24 patients), disease-related worries (25 patients), and muscle/bone pain (16 patients). Other fairly common severe symptoms included impaired social functioning (17 patients), fatigue (13 patients), and dyspnoea (nine patients).

The distribution of tumours is presented in Table 9, in which the liver was the most common location for metastases and the location with the highest tumour burden.

**Table 9. Distribution of the tumours and volumes**
The distribution of the location of tumours and the respective tumour volume (SRETVwb)

| Tumour distribution | n (%) | Median SRETVwb, ml (IQR) |
|---|---|---|
| Liver | 40 (56.3) | 18.8 (10.6–112.7) |
| Pancreas | 15 (21.1) | 1.7 (0.7–3-7) |
| Mesenteric lymph nodes | 36 (50.7) | 1.6 (0.7–4-3) |
| Gastrointestinal tract | 9 (12.7) | 1.4 (1.0–3.3) |
| Other lymph nodes | 31 (43.7) | 1.4 (0.5–4.8) |
| Skeletal metastases | 17 (23.9 | 1.2 (0.8–6.9) |
| Other | 13 (18.3) | 2.4 (1.3–4.2) |

Neither the simple linear regression between SRETVwb and the health-related summary score nor multiple linear regression – with adjustment for age, comorbidity, and treatment with a somatostatin analogue – demonstrated any correlation between the variables. Sensitivity analyses that excluded patients who had undergone extensive surgery with pancreaticoduodenectomy or those with a gap

of more than 6 months between completing the questionnaires and undergoing the PET-CT, did not alter the results.

The symptoms that troubled most patients, including diarrhoea and muscle/bone pain, displayed weak associations with increased SRETV in various anatomical locations. Diarrhoea correlated with tumour volume in the gastrointestinal tract (r = 0.31), liver (r = 0.28) and unspecified sites (r = 0.25). Meanwhile, muscle/bone pain had a weak correlation with tumour volume in the mesenteric lymph nodes (r = 0.20) but showed no correlation with skeletal metastases (r = -0.08). The total tumour volume, SRETVwb, indicated a weak positive correlation with dyspnoea (r = 0.21), diarrhoea (r = 0.23), and endocrine dysfunction (r = 0.33).

# Paper III

Out of the 200 patients who underwent a clinically necessary somatostatin receptor PET-CT and were selected for this study, 22 patients were excluded based on predetermined criteria. The study ultimately included 178 patients, whose somatostatin receptor-expressing tumour burden were subsequently segmented. The training and validation set featured PET-CT scans from 148 patients, with 118 scans used for training and 30 scans for validation. Somatostatin receptor-avid tumour lesions were segmented in 108 patients, while 40 patients did not have any somatostatin receptor-avid tumours. In the training and validation set, the radiopharmaceutical $^{68}$Ga-DOTATATE was used in 44 examinations and $^{68}$Ga-DOTATOC was used in 104 examinations. The test group consisted of 30 patients, 25 of whom had pathological uptake and five who showed no pathological uptake on the PET-CT. Before the PET-CT, 23 patients had an established diagnosis of neuroendocrine neoplasia, and four patients received their final diagnosis after the PET-CT. Three patients had no verified NET and showed no pathological uptake.

## Performance of the AI model

Of the 25 patients with somatostatin receptor-avid tumours, the AI model accurately classified 24 of these as tumour-positive (true positive). Additionally, out of the negative PET-CT examinations, the AI model correctly classified three out of five as negative (true negative). In contrast, Reader B properly identified 24 patients as true positives and five as true negatives with one patient being misclassified as a false negative.

Reader A (ground truth) segmented a total of 267 lesions with a median of three lesions per patient, ranging from 0 to 58 lesions; the median SRETVwb was 6.8 ml. Reader B segmented a total of 269 lesions with a median of 2.5 lesions per patient, and a median SRETVwb of 6.5 ml. The AI model segmented a total of 265 lesions,

with each patient having a median of 3.5 lesions and a median SRETVwb of 4.7 ml. The quantities of true positive, false positive and false negative lesions are presented in Table 10 for each reader and the AI model.

**Table 10. Classification of lesions**
Number of lesions which are true positive, false positive and false negative are presented for the AI model, Reader B and Reader A. Values are presented as total number of lesions, median number of lesions per patient with interquartile range (IQR). Sensitivity and positive predictive values (PPV) are presented last.

| | AI model vs. Reader A | AI model vs. Reader B | Reader B vs. Reader A |
|---|---|---|---|
| **True positive lesions** | | | |
| Total | 214 | 210 | 246 |
| Per patient (IQR) | 2 (0.0-12.0) | 1 (0.0-12.0 | 2.5 (1.0-14.5) |
| **False positive lesions** | | | |
| Total | 45 | 41 | 25 |
| Per patient (IQR) | 1 (0.0-2.3) | 1 (0.0-2.0) | 0.0 (0.0-1.3) |
| **False negative lesions** | | | |
| Total | 53 | 59 | 21 |
| Per patient (IQR | 1 (0.0-2.0) | 1 (0.0-3.3) | 0.0 (0.0-1.0) |
| **Sensitivity (%)** | 80 | 79 | 92 |
| **PPV (%)** | 83 | 84 | 91 |

The correlations between the AI model and the readers showed similarities for both SRETVwb and TLSREwb, as represented in the scatterplots comparing the AI model and Reader A (Figure 22A and 22B). Nevertheless, the correlation between Reader A and B exhibited a higher level (Figure 22C and 22D).
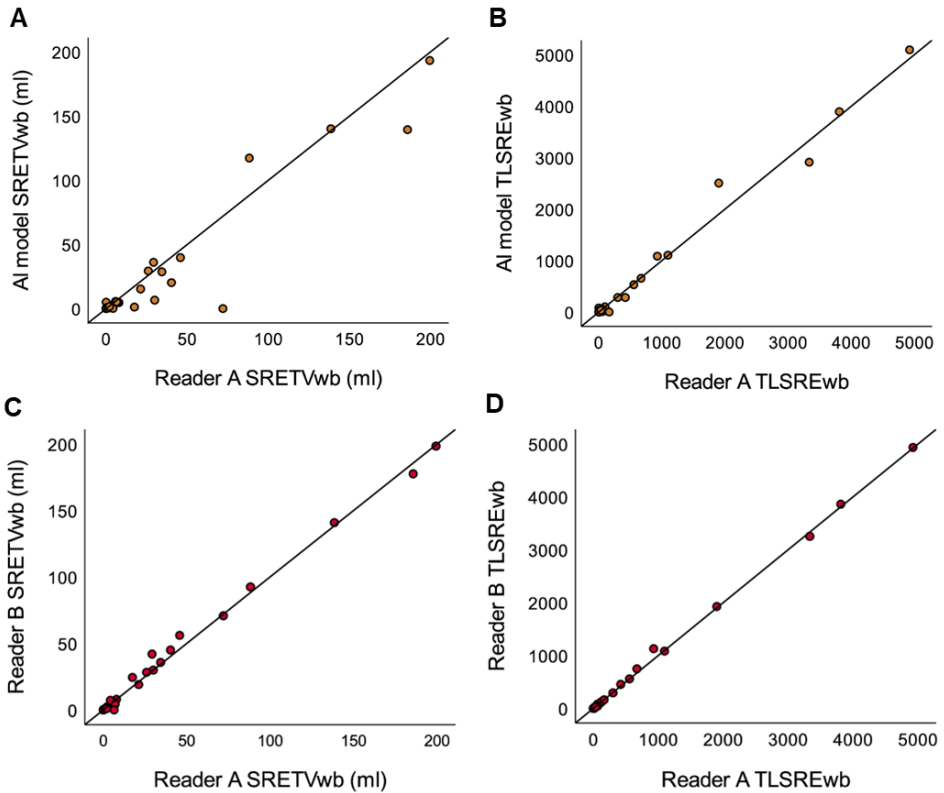
**Figure 22. Scatterplots of measurements of SRETVwb and TLSREwb**
The scatterplot in A compares the measurement of whole-body somatostatin receptor-expressing tumour volume (SRETVwb) obtained by the AI model with those obtained by Reader A ($r = 0.78$, $p<0.001$), respectively whole-body total lesion somatostatin receptor expression (TLSREwb) in B ($r = 0.83$, $p<0.001$). Scatterplots of Reader B versus Reader A showing the correlation for SRETVwb in C ($r = 0.96$, $p< 0.001$) and TLSREwb in D ($r = 0.99$, $p< 0.001$). Line of identity in figures.

The AI model experienced issues with the segmentation of mediastinal lesions and lesions with low uptake, as depicted by the outliers in Figure 22A. However, the accuracy of TLSREwb proved superior, as seen in Figure 22B, because it was less affected by lesions with low uptake or small volume. More specifically, TLSREwb, represents the sum of all SUVmean*lesion volume (ml) products which made it more robust against small or low uptake lesions. Most examinations presented high agreement, with some excellent examples of AI model segmentation shown in Figure 23.
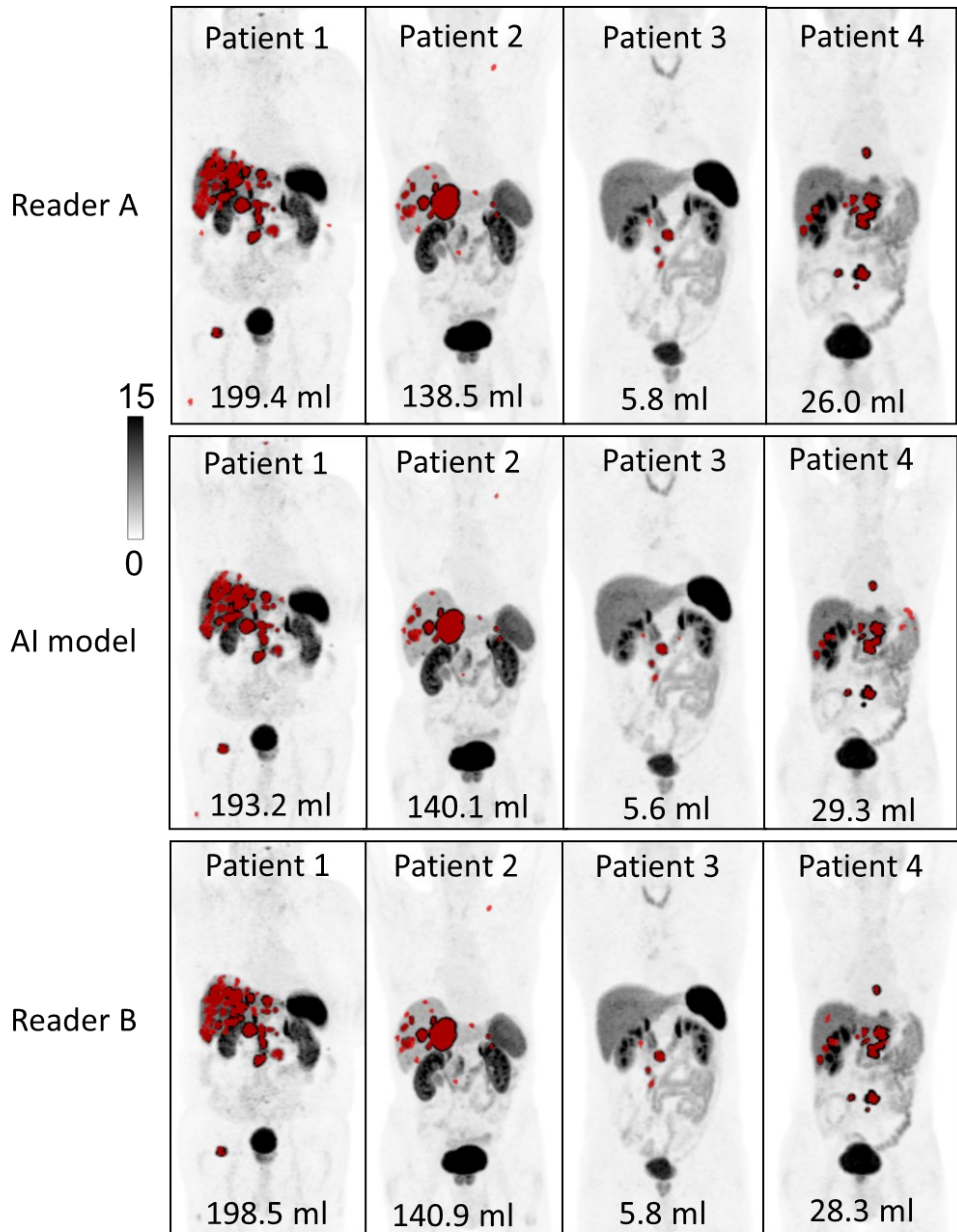
**Figure 23. Examples of tumour segmentation in four patients**
MIP-images from four patients, illustrating some of the excellent AI model segmentations compared to those of Reader A and B.

# Paper IV

A total of 31 patients with GEP-NET were included in this analysis. The median follow-up time was 21.4 months. During the study, 22 patients experienced radiological or clinical progression of the disease with a median time to progression of 17.2 months. In contrast, nine patients without progressive disease had a median follow-up of 28.7 months. Nine patients died during the study, all of whom had progressive disease. The time elapsed since diagnosis to the start of PRRT was a median of 2.5 years, and the median age at the start of treatment was 70 years. Nine patients had a tumour grade of G1, 18 patients were diagnosed as G2 and 3 patients as G3. Out of all 31 patients, 27 received all four treatments, two patients received three cycles of treatment, and two patients completed only two cycles due to disease progression or side effects. The median number of days between the baseline PET and the first cycle of PPRT was 73 days. Twenty-five patients were examined with a follow-up PET-CT, and the median number of days between the follow-up PET and the final PRRT was 53 days. SPECT-CT data were available for 29 patients. The SPECT-CT was acquired after the first cycle of PRRT and was used to estimate the mean tumour absorbed dose.
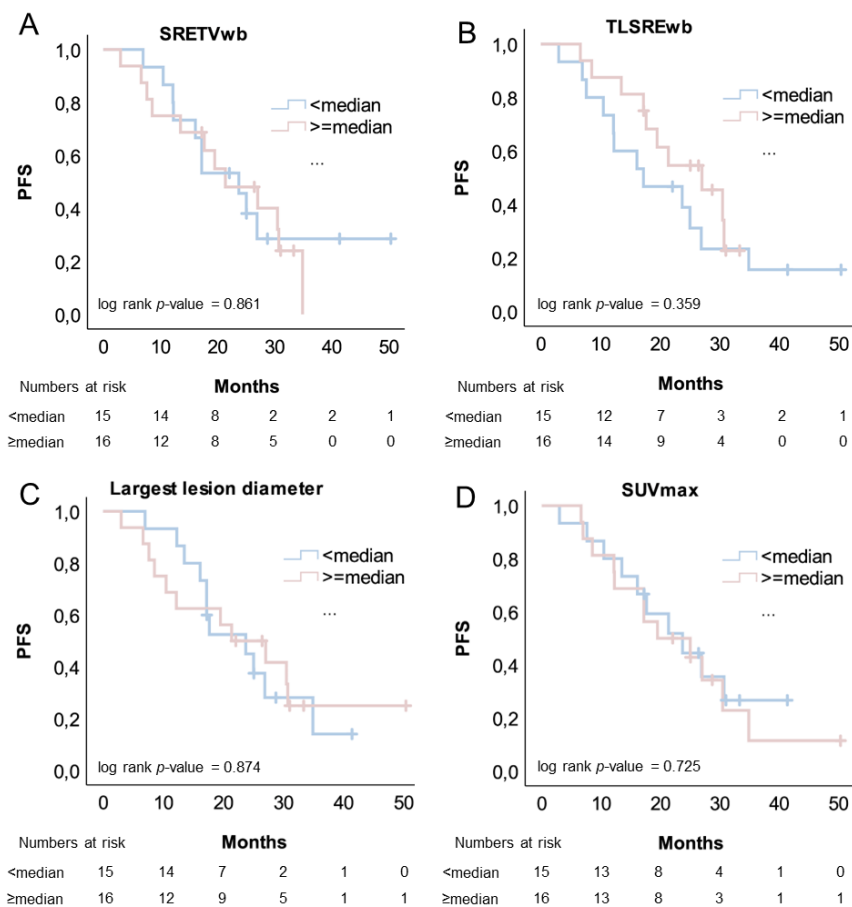
## Tumour burden

The tumour burden at baseline PET-CT (31 patients) and the first follow-up (25 patients) is presented in Table 11.

**Table 11. Tumour burden**
The tumour burden parameters at baseline and follow-up

| Quantification of tumour burden | Manual measurement | Missing |
|---|---|---|
| Baseline PET-CT | | |
|   SRETVwb, ml (IQR) | 132 (61 - 302) | |
|   TLSREwb (IQR) | 3684 (1522 - 5669) | |
|   Largest lesion diameter, mm (IQR) | 77 (44 - 101) | |
|   SUVmax (IQR) | 50 (26 - 82) | |
| Follow-up PET-CT | | 6 |
|   SRETVwb, ml (IQR) | 71 (36 - 278) | |
|   TLSREwb (IQR) | 2251 (647 - 3796) | |
|   Largest lesion diameter, mm (IQR) | 73 (35 - 114) | |
|   SUVmax (IQR) | 41 (22 - 61) | |
|   Relative change SRETVwb % (IQR) | -26 (-49 - 4) | |
|   Relative change TLSREwb % (IQR) | -35 (-72 to -14) | |
|   Relative change largest lesion diameter % (IQR) | -9 (-20 - 3) | |
|   Relative change highest SUVmax % (IQR) | -26 (-39 to -12) | |

In the initial PET-CT, none of the measurements – SRETVwb, TLSREwb, largest lesion diameter or SUVmax – exhibited any predictive value for progression-free survival after treatment with ^{177}Lu-DOTATATE PRRT when they were subgrouped by their median values (Figure 24).



**Figure 24. Kaplan Meier curves of progression-free survival (PFS) for high or low tumour burden at baseline PET-CT**
Patients were subgrouped by the median values of, (A); SRETVwb, median of 132 ml, (B); TLSREwb, sum of all lesions SUVmean*ml, median of 3684, (C); largest lesion diameter, median of 77 mm and (D); SUVmax, median of 50.

The median value of the mean tumour absorbed dose was calculated to be 25 Gy, ranging from 7–94 Gy. The mean tumour absorbed dose showed a slight tendency toward a weak negative correlation with SRETVwb at baseline, although insignificantly (Figure 25A). As revealed in Figure 25A, no patients with a tumour burden greater than 400 ml received a mean tumour absorbed dose of more than 30

84

Gy. There was no correlation found between the mean tumour absorbed dose and TLSREwb. However, a moderately strong correlation was discovered between the mean tumour absorbed dose and the highest SUVmax in the tumours (Figure 25C).
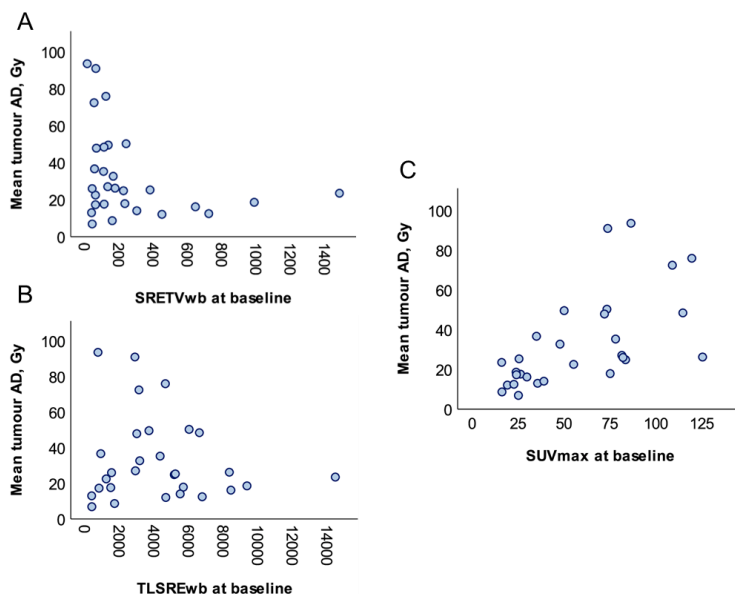


**Figure 25. Scatterplots of mean tumour absorbed dose and tumour burden**
Scatterplots of mean tumour absorbed dose (AD) and somatostatin receptor-expressing tumour volume (SRETVwb, ml) (A), total lesion somatostatin receptor expression (TLSREwb, ml*SUVmean) (B) respectively SUVmax (C) at baseline PET. Spearman rank correlation was $r$ = -0.306 $p$ = 0.106 (A), $r$ = -0.009, $p$ = 0.962 (B) and $r$ = 0.705, $p$>0.001 (C).
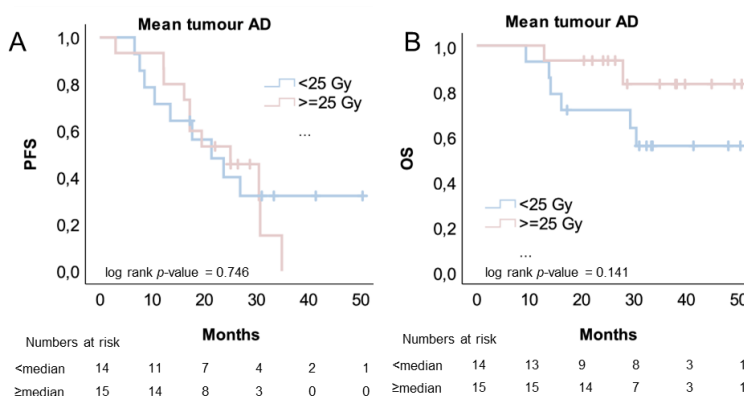


**Figure 26. Outcome for groups receiving low or high mean tumour absorbed dose**
Kaplan Meier curves illustrating no significant differences for progression-free survival (A) and overall survival (B) for groups with mean tumour absorbed dose (AD) of more or less than median (25 Gy).

When evaluating outcomes such as progression-free survival or overall survival in groups receiving above or below the median of mean tumour absorbed dose of 25 Gy, no significant differences were found. However, there was a tendency toward improved overall survival in patients receiving higher doses (Figure 26B).

Patients with a relative increase in SRETVwb, TLSREwb and the largest lesion diameter at follow-up PET-CT experienced significantly shorter progression-free survival compared to patients with stable disease or a decreasing tumour burden (Figure 27A–C). A decreased or stable SUVmax (no patients experienced an increase of more than 20%) revealed no differences in outcomes (Figure 27D).
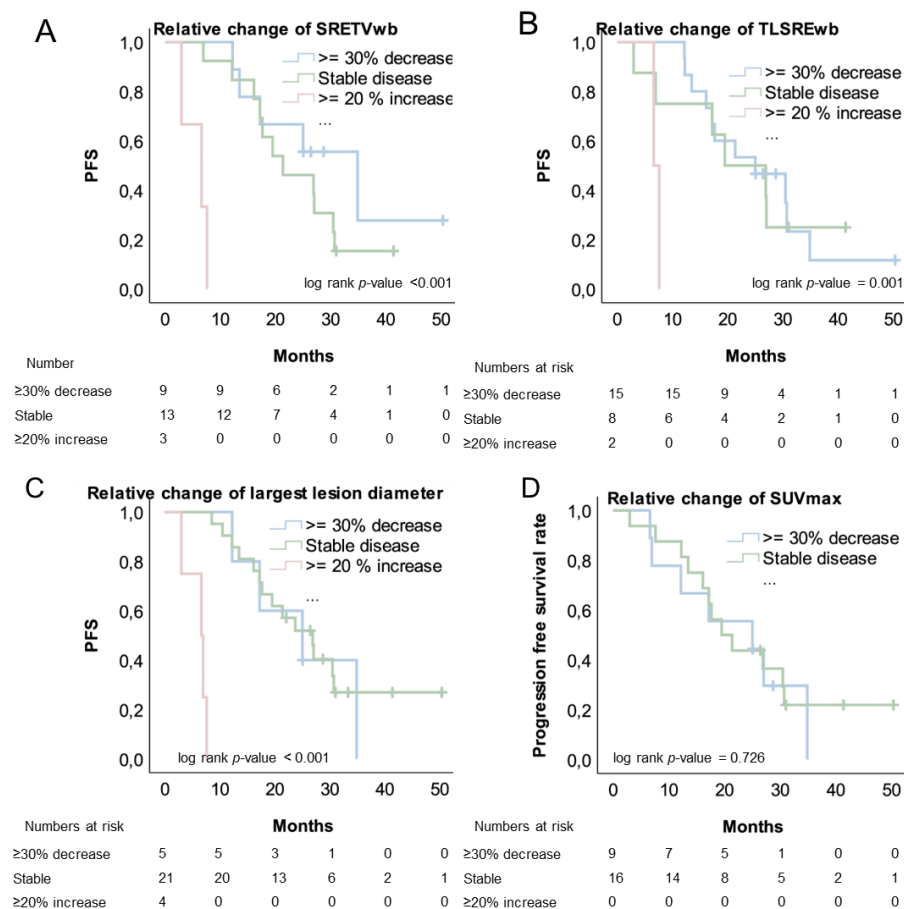


**Figure 27. Kaplan Meier curves of progression-free survival (PFS) and the relative change of tumour burden**
Kaplan Meier curves illustrating progression-free survival for different groups depending on the relative change of tumour burden at follow-up PET-CT. Tumour burden evaluted as whole-body somatostatin receptor-expressing tumour volume (SRETVwb, ml) (A), total lesion somatostatin receptor expression (TLSREwb, ml*SUVmean) (B), largest lesion diameter (C) and SUVmax (D).

When the AI model developed in Paper III was evaluated for measurements of SRETVwb and TLSREwb in this cohort, and compared with manual semi-automatic measurements, its performance was found to be inferior to that in Paper III. Specifically, the AI model failed to detect large tumours in the liver for seven patients. The Spearman rank correlation between the manual and AI model measurements was moderately strong for SRETVwb, with $r = 0.60$ and $p<0.001$, and fairly strong for TLSREwb, with $r = 0.53$ $p = 0.002$. The median SRETVwb at the baseline was calculated to be 75 ml, as compared to 132 ml for manual measurements. The levels of agreement are depicted in Figure 28.
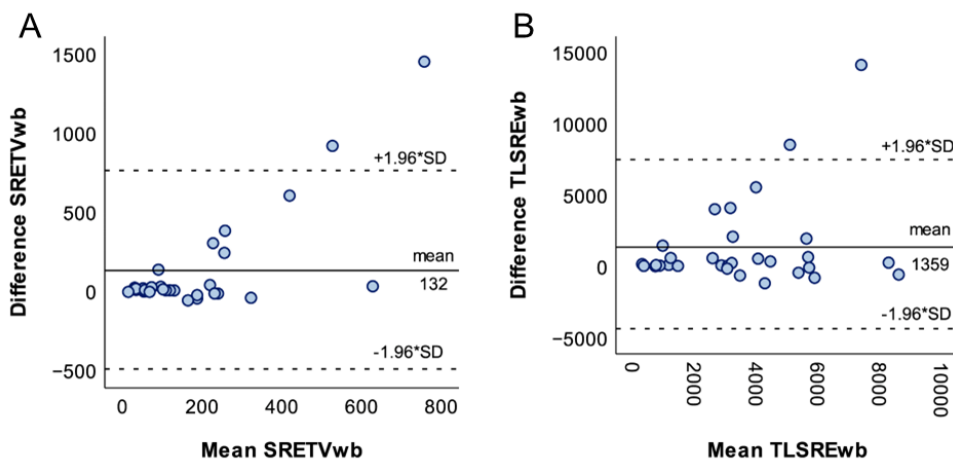


**Figure 28. Bland Altman plots**

Bland Altman plots illustrating the levels of agreement between AI model and manual measurements. Y-axis illustrates the difference, and X-axis the mean SRETVwb between AI model and manual measurements per patient.

# Discussion

## Somatostatin analogue treatment and PET-CT

Several studies have examined the relationship between long-acting somatostatin analogue treatment and the uptake of radiolabelled somatostatin analogues such as ^{68}Ga-DOTATATE or ^{68}Ga-DOTATOC in tumours and normal tissue both retrospectively and prospectively.[200-206] A common weakness in NET studies is the small sample sizes. However, a strength in determining whether somatostatin analogue treatment affects uptake at the somatostatin receptor PET-CT is the concordance all studies to date have shown in results and conclusions. The various studies evaluating aspects of ^{68}Ga-DOTATATE or ^{68}Ga-DOTATOC uptake during treatment with long-acting somatostatin analogues are presented in Table 12.

Treatment with long-acting somatostatin analogues has been proven to reduce the uptake of radiolabelled somatostatin analogues in some normal tissues such as the liver, without significantly reducing uptake in tumours (Table 12). This results in an improved tumour-to-background ratio, making tumours in the liver easier to visualise during imaging, and possibly increasing the detection of liver metastases. The reasons for these differences between tumour tissue and normal tissues remain unknown, but varying receptor internalisation and expression kinetics could partly explain this.[207, 208] The amount of circulating peptide during treatment with somatostatin analogues could also contribute to the explanation. The Uppsala group, showed in an experimental setting, that an injection of 50 µg of short-acting somatostatin analogues before the PET-CT examination resulted in a better tumour-to-normal tissue ratio than that with no pre-treatment or compared to pre-treatment with high-dose short-acting somatostatin analogues.[209] The group also investigated the uptake of ^{68}Ga-DOTATOC in four patients receiving treatment with long-acting somatostatin analogues. These patients were "pre-treated" with 400 mg short-acting somatostatin analogues and underwent three successive PET-CT examinations. These exams revealed a significantly lower uptake in both tumour and normal tissues after 1 h. However, after 4 and 7 hours, uptake in tumours was restored, but not in normal tissues, implying different receptor recycling behaviours in tumours compared to normal organs.[210]

**Table 12. Uptake at somatostatin receptor PET-CT during somatostatin analogue treatment**

Summary of studies evaluating aspects of the uptake in tumours or normal organs during treatment with long-acting somatostatin analogues when imaged with PET-CT. Significant changes are illustrated with an arrow (↑ increase or ↓ decrease), and no significant changes with an en dash (-). Long-acting somatostatin analogues (LA SSA) were used either as octreotide long-acting release (LAR) or lanreotide. Tumour to liver ratio (T/L), tumour to background ratio (T/B), Liver to background ratio (L/B).

| Study | Design and n patients | Parameters | Results |
|---|---|---|---|
| Gålne et al. 2019[200] 68Ga-DOTATATE octreotide LAR or lanreotide | Prospective. **Intraindividual** - 19 patients before and after treatment with LA SSA Interintervidual - 37 patients with LA SSA was examined by the interval since last injection | SUVmax normal liver SUVmax tumour T/L ratio | Liver↓ Tumour – T/L ratio ↑ The interval showed no signficant differences |
| Aalbersberg et al. 2019[206] 68Ga-DOTATATE lanreotide | Prospective. **Intraindividual** - 34 patients with LA SSA treatment were examined one day before and one day after injection of LA SSA | SUV max of sevaral normal tissues SUVmax tumour T/L ratio | Spleen↓ Liver↓ Tumour↑ T/L ratio↑ |
| Cherk et al. 2018[201] 68Ga-DOTATATE octreotide LAR or lanreotide | Retrospective. **Intraindividual** - 21 patients were evaluated for uptake in normal tissues and 12 patients with stable disease evaluted for uptake in tumour tissue, before and after treatment | SUVmax of several normal tissues, including liver and spleen SUVmax tumour T/L ratio | Spleen↓, Liver↓, Tumour ↑ (61% of metastatic lesions increased in SUVmax and 82% of metastatic lesions had an increase of T/L ratio) |
| Haug et al. 2011[203] 68Ga-DOTATATE octreotide LAR | Retrospective. **Interindividual** - 105 patients, comparison of 35 patients with treatment compared to 70 patients without. Intraindiviudal - 9 patients before and after treatment | SUVmax of several normal tissues including liver and spleen SUVmax tumour | Spleen↓, Liver↓ Tumour – no significant differences between the two groups or before and after treatment |
| Ayati et al. 2018[202] 68Ga-DOTATATE octreotide LAR | Retrospective. **Intraindivual** - 30 patients. Before and after treatment | Comparison of SUVmax and SUV mean in tumours and normal tissues | Spleen↓, Liver↓ Tumours - no significant differences |
| Chahid et al. 2023[204] 68Ga-DOTATATE octreotide LAR or lanreotide | Retrospecitve. **Interindividual** - 165 patients. Comparsion of 77 patients with treatment and 115 patients without treatment | Comparison of SUVmax ratios: T/B, L/B and T/L | Significant higher T/L and T/B but no signfiant difference for L/B for patients with treatment compared to those without |
| van de Weijer et al. 2024[205] 68Ga-DOTATOC lanreotide | Retrospective. **Intraindividual** - 35 patients. Before and after treatment at repeated examinations and the interval since injection of LA SSA | Comparison of SUVmax and SUVmean from tumours, normal tissue and blood pool | Blood pool ↑, Spleen↓, Liver↓ Tumours - no significant differences SUVmax in blood pool was higher for patients receiving the treatment within 5 days before the PET scan |

The concern that long-acting somatostatin analogue treatment could impair the diagnostic capability of somatostatin receptor PET-CT may not be necessary. Current guidelines from 2023 still suggest a 3–4 week interval post-administration of long-acting somatostatin analogues before PET-CT, to avert possible receptor blockade.[60] Considering all aforementioned studies, which account for different aspects of imaging the biodistribution of $^{68}$Ga-DOTATOC or $^{68}$Ga-DOTATATE during treatment with short or long-acting somatostatin analogues, this could be an overly conservative approach. Despite there being variations in biodistribution when comparing intraindividual imaging with or without long-acting somatostatin analogues, these variations primarily originate from the notable change in normal tissue uptake. Although, slight variations depending on the time since injection cannot be ruled out, even though neither our study nor the one by Van de Weijer et al. demonstrated significant differences in tumours based on injection interval.[200, 205] Instead, Van de Weijer et al. reported a significantly higher uptake in the blood pool if the injection time was less than 5 days and a significant correlation between the blood-pool uptake and the tumour and organ uptake.[205] Given the limited size of both studies, small variations in the tumour uptake based on the time since injection cannot be disregarded. Absolute comparison of SUV in tumours should still be treated with caution as various factors could influence the uptake. However, in conclusion, it seems reasonably safe to say that patients do not need to delay imaging with somatostatin receptor PET-CT commencing important treatment with long-acting somatostatin analogues. It has been demonstrated in several studies that the tumour-to-liver ratio significantly increases, potentially improving detection of liver metastases.

Interestingly, the decreased uptake of $^{68}$Ga-DOTATOC or $^{68}$Ga-DOTATATE in normal tissues during treatment with long-acting somatostatin analogues, while maintaining similar uptake in tumours, along with the antiproliferative effects of these analogues, could influence treatment strategies. The combination of long-acting somatostatin analogues and PRRT could potentially improve tumour control[211] and theoretically lessen the absorbed dose to normal tissues. In the NETTER-1 study, comparing high-dose long-acting somatostatin analogues (60 mg) with $^{177}$Lu-DOTATATE, patients in the $^{177}$Lu treatment group received a 30 mg dose of the long-acting somatostatin analogue 4 h after each cycle, and repeated in between $^{177}$Lu-DOTATATE-infusions. However, this regimen is not always followed and sometimes only $^{177}$Lu-DOTATATE treatment, without concurrent somatostatin analogue therapy, is provided.

No prospective study has analysed the effect of combining long-acting somatostatin analogues with PRRT compared to using PRRT alone. A retrospective study examined the survival and response rates in patients treated with either long-acting somatostatin analogues in conjunction with PRRT or as maintenance therapy following PRRT, compared to those receiving PRRT alone.[211] The results suggested better outcomes for patients receiving the analogues.[211] However, to prevent

potential interference of the somatostatin receptor with PRRT, patients discontinued injections of long-acting somatostatin analogues 4–6 weeks before PRRT.[211]

A prospective study considered the initiation of long-acting somatostatin analogues post-PRRT in patients who demonstrated disease control.[212] It found no outcome benefits for those patients receiving the analogues compared to those not receiving them.[212] It is evident that our understanding of the added value of combining long-acting somatostatin analogues with PRRT or determining the optimal interval for injections of the analogues in relation to PRRT remains limited.

# Health-related quality of life and tumour burden

When treating patients with metastasised NET, the self-reported quality of life gains importance, as the likelihood of cure is low, the projected survival time may be prolonged, and enhanced quality of life is a crucial treatment outcome. We noticed worthiness in studying the association between the total tumour burden in patients with GEP-NET and their health-related quality of life since no prior studies have undertaken this exploration.

Theoretically, a large neuroendocrine tumour burden could impact various aspects of health-related quality of life. An increased volume of hormone-producing tumours, such as functioning NETs, could exacerbate hormone-related symptoms. In addition, a larger tumour burden is more likely to cause symptoms related to tumour location, such as pain, gastrointestinal obstruction, or other symptoms, by interfering with normal organ function or homeostasis. Surgery aimed at reducing the tumour load could be beneficial even if a cure is not possible and is sometimes applied when NET-symptoms cannot be controlled through medication. Presumably, patients may gradually adapt to symptoms from these typically slow-growing tumours, as they might "get used" to their tumour burden and symptoms.

Indeed, our findings in Paper II revealed no significant correlation between tumour volume and the health-related quality of life summary score. Several conceivable reasons could explain these results. First, as questionnaire completion is voluntary, a self-selection bias may occur, where only certain patients choose to respond, potentially influencing the outcomes. Similar to other survey studies,[213] only 67% of the patients returned the forms, resulting in a 33% non-response rate. We were unable to access the medical records of the non-participating patients without their informed consent, so we remain unaware of these patients' background variables. In Paper II, the overall health-related quality of life was quite high within our cohort, and a mere 25% of the patients had a total tumour volume of ≥50 ml. In contrast, 75% of the patients in Paper IV had a total tumour volume of ≥ 61 ml. The relatively minor tumour burden in Paper II may have impacted the likelihood of discovering a significant correlation between total tumour volume and health-related quality of

life. Similarly, disease progression might play a more relevant role in patients' health-related quality of life than the specific tumour volume.

In a Netherlands based study involving 265 patients, health-related quality of life was assessed using the QLQ-C30 before and after the patients received PRRT.[214] Significant improvements in global health and symptomatology were observed after treatment, specifically among patient subgroups presenting with certain symptoms before treatment. Interestingly, the subgroup that exhibited the most marked improvement in global health scores was the one with progressive disease, surpassing patients with stabilised disease or a partial response.[214] The reason for this phenomenon is unclear. Patients with progressive disease may have had more advanced stages of the condition, reflected in their significantly lower initial global health scores.[214] Since there might not have been any alternative treatment options for these individuals, their expectations from treatment could have been relatively high. Despite progressive disease significantly impacting quality of life and the treatment not being sufficient for disease stabilisation, anti-tumour effects from the treatment might have contributed to improvements in their quality of life.

In Paper II, we were unable to adjust for progressive disease. Nevertheless, exploring the relationship between tumour burden and quality of life in the context of changing tumour burden would be an interesting avenue for future research.

Health-related quality of life is multifaceted, with numerous factors influencing patients' mental and physical health, as well as their perception of the disease and its symptoms. One study of breast cancer patients indicated that negative illness perceptions were associated with poor health-related quality of life.[215] While this has not been evaluated in NET patients, it presents an intriguing possibility, as illness perception could potentially be a path for intervention.

Contrary to our findings of a relatively high mean summary score for health-related quality of life in this cohort, several specific symptoms significantly bothered patients. We found a weak positive correlation between carcinoid-related symptoms and both total tumour volume and tumour volume in specific anatomical locations, such as the gastrointestinal tract and liver. These results suggest that even though some of the symptoms patients experience, which are related to their disease and reflected in specific symptom questionnaires, are not captured in the overall health-related quality of life measure. This implies that it might be important to not only evaluate the health-related quality of life in NET patients but also assess the specific NET-associated symptoms with the detailed questionnaires available.

# Quantification of tumour burden

Measuring total tumour burden is a time-intensive task, usually not applied in clinical practice due to its lengthiness and incompatibility with efficient approaches. Inter-observer variability tends to be higher when measuring tumour burden manually compared to semi-automatic methods.[216] A standardised fully automatic method to measure tumour burden could potentially enhance reproducibility in comparison to manual measurements.[217, 218] Moreover, a few studies propose comparable prognostic value for outcome analyses, despite minor differences in the chosen segmentation method.[219, 220] These results allude to the idea that the accuracy of the delineation method may not be as central as reproducibility and consistency.

Measurements of total tumour burden as SRETVwb at somatostatin receptor PET-CT could enhance prognostication, improve follow-up accuracy, and provide a rationale for treatment approaches. The differences in tumour volume might be detected earlier through measurements of volume compared to diameters, which are provided in the imaging report in clinical practice. There is no consensus about the optimal segmenting approach for SRETVwb, with several studies using different methods. We applied a semi-automatic method using a fixed relative threshold, segmenting 50% of SUVmax, but the manual delineation of tumours was often required to avoid adjacent uptake from the tumours or background. Other segmenting approaches for SRETVwb exist, some employing a fixed or adaptive background threshold such as normal liver parenchyma.[96, 221, 222]

Several studies use software that semi-automatically segment all tissue with an uptake above a threshold of 1.5*(SUVmean in normal liver + 2 standard deviations (SD)) and then complements it by manual removal of false-positive lesions.[83, 92, 95] Some studies using background threshold-based methods have shown similar results, with worse progression-free survival or overall survival for larger SRETVwb.[83, 96, 221] However, a few of the background threshold-based studies did not find such strong correlations between tumour volume and progression-free survival or overall survival as others. [92, 95, 222]

All segmenting methods come with their benefits and drawbacks. In the threshold-based method used by Thullier et al., SRETVwb was 0 ml for five patients, even though they had somatostatin receptor-expressing tumours.[96] This discrepancy occurred because the uptake in their tumours was lower than in the liver for those patients.[96] Fixed threshold-based methods, may overestimate larger tumours due to partial volume effects. Conversely, fixed relative threshold-based method of 40% or 50% of SUVmax might underestimate the volume for high uptake and overestimate for a low SUVmax.[87] Necrotic cores are rarely included when segmenting tumour volumes using uptake at PET-CT, but they are included when measuring the diameter.[79] This can be both a disadvantage and an advantage as the PET-CT measurements more accurate assess the viable tumour burden.

Table 13 provides a summary of studies evaluating various segmenting methods of SRETVwb from somatostatin receptor PET-CT images. All studies were conducted in different clinical settings, which is why the results are not wholly transferable.

**Table 13. Tumour burden at somatostatin receptor PET-CT**

Overview of studies evaluating the prognostic or predictive value of whole-body somatostatin receptor tumour volume (SRETVwb) and whole-body total lesion somatostatin receptor expression (TLSREwb) at somatostatin receptor (SSTR) PET-CT. Progression-free survival (PFS), overall survival (OS), long-acting somatostatin analogues (LA SSA). Comments by the author are marked with an asterix (*).

| Study and disease/grade | N subjects | Parameters | Segmenting method | Conclusion and comments* |
|---|---|---|---|---|
| Toriihara et al. 2019[91] Retrospective NET G1-G2 ^{68}Ga-DOTATATE | 92 patients with pathologically diagnosed NET (G1-G2) of whom 76* had SSTR-avid lesions | SRETVwbT LSREwb PFS | Fixed relative treshold, 50% of SUVmax | SRETVwb (≥11 ml) was a prognostic risk factor for the assessment of PFS in both univariate and multivariate analyses. *Inclusion of patients without SSTR avid tumours make results uncertain. |
| Tirosh et al. 2018[221] Prospective NET G1-G3 ^{68}Ga-DOTATATE | 184 patients with SSTR avid lesions, 128 patients had metastases and 11 patients locally advanced disease | SRETVwb PFS, OS | Individualised SUVmax threshold-based approach with automatic demarcation of tumours + manual correction | SRETVwb (≥7 ml) was a prognostic risk factor for the assessment of PFS and SRETVwb (≥36 ml) was a prognostic risk factor for the assessment of OS, in both univariate and multivariate analyses. |
| Thuillier et al. 2022[96] Retrospective NET G1-G3 ^{68}Ga-DOTATOC | 84 patients NET (G1-G3) with SSTR avid lesions | SRETVwbT LSREwb PFS, OS | Individualised treshold based segmentation depending on SUVmax in healthy liver | SRETVwb ≥39 ml and TLSREwb >307 were prognostic risk factors for assessment of PFS and OS. SRETVwb ≥39 ml was the only risk factor of PFS in multivariate analyses. |
| Chen et al. 2022[92] Retrospective Well-differentiated NET ^{68}Ga-DOTANOC | 204 patients who had no prior treatment, SSTR-avid lesions >liver and receivded LA SSA as first line treatment were included | Log transform-ation of SRETVwb and TLSREwb PFS, OS | Background treshold: 1.5xSUVmean liver + 2 SD or 0.67xSUVmean spleen + 2 SD or Fixed relative treshold based on 30,40 and 50% of SUVmax | Background treshold based parameters based were not associated with OS Log SRETV 30, 40 and 50% of SUVmax were all independently associated with OS with a minor preference for LogSRETV30 |
| Kim et al 2020[95] Retrospective GEP-NET G1-G3 ^{68}Ga-DOTATOC | 31 patients receiving treatment with LA-SSA after PET | SRETVwb TLSREwb PFS | Background treshold, based on 1.5xSUVmean liver + 2 SD | SRETVwb ≥ 59 ml was a significant risk factor for the assessment of PFS in univariate analysis but not in the multivariate analysis (p=0.07). |

**Table 13.**
(continued)

| Study and disease/grade | N subjects | Parameters | Segmenting method | Conclusion and comments* |
|---|---|---|---|---|
| Carlsen et al. 2021[83] Prospective NET G1-G3 ^{64}Cu-DOTATATE | 116 patients with imaged with PET-CT for staging or follow-up | SRETVwb PFS, OS | Background treshold, based on 1.5xSUVmean liver + 2 SD | Higher SRETVwb was associated with worse PFS and OS in univariate analysis |
| Gallicchio et al. 2022[93] Retrospective GEP-NET ^{68}Ga-DOTATOC | 42 patients were examined with PET-CT before surgery | SRETVwb, TLSREwb event-free survival | Fixed relative treshold of 42% of SUVmax | SRETVwb >2.5 ml was a significant risk factor assessing event free survival after surgery on univariate analyses |
| Ohnona et al. 2018[94] Prospective Pancreatic NET G1 and G2 ^{68}Ga-DOTATOC | 50 patients with ≥1 SSTR avid lesion Different treatments after PET-CT | SRETVwb PFS | Fixed relative treshold of 41% of SUVmax | SRETVwb >14 ml was a significant prognostic risk factor for assessment of PFS in both univariate and multivariate analyses. |
| Pauwels et al. 2020[222] Post-hoc analysis of previous prospective study NET ^{68}Ga-DOTATOC | 43 patients who received PRRT with ^{90}Y-DOTATOC | SRETVwb, TLSREwb PFS, OS | Individualised SUVmax threshold-based approach with automatic demarcation of tumours + manual correction | A baseline tumour volume > 578 ml (75th percentile) was associated with poorer OS on univariate analysis but not multivariate analysis |
| Ortega et al. 2021[223] Prospective multicenter study Well-differentiated NET ^{68}Ga-DOTATATE | 91 patients were examined with PET-CT before ^{177}Lu-DOTATATE | SRETVwb(L) SRETVwb(S) PFS, OS | Inhouse developed semiautomatic treshold based method with manual corrections. Treshold were set at reference tissue in liver SRETVwb(L) and spleen SRETVwb(S) | Not significant (p=0.12 and p=0.06), but there was a tendency for worse outcomes for patients with smaller SRETVwb for both SRETVwb(L) and (S). *The tumour volume was twice as high when the liver was set as treshold (L) compared to the spleen (S), indicating uncertainty in this segmentation method |
| Lee et al.2024[224] Retrospective NET ^{68}Ga-DOTATATE | 94 patients examined with SSTR PET-CT before ^{177}Lu-DOTATATE | SRETVwb PFS, OS | Background treshold, based on 1.5xSUVmean liver + 2 SD | SRETVwb >325 ml was a significant risk factor for worse PFS/OS. *6 patients had SRETVwb 0 ml due to tumours with uptake below the treshold. No multivariate analysis for other risk factors was performed. |

In conclusion, no perfect method for measuring SRETVwb has been established yet. One advantage of fixed relative threshold-based methods is that they can also include tumours with lower uptake, in contrast to methods using a threshold relative to the liver where lesions with low uptake are omitted. Tumours with low uptake could potentially be more aggressive in nature,[83, 104] and including them in the total tumour volume could be valuable.

Perhaps the different methods will yield similar results regardless of the chosen method, or a preference might exist for fixed relative threshold-based methods over background threshold-based methods, as suggested by the largest study conducted by Chen et al.[92] A potential solution to some issues related to tumour segmentation could be the development of an automatic AI method for measuring tumour volume. If the tumour volume is automatically provided for each PET-CT examination, this could prove crucial for evaluating disease status and treatment response. Perfect accuracy may not be as important as the reproducibility and efficiency in a clinical setting. Also, intra- and inter-reader variability could decrease in comparison to manual or semi-automatic methods. In Paper III, we took several steps towards creating an AI model, demonstrating the feasibility of developing a high-performance AI model to measure tumour burden at somatostatin receptor PET-CT. Our model's performance matched that of an AI model developed by Carlsen et al., which assessed tumour burden using $^{64}$Cu-DOTATATE PET-CT images.[225] However, our AI model was not perfect, and it performed worse when evaluated in the PRRT treated patient cohort in Paper IV. This emphasises the need for validating new AI tools in the clinical context where they are intended to be used. It is critical to assess all aspects of an AI model's contributions when incorporating them into clinical practice, ideally in a systematic manner, as outlined in Table 7.

The development of AI models will undoubtedly accelerate in the future. This growth is spurred by advancements in technology, the expanding availability of data, as seen in The European Cancer Imaging Initiative (EUCAIM),[226] and the escalating demand for AI solutions to enhance cancer diagnostics and treatments. Additionally, AI offers the potential to construct prediction models based on a variety of parameters including clinical, pathological, and imaging data.

# Quantification of tumours in relationship to response to treatment

Interpreting an absolute change in the uptake of $^{68}$Ga-DOTATOC or $^{68}$Ga-DOTATATE, as measured through SUVmax or SUVmean at baseline and follow-up imaging with PET-CT, can be challenging due to the plethora of factors that could potentially influence the uptake. Factors such as different treatments can affect uptake in tumours or normal tissue. Furthermore, discrepancies in patient

weight, administered radiopharmaceutical dose, technical aspects, motion artefacts, a variation in total tumour volume, and individual tumour lesion volume might influence the SUVmax measurements. Therefore, interpreting changes in uptake may not be straightforward. The explorative analysis in Paper I highlighted notable differences in the change of SUVmax depending on whether clinical disease status was seen as a progressive disease, stable disease, or regression of disease. However, there was an overlap between these groups, and a change in SUVmax does not directly translate to a clinical interpretation of disease status. A potential resolution to some of these issues may lie in evaluating relative tumour uptake, defined by the ratio of the uptake in normal liver, spleen, or blood pool. A variety of studies have indeed evidenced that the tumour-to-liver ratio surpasses SUVmax in predicting the response to PRRT.[227, 228] Nevertheless, since the uptake in the blood pool is higher for patients receiving long-acting somatostatin analogues within 5 days preceding the PET-CT,[206] and the uptake in liver or spleen has been observed to decrease post initiation of treatment with long-acting somatostatin analogues,[200, 206] comparing changes in these ratios might still be hard to decipher.

We did not uncover any correlation between the highest SUVmax and progression-free survival or overall survival in Paper IV. This finding aligns with other studies, which report no correlation between SUVmax and outcome.[229] However, some research has observed a connection between SUVmax and treatment responsiveness.[224, 229] A potential explanation for these inconsistent results could be tumour heterogeneity across different studies and a selection bias, as tumour uptake is already assessed for PRRT eligibility.

In Paper IV, we did not observe any predictive value for baseline tumour burden assessed as SRETVwb, TLSREwb, largest lesion diameter, or SUVmax in predicting response to PRRT with $^{177}$Lu-DOTATATE. Only a handful of studies have evaluated the total SRETV at pretherapy PET-CT as a potential predictive biomarker for outcomes following PRRT.[222-224] Ortega et al. evaluated different quantitative parameters from $^{68}$Ga-DOTATATE PET-CT images both before and during PRRT.[223] Baseline somatostatin receptor PET-CT tumour volume was not found to be significantly associated with treatment response, although there was nearly a significant inverse relationship with a mean tumour volume of 364 ml for responders versus 151 ml for non-responders (p = 0.06).[223] In contrast, Lee et al. discovered worse progression-free survival and overall survival in patients with tumour volume exceeding 325 ml.[224] Pauwels et al. assessed patients who received PRRT with $^{90}$Y-DOTATOC and found that a baseline tumour volume larger than 578 ml was linked with poorer overall survival in a univariate analysis but not in a multivariate analysis.[222]

Moreover, some studies have assessed partial tumour burden, typically only examining the liver or the size of the largest tumour lesion. For example, in the treatment group that only received high-dose octreotide in the NETTER-1 study, a correlation was observed between a higher tumour load in the liver and shortened

progression-free survival. However, neither progression-free survival nor overall survival showed significant differences in the ^{177}Lu-DOTATATE treatment group based on the liver's tumour load. Instead, an absence of large tumour lesions (>30 mm in diameter) was associated with improved progression-free survival.[136] Contrary to the NETTER-1 study, a retrospective study found shorter overall survival when the liver's tumour load was >25%.[230] On the other hand, Kwekkeboom et al. evaluated the tumour response after PRRT in 310 patients with GEP-NET. They found a positive correlation between higher remission rates and high uptake in tumours before treatment, along with a limited number of liver metastases.[137]

Overall, the results from various studies on the predictive value of tumour burden are inconsistent. This discrepancy could be partly explained by differences in segmentation methods, the inclusion of various patient subgroups, small study populations, and the prospect that other factors – such as tumour grade, the rate of disease progression before PRRT, and the presence of ^{18}F-FDG-avid lesions – may be more important for the outcome than the actual tumour burden.

The optimal levels of the absorbed dose for all tumours have yet to be determined. We found the median of the mean tumour absorbed dose in cycle 1 to be 25 Gy compared to two recent studies that found a median tumour absorbed dose of 33 Gy, and 32 Gy in target lesions, respectively.[231, 232] Contrary to our findings, both studies reported longer progression-free survival for patients receiving higher doses.[231, 232] Although there was a tendency for better overall survival for patients receiving higher doses in Paper IV, the difference was not statistically significant. These results, combined with the finding that no patients with a tumour burden >400 ml received a mean tumour absorbed dose >30 Gy, suggest that further study in a larger cohort is warranted. There may be potential to improve treatment outcomes with ^{177}Lu-DOTATATE by treating patients with a large tumour burden differently.

# Strengths and limitations

The strength of **Paper I**, the Gapetto trial, lies in its prospective design, which provides more robust evidence for decision-making than retrospective studies. However, during the observational "real-world" Gapetto trial, several limitations were identified. As an observational study conducted in a clinical setting, there was some loss of information due to missing data. Performing an observational study – where one cannot control when patients initiate treatment or when follow-up examinations occur – resulted in a limited number of patients available for subgroup analysis. Other weaknesses included the relatively long time interval between the PET-CT scan before treatment initiation and the follow-up PET-CT scan, as well as the lack of correlations with tumour burden or blood-based tumour makers.

**Paper II** holds significance as it is, to our knowledge, the first study to investigate whether total tumour burden correlates with health-related quality of life and symptoms in GEP-NET patients. Knowledge in this area is incredibly valuable when individualising a patient's treatment. The population-based design is another strength, minimising selection bias. A notable limitation is the number of patients who did not respond to the questionnaires. Due to the population-based design, and the inclusion of all eligible patients, no power analysis was conducted; however, a potential power issue cannot not be ruled out.

In **Papers II-IV**, there are limitations concerning the method of measuring tumour volume. Currently, there is no validated method available for measuring the somatostatin receptor-expressing tumour volume, and such measurements can be performed in a variety of ways. We opted to measure tumours using the only method described in a few studies at the time, which also had shown potential prognostic value.[91] Although outlining tumours with 50% of SUVmax has displayed promise, this method has limitations when segmenting highly complex tumours. When the tumours were large, complex, and featured necrosis, along with a high uptake in certain parts, it is possibly that not all viable tumour volumes were accounted for. Tumours might have been underestimated, or overestimated if they had a low uptake relative to the background. Moreover, lesions demonstrating a decrease in uptake at the follow-up, could appear larger using this method, even if the tumour margins remain the same.[87]

Small lesions are often underestimated at PET images due to factors like partial volume effects, limited spatial resolution, motion artefacts, low contrast, and the

impact of noise.[233, 234] It was not possible to correct for all these limitations that affect tumour measurements on PET-CT images. Furthermore, all segmentation techniques have their own unique limitations.[79] However, a strength of our method is that the largest study evaluating different segmentation techniques found the relative fixed threshold method to be superior to fixed threshold-based methods.[92]

Throughout this thesis, the production of $^{68}$Ga-DOTATATE was altered to $^{68}$Ga-DOTATOC, which is why both radiopharmaceuticals are encompassed in **Papers II–IV**. This change could be seen as a weakness, given that the affinity profiles for somatostatin receptors differ slightly, potentially leading to small differences in tumour segmentation. However, the inclusion of two tracers might also be considered a strength, particularly showcased in **Paper III** during the training of the AI model. Moreover, the ability of our AI model to analyse both tracers was a prerequisite, as they were used for the baseline PET-CT examination for patients included in **Paper IV**.

A general drawback of conducting manual or semi-automatic tumour segmentation is its significant time consumption, which likely contributes to the scarcity of studies in this field. A key strength of this thesis lies in addressing these segmentation issues and time constraints by developing and assessing an AI model. Due to the rarity of NET disease, coupled with cost and time restrictions, the training and validation set for the AI model development was limited to 148 patients. The AI model would likely have exhibited superior performance if more patients had been included.

The retrospective nature of **Paper IV** introduces several weaknesses. The main one is that fewer patients than initially expected were included, primarily due to a longer time interval between the PET-CT and the start of treatment than stipulated in the inclusion/exclusion criteria. Some of these prolonged time intervals could have been related to the COVID-19 pandemic situation where any extra examination was thoroughly weighed against the risks of travelling to and visiting the hospital. The small sample size might have led to an underpowered study. However, a strength of this small study is that we correlated tumour burden to the estimated mean tumour absorbed dose and evaluated the outcome in relation to this dose, thus investigating not just the correlation but also a possible causal explanation. This measurement might be valuable for predicting treatment response and warrants further study.

# Conclusions

- Initiation of treatment with long-acting somatostatin analogues reduced the uptake in normal liver tissue, but the uptake in tumours remained largely unaltered by the treatment or the interval since injection. This resulted in a higher tumour-to-liver ratio, potentially enhancing tumour detection.

- The findings from Paper I, combined with those from similar studies, suggest that patients may not need to postpone initiating treatment with long-acting somatostatin analogues before undergoing PET-CT. The EANM guidelines, which recommend scheduling the PET-CT exam 3–4 weeks post the last injection, may be unnecessarily complicated and could probably be revised.

- No association was found between the summary score of health-related quality of life and total tumour burden. These results indicate that other factors may be more significant for the health-related quality of life of patients with metastasised NET disease.

- The development of an AI model for tumour segmentation is feasible, although further enhancements are required before it can be implemented in clinical practice.

- We were unable to find predictive value in various measures of tumour burden from baseline somatostatin receptor PET-CT for treatment outcomes with ^{177}Lu-DOTATATE.

- A moderately strong correlation was found between the highest SUVmax and mean tumour absorbed dose. This is consistent with the value of high uptake at pretherapy somatostatin receptor PET-CT for the selection of patients for PRRT. The mean tumour absorbed dose at first treatment cycle did not significantly predict treatment outcomes in this small cohort.

- Unsurprisingly, an increase in tumour burden, measured as SRETVwb, TLSREwb, or tumour diameter at the first follow-up after PRRT, was predictive of a worse outcome.

# Future perspectives

PET-CT stands as an invaluable imaging method for diagnostics, staging, and follow-up purposes. Imaging biomarkers determined at somatostatin receptor PET-CT could play a pivotal role in the future as they might provide additional information for prognostication or predicting treatment response. Currently, there are no established quantitative imaging biomarkers at somatostatin receptor PET-CT for predicting response to PRRT.

Overall, PRRT with ^{177}Lu-DOTATATE is a highly effective treatment option for patients with well-differentiated NETs, with numerous strategies currently being explored to further enhance patient care.[235] Though PRRT increases health-related quality of life and extends progression free survival time, there is an essential need for improved patient selection and treatment optimisation. Not all patients respond to the treatment, and PRRT is both costly and associated with potentially serious side effects.

Additionally, NET is a heterogeneous disease, yet the standard ^{177}Lu-DOTATATE treatment does not account for specific disease characteristics like disease grade, distribution, tumour volume and size of individual lesions. The standard regimen also overlooks certain patient characteristics, such as body mass. In the future, personalised PRRT could involve the selection of radionuclides (like ^{177}Lu or ^{90}Y) depending on lesion size, or the adjustment of the administered activity or number of cycles, based on tumour burden, dosimetry, or patient characteristics that are not currently considered. Furthermore, it would be valuable to study the relationship between the mean tumour absorbed dose in relation to outcomes in a larger cohort of patients.

The future may see validated imaging biomarkers assisting in these decisions. Identifying reliable imaging biomarkers for predicting responses to PRRT holds considerable potential to enhance treatment outcomes and cost-effectiveness, thereby generating significant interest for further studies.

This thesis has evaluated aspects of quantitative imaging parameters from somatostatin receptor PET-CT in relation to treatment, health-related quality of life, and AI. Regarding treatment with long-acting somatostatin analogues, the number of published papers to date, all pointing in the same direction, suggests that further research in this area may be less warranted.

Evaluating health-related quality of life is crucial when introducing new treatments. Although we did not find any evidence of worse health-related quality of life concerning tumour volume in our cohort, it might be interesting to study this in a cohort with a higher tumour burden, as with the patients selected for PRRT in Paper IV. It would also be beneficial to assess health-related quality of life in relation to disease status, such as complete or partial response, stable disease or progressive disease, as evaluated with somatostatin receptor PET-CT. Health-related quality of life may deteriorate before significant changes are detectable by PET-CT imaging.

AI models in healthcare will undoubtedly play a significant role in clinical practice in the near future. This thesis developed and evaluated an AI model for estimating tumour burden. However, AI models are not always developed in the environments where they will later be applied, which may involve different hardware or software, or diverse patient characteristics. The results in Paper IV underscore the importance of comprehensive evaluation when integrating new AI models into clinical workflows, including assessing sensitivity and specificity, changes in workload, time efficiency, and other pertinent factors.

Finally, the combination of somatostatin receptor PET-CT and $^{18}$F-FDG PET-CT imaging, also known as dual-imaging, offers a comprehensive overview of disease status throughout the body and has prognostic value for certain patients. The presentation of somatostatin receptor PET-CT findings and dual-imaging could potentially benefit clinical decision-making and research via the use of standardised reporting systems. Incorporating the use of SSTR-RADS 1.0 or NETPET score into clinical workflow could improve reporting for diagnosis, treatment planning, and research, while also lessening inter- and intra-reader variability.

# Errata

- Paper III, Figure 2.

  In the CONSORT diagram of the retrospective study, the "Training group (n=138)" should be corrected to "Training group (n = 118)".

- Paper III, Table 4. Table text.

  In the table text the mention of "median volume (ml) and median TLSREwb" should be removed as these values are not included in the table.

  Revised table text:

  Number of lesions which are true positive, false positive and false negative for the AI model versus Reader A, the AI model versus Reader B and Reader B versus Reader A. Values are total number of lesions, median number of lesions per patient, with interquartile range (IQR). Sensitivity and positive predictive value (PPV) are also presented for each comparison.

# Acknowledgements

Jag vill rikta ett varmt och innerligt tack till *alla* som på något sätt har stöttat och hjälpt mig under mina doktorandstudier – ni är många. Ett hjärtligt tack vill jag också framföra till alla *patienter* som deltagit i våra studier, ert bidrag är ovärderligt!

Min huvudhandledare, *Elin Trägårdh* - Jag är så tacksam för att du gav mig chansen att få bli din doktorand. Med din flexibla och lyhörda handledning har du med stor erfarenhet väglett mig. Du är en inspiration och förebild med allt du gör både i kliniken och i forskningen. När jag nu ska lämna den trygga platsen under dina vingar är jag glad att jag fortfarande får ha dig som kollega i det kliniska arbetet. Dessutom ser jag fram emot framtida samarbeten!

Min bihandledare *Anna Sundlöv*, hur ska jag kunna tacka dig? Du hade Gapetto i bakfickan när jag behövde ett vetenskapligt arbete under ST:n. Du har hjälpt till med så mycket under alla de här åren, både på ett personligt och vetenskapligt plan. Du har med din djupa kunskap, ditt metodiska arbetssätt och med konsten att ställa de rätta frågorna hela tiden inspirerat och väglett mig.

*Olof Enqvist*, min bihandledare som kan allt om AI. Utan din hjälp, kunskap och erfarenhet hade jag kört fast vid förkortningen för artificiell intelligens. Och jag vet att jag har frågat tusen frågor om hur AI fungerar, och du svarar så pedagogiskt och bra, och kanske har jag blivit lite klokare på vägen också.

Min bihandledare *Johan Wasselius*, tack för kloka tankar under resans gång och inte minst överlevnadsknep för arbetsdagen och bra tips inför framtida forskning.

*Jonas Jögi*, min nuvarande chef på Klinisk Fysiologi and Nuklearmedicin. Tack för att du anställde mig och gav mig chansen att förverkliga mina drömmar om att få kombinera forskningen med kliniskt arbete inom radiologi och nuklearmedicin!

*Peter Hochbergs*, verksamhetschef för verksamhetsområde Bild och Funktion. Stort tack för att du gav mig möjligheten att bli doktorand och få forska under min ST.

*Fredrik Stålhammar*, min eviga handledare (under ovanligt lång röntgen-ST). Tack för all hjälp, alla samtal och all kunskap du så generöst delar med dig av. Jag ser alltid fram emot nästa lunch med dig!

*Ulrika Bitzén*, min nya handledare på nuklearmedicin, du kan otroligt mycket och det är alltid lärorikt att diskutera med dig. Jag är också otroligt tacksam för att du lyckats frigöra så mycket forskningstid till mig, det hade aldrig gått annars!

# References

1. Oronsky B, Ma PC, Morgensztern D, Carter CA. Nothing But NET: A Review of Neuroendocrine Tumors and Carcinomas. Neoplasia. 2017;19(12):991-1002.
2. Kaltsas GA, Besser GM, Grossman AB. The Diagnosis and Medical Management of Advanced Neuroendocrine Tumors. Endocrine reviews. 2004;25(3):458-511.
3. WHO Classification of Tumours Editorial Board. Digestive system tumors. Lyon (France): International Agency for Research on Cancer; 2019.
4. Tsoucalas G, Karamanou M, Androutsos G. The eminent German pathologist Siegfried Oberndorfer (1876-1944) and his landmark work on carcinoid tumors. Ann Gastroenterol. 2011;24(2):98-100.
5. Modlin IM, Shapiro MD, Kidd M, Eick G. Siegfried oberndorfer and the evolution of carcinoid disease. Arch Surg. 2007;142(2):187-97.
6. Oberndorfer S. Karzinoide tumoren des dunndarms. Frankf Zschr Path. 1907;1:426.
7. Ransom W. A CASE OF PRIMARY CARCINOMA OF THE ILEUM. The Lancet. 1890;136(3507):1020-3.
8. Dasari A, Shen C, Halperin D, Zhao B, Zhou S, Xu Y, et al. Trends in the incidence, prevalence, and survival outcomes in patients with neuroendocrine tumors in the United States. JAMA oncology. 2017;3(10):1335-42.
9. Fraenkel M, Kim M, Faggiano A, de Herder WW, Valk GD. Incidence of gastroenteropancreatic neuroendocrine tumours: a systematic review of the literature. Endocrine-related cancer. 2014;21(3):R153-63.
10. Hofland J, Kaltsas G, de Herder WW. Advances in the Diagnosis and Management of Well-Differentiated Neuroendocrine Neoplasms. Endocrine reviews. 2020;41(2):371-403.
11. Hassan MM, Phan A, Li D, Dagohoy CG, Leary C, Yao JC. Risk factors associated with neuroendocrine tumors: A U.S.-based case–control study. International Journal of Cancer. 2008;123(4):867-73.
12. Anlauf M, Garbrecht N, Bauersfeld J, Schmitt A, Henopp T, Komminoth P, et al. Hereditary neuroendocrine tumors of the gastroenteropancreatic system. Virchows Archiv. 2007;451(1):29-38.
13. Leoncini E, Carioli G, La Vecchia C, Boccia S, Rindi G. Risk factors for neuroendocrine neoplasms: a systematic review and meta-analysis. Annals of Oncology. 2016;27(1):68-81.
14. Bogaards M, May AM, Hassan FA, Valk GD, van Leeuwaarde RS. Lifestyle Factors and Development and Natural Course of Gastroenteropancreatic Neuroendocrine Tumors: A Review of the Literature. Neuroendocrinology. 2023;113(4):381-94.

15. Rindi G, Mete O, Uccella S, Basturk O, La Rosa S, Brosens LAA, et al. Overview of the 2022 WHO Classification of Neuroendocrine Neoplasms. Endocrine Pathology. 2022;33(1):115-54.

16. Nagtegaal ID, Odze RD, Klimstra D, Paradis V, Rugge M, Schirmacher P, et al. The 2019 WHO classification of tumours of the digestive system. Histopathology. 2020;76(2):182-8.

17. Assarzadegan N, Montgomery E. What is New in the 2019 World Health Organization (WHO) Classification of Tumors of the Digestive System: Review of Selected Updates on Neuroendocrine Neoplasms, Appendiceal Tumors, and Molecular Testing. Arch Pathol Lab Med. 2021;145(6):664-77.

18. Mete O, Asa SL, Gill AJ, Kimura N, de Krijger RR, Tischler A. Overview of the 2022 WHO Classification of Paragangliomas and Pheochromocytomas. Endocr Pathol. 2022;33(1):90-114.

19. Nicholson AG, Tsao MS, Beasley MB, Borczuk AC, Brambilla E, Cooper WA, et al. The 2021 WHO Classification of Lung Tumors: Impact of Advances Since 2015. J Thorac Oncol. 2022;17(3):362-87.

20. Pavel M, Öberg K, Falconi M, Krenning EP, Sundin A, Perren A, Berruti A. Gastroenteropancreatic neuroendocrine neoplasms: ESMO Clinical Practice Guidelines for diagnosis, treatment and follow-up. Ann Oncol. 2020;31(7):844-60.

21. (UICC) UfICC. The TNM Classification of Malignant Tumours, 8th Edition: Wiley Blackwell; 2016.

22. Dasari A, Shen C, Devabhaktuni A, Nighot R, Sorbye H. Survival According to Primary Tumor Location, Stage, and Treatment Patterns in Locoregional Gastroenteropancreatic High-grade Neuroendocrine Carcinomas. Oncologist. 2022;27(4):299-306.

23. Sorbye H, Welin S, Langer SW, Vestermark LW, Holt N, Osterlund P, et al. Predictive and prognostic factors for treatment and survival in 305 patients with advanced gastrointestinal neuroendocrine carcinoma (WHO G3): the NORDIC NEC study. Ann Oncol. 2013;24(1):152-60.

24. Dasari A, Mehta K, Byers LA, Sorbye H, Yao JC. Comparative study of lung and extrapulmonary poorly differentiated neuroendocrine carcinomas: A SEER database analysis of 162,983 cases. Cancer. 2018;124(4):807-15.

25. Lithgow K, Venkataraman H, Hughes S, Shah H, Kemp-Blake J, Vickrage S, et al. Well-differentiated gastroenteropancreatic G3 NET: findings from a large single centre cohort. Sci Rep. 2021;11(1):17947.

26. Rindi G, Villanacci V, Ubiali A. Biological and Molecular Aspects of Gastroenteropancreatic Neuroendocrine Tumors. Digestion. 2000;62(Suppl. 1):19-26.

27. Kvols LK. Metastatic carcinoid tumors and the malignant carcinoid syndrome. Annals of the New York Academy of Sciences. 1994;733:464-70.

28. Raphael MJ, Chan DL, Law C, Singh S. Principles of diagnosis and management of neuroendocrine tumours. Cmaj. 2017;189(10):E398-e404.

29. Hofland J, Falconi M, Christ E, Castaño JP, Faggiano A, Lamarca A, et al. European Neuroendocrine Tumor Society 2023 guidance paper for functioning

pancreatic neuroendocrine tumour syndromes. Journal of Neuroendocrinology. 2023;35(8):e13318.

30. Perri G, Prakash LR, Katz MHG. Pancreatic neuroendocrine tumors. Current Opinion in Gastroenterology. 2019;35(5):468-77.

31. Modlin IM, Kidd M, Latich I, Zikusoka MN, Shapiro MD. Current Status of Gastrointestinal Carcinoids. Gastroenterology. 2005;128(6):1717-51.

32. Lips CJ, Lentjes EG, Höppener JW. The spectrum of carcinoid tumours and carcinoid syndromes. Annals of Clinical Biochemistry. 2003;40(6):612-27.

33. Rubin de Celis Ferrari AC, Glasberg J, Riechelmann RP. Carcinoid syndrome: update on the pathophysiology and treatment. Clinics (Sao Paulo). 2018;73(suppl 1):e490s.

34. Caplin ME, Buscombe JR, Hilson AJ, Jones AL, Watkinson AF, Burroughs AK. Carcinoid tumour. Lancet. 1998;352(9130):799-805.

35. Patel YC. Somatostatin and its receptor family. Front Neuroendocrinol. 1999;20(3):157-98.

36. Cakir M, Dworakowska D, Grossman A. Somatostatin receptor biology in neuroendocrine and pituitary tumours: part 1--molecular pathways. J Cell Mol Med. 2010;14(11):2570-84.

37. Modlin IM, Pavel M, Kidd M, Gustafsson BI. Review article: somatostatin analogues in the treatment of gastroenteropancreatic neuroendocrine (carcinoid) tumours. Alimentary pharmacology & therapeutics. 2010;31(2):169-88.

38. Reichlin S. Secretion of somatostatin and its physiologic function. J Lab Clin Med. 1987;109(3):320-6.

39. Reubi JC. Peptide receptors as molecular targets for cancer diagnosis and therapy. Endocrine reviews. 2003;24(4):389-427.

40. Eychenne R, Bouvry C, Bourgeois M, Loyer P, Benoist E, Lepareur N. Overview of Radiolabeled Somatostatin Analogs for Cancer Imaging and Therapy. Molecules. 2020;25(17).

41. Hofland LJ, Lamberts SW. The pathophysiological consequences of somatostatin receptor internalization and resistance. Endocrine reviews. 2003;24(1):28-47.

42. de Herder WW, Hofland LJ, van der Lely AJ, Lamberts SW. Somatostatin receptors in gastroentero-pancreatic neuroendocrine tumours. Endocrine-related cancer. 2003;10(4):451-8.

43. Hoyer D, Lübbert H, Bruns C. Molecular pharmacology of somatostatin receptors. Naunyn Schmiedebergs Arch Pharmacol. 1994;350(5):441-53.

44. Krenning EP, Kwekkeboom DJ, Bakker WH, Breeman WA, Kooij PP, Oei HY, et al. Somatostatin receptor scintigraphy with [111In-DTPA-D-Phe1]- and [123I-Tyr3]-octreotide: the Rotterdam experience with more than 1000 patients. European journal of nuclear medicine. 1993;20(8):716-31.

45. Frangos S, Buscombe JR. Why should we be concerned about a "g"? European journal of nuclear medicine and molecular imaging. 2019;46(2):519-.

46. Ambrosini V, Kunikowska J, Baudin E, Bodei L, Bouvier C, Capdevila J, et al. Consensus on molecular imaging and theranostics in neuroendocrine neoplasms. Eur J Cancer. 2021;146:56-73.

47. Verburg FA, Heinzel A, Hänscheid H, Mottaghy FM, Luster M, Giovanella L. Nothing new under the nuclear sun: towards 80 years of theranostics in nuclear medicine. European journal of nuclear medicine and molecular imaging. 2014;41(2):199-201.

48. Nationellt vårdprogram neuroendokrina buktumörer Stockholm: Regionala cancercentrum i samverkan; 2021-05-04 [version 3.0:[Available from: https://kunskapsbanken.cancercentrum.se/diagnoser/neuroendokrina-buktumorer/vardprogram/.

49. Modlin IM, Gustafsson BI, Moss SF, Pavel M, Tsolakis AV, Kidd M. Chromogranin A--biological function and clinical utility in neuro endocrine tumor disease. Ann Surg Oncol. 2010;17(9):2427-43.

50. Eriksson B, Öberg K, Stridsberg M. Tumor Markers in Neuroendocrine Tumors. Digestion. 2000;62(suppl 1)(Suppl. 1):33-8.

51. Modlin IM, Drozdov I, Alaimo D, Callahan S, Teixiera N, Bodei L, Kidd M. A multianalyte PCR blood test outperforms single analyte ELISAs (chromogranin A, pancreastatin, neurokinin A) for neuroendocrine tumor detection. Endocrine-related cancer. 2014;21(4):615-28.

52. Knigge U, Capdevila J, Bartsch DK, Baudin E, Falkerby J, Kianmanesh R, et al. ENETS Consensus Recommendations for the Standards of Care in Neuroendocrine Neoplasms: Follow-Up and Documentation. Neuroendocrinology. 2017;105(3):310-9.

53. Öberg K, Califano A, Strosberg JR, Ma S, Pape U, Bodei L, et al. A meta-analysis of the accuracy of a neuroendocrine tumor mRNA genomic biomarker (NETest) in blood. Ann Oncol. 2020;31(2):202-12.

54. Puliani G, Di Vito V, Feola T, Sesti F, Centello R, Pandozzi C, et al. NETest: A Systematic Review Focusing on the Prognostic and Predictive Role. Neuroendocrinology. 2021;112(6):523-36.

55. Elias D, Lefevre JH, Duvillard P, Goéré D, Dromain C, Dumont F, Baudin E. Hepatic metastases from neuroendocrine tumors with a "thin slice" pathological examination: they are many more than you think. Ann Surg. 2010;251(2):307-10.

56. Shi W, Johnston CF, Buchanan KD, Ferguson WR, Laird JD, Crothers JG, McIlrath EM. Localization of neuroendocrine tumours with [111In] DTPA-octreotide scintigraphy (Octreoscan): a comparative study with CT and MR imaging. Qjm. 1998;91(4):295-301.

57. Kwekkeboom DJ, Krenning EP. Somatostatin receptor imaging. Seminars in Nuclear Medicine. 2002;32(2):84-91.

58. Maxwell JE, Sherman SK, Menda Y, Wang D, O'Dorisio TM, Howe JR. Limitations of somatostatin scintigraphy in primary small bowel neuroendocrine tumors. J Surg Res. 2014;190(2):548-53.

59. Bozkurt MF, Virgolini I, Balogova S, Beheshti M, Rubello D, Decristoforo C, et al. Guideline for PET/CT imaging of neuroendocrine neoplasms with (68)Ga-DOTA-conjugated somatostatin receptor targeting peptides and (18)F-DOPA. European journal of nuclear medicine and molecular imaging. 2017;44(9):1588-601.

60. Hope TA, Allen-Auerbach M, Bodei L, Calais J, Dahlbom M, Dunnwald LK, et al. SNMMI Procedure Standard/EANM Practice Guideline for SSTR PET: Imaging Neuroendocrine Tumors. Journal of Nuclear Medicine. 2023;64(2):204-10.

61. Bailey DL, Townsend DW, Valk PE, Maisey MN. Positron Emission Tomography: Basic Sciences: Springer London; 2005.

62. Boellaard R, Delgado-Bolton R, Oyen WJ, Giammarile F, Tatsch K, Eschner W, et al. FDG PET/CT: EANM procedure guidelines for tumour imaging: version 2.0. European journal of nuclear medicine and molecular imaging. 2015;42(2):328-54.

63. Kapoor V, McCook BM, Torok FS. An introduction to PET-CT imaging. Radiographics. 2004;24(2):523-43.

64. Evangelista L, Ravelli I, Bignotto A, Cecchin D, Zucchetta P. Ga-68 DOTA-peptides and F-18 FDG PET/CT in patients with neuroendocrine tumor: A review. Clin Imaging. 2020;67:113-6.

65. SomaKit TOC:EPAR Product Information Internet: European Medicines Agency; 2017 Feb 20 [updated 2024 March 03; cited 2024 22th April]. Available from: https://www.ema.europa.eu/en/medicines/human/EPAR/somakit-toc#product-info.

66. Velikyan I. 68Ga-Based radiopharmaceuticals: production and application relationship. Molecules. 2015;20(7):12913-43.

67. Bakgrundsstrålning Internet: Strålsäkerhetsmyndigheten; 2019 [cited 2024 5 April ].

68. Schofield R, King L, Tayal U, Castellano I, Stirrup J, Pontana F, et al. Image reconstruction: Part 1 – understanding filtered back projection, noise and image acquisition. Journal of Cardiovascular Computed Tomography. 2020;14(3):219-25.

69. Goldman LW. Principles of CT and CT Technology. Journal of Nuclear Medicine Technology. 2007;35(3):115-28.

70. Davenport MS, Perazella MA, Yee J, Dillman JR, Fine D, McDonald RJ, et al. Use of Intravenous Iodinated Contrast Media in Patients with Kidney Disease: Consensus Statements from the American College of Radiology and the National Kidney Foundation. Radiology. 2020;294(3):660-8.

71. Badiee S, Franc BL, Webb EM, Chu B, Hawkins RA, Coakley F. Role of IV Iodinated Contrast Material in 18F-FDG PET/CT of Liver Metastases. American Journal of Roentgenology. 2008;191(5):1436-9.

72. Fleischmann D, Kamaya A. Optimal vascular and parenchymal contrast enhancement: the current state of the art. Radiol Clin North Am. 2009;47(1):13-26.

73. Mansi L. Eugene C. Lin and Abass Alavi (Eds): PET and PET/CT. A Clinical Guide. Third Edition: Thieme Medical Publishers, New York, 2019. ISBN: 9781626231344. European journal of nuclear medicine and molecular imaging. 2019;46.

74. Ross S. Q.Clear Internet: GE Healthcare;  [cited 2024 5 April]. DOC1474189, Rev 3:[

75. Tong S, Alessio AM, Kinahan PE. Image reconstruction for PET/CT scanners: past achievements and future challenges. Imaging Med. 2010;2(5):529-45.

76. Harvey A. Ziessman JPOM, James H. Thrall. Nuclear Medicine the Requisites. Fourth Edition ed2014.

77. Vanderhoek M, Perlman SB, Jeraj R. Impact of the definition of peak standardized uptake value on quantification of treatment response. Journal of nuclear medicine : official publication, Society of Nuclear Medicine. 2012;53(1):4-11.

78. Wahl RL, Jacene H, Kasamon Y, Lodge MA. From RECIST to PERCIST: Evolving Considerations for PET Response Criteria in Solid Tumors. Journal of Nuclear Medicine. 2009;50(Suppl 1):122S-50S.

79. Foster B, Bagci U, Mansoor A, Xu Z, Mollura DJ. A review on segmentation of positron emission tomography images. Computers in Biology and Medicine. 2014;50:76-96.

80. Campana D, Ambrosini V, Pezzilli R, Fanti S, Labate AM, Santini D, et al. Standardized uptake values of (68)Ga-DOTANOC PET: a promising prognostic tool in neuroendocrine tumors. Journal of nuclear medicine : official publication, Society of Nuclear Medicine. 2010;51(3):353-9.

81. Kratochwil C, Stefanova M, Mavriopoulou E, Holland-Letz T, Dimitrakopoulou-Strauss A, Afshar-Oromieh A, et al. SUV of [68Ga]DOTATOC-PET/CT Predicts Response Probability of PRRT in Neuroendocrine Tumors. Mol Imaging Biol. 2015;17(3):313-8.

82. Liberini V, Huellner MW, Grimaldi S, Finessi M, Thuillier P, Muni A, et al. The Challenge of Evaluating Response to Peptide Receptor Radionuclide Therapy in Gastroenteropancreatic Neuroendocrine Tumors: The Present and the Future. Diagnostics (Basel). 2020;10(12).

83. Carlsen EA, Johnbeck CB, Loft M, Pfeifer A, Oturai P, Langer SW, et al. Semiautomatic Tumor Delineation for Evaluation of (64)Cu-DOTATATE PET/CT in Patients with Neuroendocrine Neoplasms: Prognostication Based on Lowest Lesion Uptake and Total Tumor Volume. Journal of nuclear medicine : official publication, Society of Nuclear Medicine. 2021;62(11):1564-70.

84. Binderup T, Knigge U, Loft A, Mortensen J, Pfeifer A, Federspiel B, et al. Functional Imaging of Neuroendocrine Tumors: A Head-to-Head Comparison of Somatostatin Receptor Scintigraphy, ^{123}I-MIBG Scintigraphy, and ^{18}F-FDG PET. Journal of Nuclear Medicine. 2010;51(5):704-12.

85. Bahri H, Laurence L, Edeline J, Leghzali H, Devillers A, Raoul J-L, et al. High Prognostic Value of ^{18}F-FDG PET for Metastatic Gastroenteropancreatic Neuroendocrine Tumors: A Long-Term Evaluation. Journal of Nuclear Medicine. 2014;55(11):1786-90.

86. Udupa JK, Odhner D, Zhao L, Tong Y, Matsumoto MM, Ciesielski KC, et al. Body-wide hierarchical fuzzy modeling, recognition, and delineation of anatomy in medical images. Med Image Anal. 2014;18(5):752-71.

87. Im HJ, Bradshaw T, Solaiyappan M, Cho SY. Current Methods to Define Metabolic Tumor Volume in Positron Emission Tomography: Which One is Better? Nucl Med Mol Imaging. 2018;52(1):5-15.

88. Liu J, Dong M, Sun X, Li W, Xing L, Yu J. Prognostic Value of 18F-FDG PET/CT in Surgical Non-Small Cell Lung Cancer: A Meta-Analysis. PLoS One. 2016;11(1):e0146195-e.

89.     Arshad MA, Gitau S, Tam H, Park WE, Patel NH, Rockall A, et al. Optimal method for metabolic tumour volume assessment of cervical cancers with inter-observer agreement on [18F]-fluoro-deoxy-glucose positron emission tomography with computed tomography. European journal of nuclear medicine and molecular imaging. 2020.

90.     Abdulrezzak U, Kurt YK, Kula M, Tutus A. Combined imaging with 68Ga-DOTA-TATE and 18F-FDG PET/CT on the basis of volumetric parameters in neuroendocrine tumors. Nuclear Medicine Communications. 2016;37(8).

91.     Toriihara A, Baratto L, Nobashi T, Park S, Hatami N, Davidzon G, et al. Prognostic value of somatostatin receptor expressing tumor volume calculated from (68)Ga-DOTATATE PET/CT in patients with well-differentiated neuroendocrine tumors. European journal of nuclear medicine and molecular imaging. 2019;46(11):2244-51.

92.     Chen L, Jumai N, He Q, Liu M, Lin Y, Luo Y, et al. The role of quantitative tumor burden based on [68 Ga]Ga-DOTA-NOC PET/CT in well-differentiated neuroendocrine tumors: beyond prognosis. European journal of nuclear medicine and molecular imaging. 2023;50(2):525-34.

93.     Gallicchio R, Giordano A, Milella M, Storto R, Pellegrino T, Nardelli A, et al. Ga-68-Edotreotide Positron Emission Tomography/Computed Tomography Somatostatin Receptors Tumor Volume Predicts Outcome in Patients With Primary Gastroenteropancreatic Neuroendocrine Tumors. Cancer Control. 2023;30:10732748231152328.

94.     Ohnona J, Nataf V, Gauthe M, Balogova S, Belissant Benesty O, Zhang-Yin J, et al. Prognostic value of functional tumor burden on 68Ga-DOTATOC PET/CT in patients with pancreatic neuro-endocrine tumors. Neoplasma. 2019;66(1):140-8.

95.     Kim YI, Yoo C, Oh SJ, Lee SJ, Kang J, Hwang HS, et al. Tumour-to-liver ratio determined by [(68)Ga]Ga-DOTA-TOC PET/CT as a prognostic factor of lanreotide efficacy for patients with well-differentiated gastroenteropancreatic-neuroendocrine tumours. EJNMMI Res. 2020;10(1):63.

96.     Thuillier P, Liberini V, Grimaldi S, Rampado O, Gallio E, Santi BD, et al. Prognostic Value of Whole-Body PET Volumetric Parameters Extracted from ^{68}Ga-DOTATOC PET/CT in Well-Differentiated Neuroendocrine Tumors. Journal of Nuclear Medicine. 2022;63(7):1014-20.

97.     Chan DL, Bernard EJ, Schembri G, Roach PJ, Johnson M, Pavlakis N, et al. High Metabolic Tumour Volume on 18-Fluorodeoxyglucose Positron Emission Tomography Predicts Poor Survival from Neuroendocrine Neoplasms. Neuroendocrinology. 2020;110(11-12):950-8.

98.     Kim HS, Choi JY, Choi DW, Lim HY, Lee JH, Hong SP, et al. Prognostic Value of Volume-Based Metabolic Parameters Measured by (18)F-FDG PET/CT of Pancreatic Neuroendocrine Tumors. Nucl Med Mol Imaging. 2014;48(3):180-6.

99.     Langen Stokmo H, Aly M, Bowitz Lothe IM, Borja AJ, Mehdizadeh Seraj S, Ghorpade R, et al. Volumetric parameters from [(18 F]FDG PET/CT predicts survival in patients with high-grade gastroenteropancreatic neuroendocrine neoplasms. J Neuroendocrinol. 2022;34(7):e13170.

100. Binderup T, Knigge U, Johnbeck CB, Loft A, Berthelsen AK, Oturai P, et al. ^{18}F-FDG PET is Superior to WHO Grading as a Prognostic Tool in Neuroendocrine Neoplasms and Useful in Guiding PRRT: A Prospective 10-Year Follow-up Study. Journal of Nuclear Medicine. 2021;62(6):808-15.

101. Majala S, Seppänen H, Kemppainen J, Sundström J, Schalin-Jäntti C, Gullichsen R, et al. Prediction of the aggressiveness of non-functional pancreatic neuroendocrine tumors based on the dual-tracer PET/CT. EJNMMI Res. 2019;9(1):116.

102. Chan DL, Hayes AR, Karfis I, Conner A, Mileva M, Bernard E, et al. [^{18}F]FDG PET/CT–Avid Discordant Volume as a Biomarker in Patients with Gastroenteropancreatic Neuroendocrine Neoplasms: A Multicenter Study. Journal of Nuclear Medicine. 2024;65(2):185-91.

103. Janson ET, Knigge U, Dam G, Federspiel B, Grønbaek H, Stålberg P, et al. Nordic guidelines 2021 for diagnosis and treatment of gastroenteropancreatic neuroendocrine neoplasms. Acta Oncologica. 2021;60(7):931-41.

104. Chan DL, Pavlakis N, Schembri GP, Bernard EJ, Hsiao E, Hayes A, et al. Dual Somatostatin Receptor/FDG PET/CT Imaging in Metastatic Neuroendocrine Tumours: Proposal for a Novel Grading Scheme with Prognostic Significance. Theranostics. 2017;7(5):1149-58.

105. Werner RA, Solnes LB, Javadi MS, Weich A, Gorin MA, Pienta KJ, et al. SSTR-RADS Version 1.0 as a Reporting System for SSTR PET Imaging and Selection of Potential PRRT Candidates: A Proposed Standardization Framework. Journal of Nuclear Medicine. 2018;59(7):1085-91.

106. Weinreb JC, Barentsz JO, Choyke PL, Cornud F, Haider MA, Macura KJ, et al. PI-RADS Prostate Imaging - Reporting and Data System: 2015, Version 2. Eur Urol. 2016;69(1):16-40.

107. Orel SG, Kay N, Reynolds C, Sullivan DC. BI-RADS categorization as a predictor of malignancy. Radiology. 1999;211(3):845-50.

108. Russ G, Bonnema Steen J, Erdogan Murat F, Durante C, Ngu R, Leenhardt L. European Thyroid Association Guidelines for Ultrasound Malignancy Risk Stratification of Thyroid Nodules in Adults: The EU-TIRADS. European Thyroid Journal. 2017;6(5):225-37.

109. Schwartz LH, Panicek DM, Berk AR, Li Y, Hricak H. Improving Communication of Diagnostic Radiology Findings through Structured Reporting. Radiology. 2011;260(1):174-81.

110. Grawe F, Ebner R, Geyer T, Beyer L, Winkelmann M, Sheikh GT, et al. Validation of the SSTR-RADS 1.0 for the structured interpretation of SSTR-PET/CT and treatment planning in neuroendocrine tumor (NET) patients. European Radiology. 2023;33(5):3416-24.

111. Chan DL, Hayes AR, Karfis I, Conner A, Furtado O'Mahony L, Mileva M, et al. Dual [68Ga]DOTATATE and [18F]FDG PET/CT in patients with metastatic gastroenteropancreatic neuroendocrine neoplasms: a multicentre validation of the NETPET score. British Journal of Cancer. 2023;128(4):549-55.

112. Plöckinger U, Rindi G, Arnold R, Eriksson B, Krenning EP, de Herder WW, et al. Guidelines for the diagnosis and treatment of neuroendocrine gastrointestinal

tumours. A consensus statement on behalf of the European Neuroendocrine Tumour Society (ENETS). Neuroendocrinology. 2004;80(6):394-424.

113. Gudmundsdottir H, Habermann EB, Vierkant RA, Starlinger P, Thiels CA, Warner SG, et al. Survival and Symptomatic Relief After Cytoreductive Hepatectomy for Neuroendocrine Tumor Liver Metastases: Long-Term Follow-up Evaluation of More Than 500 Patients. Ann Surg Oncol. 2023;30(8):4840-51.

114. Caplin ME, Pavel M, Cwikla JB, Phan AT, Raderer M, Sedlackova E, et al. Lanreotide in metastatic enteropancreatic neuroendocrine tumors. The New England journal of medicine. 2014;371(3):224-33.

115. Rinke A, Müller HH, Schade-Brittinger C, Klose KJ, Barth P, Wied M, et al. Placebo-controlled, double-blind, prospective, randomized study on the effect of octreotide LAR in the control of tumor growth in patients with metastatic neuroendocrine midgut tumors: a report from the PROMID Study Group. Journal of clinical oncology : official journal of the American Society of Clinical Oncology. 2009;27(28):4656-63.

116. Rinke A, Wittenberg M, Schade-Brittinger C, Aminossadati B, Ronicke E, Gress TM, et al. Placebo-Controlled, Double-Blind, Prospective, Randomized Study on the Effect of Octreotide LAR in the Control of Tumor Growth in Patients with Metastatic Neuroendocrine Midgut Tumors (PROMID): Results of Long-Term Survival. Neuroendocrinology. 2017;104(1):26-32.

117. Pusceddu S, Prinzi N, Raimondi A, Corti F, Buzzoni R, Di Bartolomeo M, et al. Entering the third decade of experience with octreotide LAR in neuroendocrine tumors: A review of current knowledge. Tumori. 2018:300891618765362.

118. Virgolini I, Ambrosini V, Bomanji JB, Baum RP, Fanti S, Gabriel M, et al. Procedure guidelines for PET/CT tumour imaging with 68Ga-DOTA-conjugated peptides: 68Ga-DOTA-TOC, 68Ga-DOTA-NOC, 68Ga-DOTA-TATE. European journal of nuclear medicine and molecular imaging. 2010;37(10):2004-10.

119. Kwekkeboom DJ, Kam BL, van Essen M, Teunissen JJ, van Eijck CH, Valkema R, et al. Somatostatin-receptor-based imaging and therapy of gastroenteropancreatic neuroendocrine tumors. Endocrine-related cancer. 2010;17(1):R53-73.

120. Johnstone RW, Ruefli AA, Lowe SW. Apoptosis: A Link between Cancer Genetics and Chemotherapy. Cell. 2002;108(2):153-64.

121. Öberg K. Interferon in the Management of Neuroendocrine GEP-Tumors : A Review. Digestion. 2000;62(Suppl. 1):92-7.

122. Cazzato RL, Hubelé F, De Marini P, Ouvrard E, Salvadori J, Addeo P, et al. Liver-Directed Therapy for Neuroendocrine Metastases: From Interventional Radiology to Nuclear Medicine Procedures. Cancers (Basel). 2021;13(24).

123. Pavel M, Valle JW, Eriksson B, Rinke A, Caplin M, Chen J, et al. ENETS Consensus Guidelines for the Standards of Care in Neuroendocrine Neoplasms: Systemic Therapy - Biotherapy and Novel Targeted Agents. Neuroendocrinology. 2017;105(3):266-80.

124. de Mestier L, Zappa M, Hentic O, Vilgrain V, Ruszniewski P. Liver transarterial embolizations in metastatic neuroendocrine tumors. Rev Endocr Metab Disord. 2017;18(4):459-71.

125.  Nationellt vårdprogram tjock och ändtarmscancer Version 3.1: Regionala Cancercentrum i Samverkan; 2023-02-03 [Available from: https://kunskapsbanken.cancercentrum.se/globalassets/cancerdiagnoser/tjock-- och-andtarm-anal/vardprogram/nationellt-vardprogram-tjock-andtarmscancer.pdf.

126.  Kulke MH, Hörsch D, Caplin ME, Anthony LB, Bergsland E, Öberg K, et al. Telotristat Ethyl, a Tryptophan Hydroxylase Inhibitor for the Treatment of Carcinoid Syndrome. Journal of clinical oncology : official journal of the American Society of Clinical Oncology. 2017;35(1):14-23.

127.  Hicks RJ, Kwekkeboom DJ, Krenning E, Bodei L, Grozinsky-Glasberg S, Arnold R, et al. ENETS Consensus Guidelines for the Standards of Care in Neuroendocrine Neoplasia: Peptide Receptor Radionuclide Therapy with Radiolabeled Somatostatin Analogues. Neuroendocrinology. 2017;105(3):295-309.

128.  Dash A, Chakraborty S, Pillai MRA, Knapp FF. Peptide Receptor Radionuclide Therapy: An Overview. Cancer Biotherapy and Radiopharmaceuticals. 2015;30(2):47-71.

129.  Hennrich U, Kopka K. Lutathera(®): The First FDA- and EMA-Approved Radiopharmaceutical for Peptide Receptor Radionuclide Therapy. Pharmaceuticals (Basel). 2019;12(3).

130.  Brabander T, van der Zwan WA, Teunissen JJM, Kam BLR, Feelders RA, de Herder WW, et al. Long-Term Efficacy, Survival, and Safety of [(177)Lu-DOTA(0),Tyr(3)]octreotate in Patients with Gastroenteropancreatic and Bronchial Neuroendocrine Tumors. Clinical cancer research : an official journal of the American Association for Cancer Research. 2017;23(16):4617-24.

131.  Strosberg J, El-Haddad G, Wolin E, Hendifar A, Yao J, Chasen B, et al. Phase 3 Trial of (177)Lu-Dotatate for Midgut Neuroendocrine Tumors. The New England journal of medicine. 2017;376(2):125-35.

132.  Kwekkeboom DJ, Teunissen JJ, Bakker WH, Kooij PP, de Herder WW, Feelders RA, et al. Radiolabeled somatostatin analog [177Lu-DOTA0,Tyr3]octreotate in patients with endocrine gastroenteropancreatic tumors. Journal of clinical oncology : official journal of the American Society of Clinical Oncology. 2005;23(12):2754-62.

133.  Park S, Parihar AS, Bodei L, Hope TA, Mallak N, Millo C, et al. Somatostatin Receptor Imaging and Theranostics: Current Practice and Future Prospects. Journal of Nuclear Medicine. 2021;62(10):1323-9.

134.  Hope TA, Calais J, Zhang L, Dieckmann W, Millo C. ^{111}In-Pentetreotide Scintigraphy Versus ^{68}Ga-DOTATATE PET: Impact on Krenning Scores and Effect of Tumor Burden. Journal of Nuclear Medicine. 2019;60(9):1266-9.

135.  Cremonesi M, Ferrari M, Bodei L, Tosi G, Paganelli G. Dosimetry in Peptide Radionuclide Receptor Therapy: A Review. Journal of Nuclear Medicine. 2006;47(9):1467-75.

136.  Strosberg J, Kunz PL, Hendifar A, Yao J, Bushnell D, Kulke MH, et al. Impact of liver tumour burden, alkaline phosphatase elevation, and target lesion size on treatment outcomes with (177)Lu-Dotatate: an analysis of the NETTER-1 study.

European journal of nuclear medicine and molecular imaging. 2020;47(10):2372-82.

137. Kwekkeboom DJ, de Herder WW, Kam BL, van Eijck CH, van Essen M, Kooij PP, et al. Treatment with the radiolabeled somatostatin analog [177 Lu-DOTA 0,Tyr3]octreotate: toxicity, efficacy, and survival. Journal of clinical oncology : official journal of the American Society of Clinical Oncology. 2008;26(13):2124-30.

138. Garske-Román U, Sandström M, Fröss Baron K, Lundin L, Hellman P, Welin S, et al. Prospective observational study of (177)Lu-DOTA-octreotate therapy in 200 patients with advanced metastasized neuroendocrine tumours (NETs): feasibility and impact of a dosimetry-guided study protocol on outcome and toxicity. European journal of nuclear medicine and molecular imaging. 2018;45(6):970-88.

139. Sundlöv A, Sjögreen-Gleisner K, Svensson J, Ljungberg M, Olsson T, Bernhardt P, Tennvall J. Individualised (177)Lu-DOTATATE treatment of neuroendocrine tumours based on kidney dosimetry. European journal of nuclear medicine and molecular imaging. 2017;44(9):1480-9.

140. Nicolini S, Bodei L, Bongiovanni A, Sansovini M, Grassi I, Ibrahim T, et al. Combined use of 177Lu-DOTATATE and metronomic capecitabine (Lu-X) in FDG-positive gastro-entero-pancreatic neuroendocrine tumors. European journal of nuclear medicine and molecular imaging. 2021;48(10):3260-7.

141. Stokke C, Gabiña PM, Solný P, Cicone F, Sandström M, Gleisner KS, et al. Dosimetry-based treatment planning for molecular radiotherapy: a summary of the 2017 report from the Internal Dosimetry Task Force. EJNMMI Physics. 2017;4(1):27.

142. Siegel JA, Thomas SR, Stubbs JB, Stabin MG, Hays MT, Koral KF, et al. MIRD Pamphlet No. 16: Techniques for Quantitative Radiopharmaceutical Biodistribution Data Acquisition and Analysis for Use in Human Radiation Dose Estimates. Journal of Nuclear Medicine. 1999;40(2):37S-61S.

143. IRCP. The 2007 Recommendations of the International Commission on Radiological Protection: IRCP; 2007.

144. Group F-NBW. BEST (Biomarkers, EndpointS, and other Tools) Co-published by National Institutes of Health (US), Bethesda (MD). 2016, updated 2021 [cited 2024 May 20]. Available from: https://www.ncbi.nlm.nih.gov/books/NBK338448/.

145. NCI Dictionary of Cancer Terms Internet: United States government, National Cancer Institute; 2024 [Available from: https://www.cancer.gov/publications/dictionaries/cancer-terms/def/biomarker.

146. O'Connor JP, Aboagye EO, Adams JE, Aerts HJ, Barrington SF, Beer AJ, et al. Imaging biomarker roadmap for cancer studies. Nat Rev Clin Oncol. 2017;14(3):169-86.

147. FDA-NIH Biomarker Working Group. BEST (Biomarkers, EndpointS, and other Tools) Internet: Food and Drug Administration (US), Co-published by National Institutes of Health (US); 2016 [Understanding Prognostic versus Predictive Biomarkers.:[Available from: https://www.ncbi.nlm.nih.gov/books/NBK402284/.

148. Chiu F-Y, Yen Y. Imaging biomarkers for clinical applications in neuro-oncology: current status and future perspectives. Biomarker Research. 2023;11(1):35.

149. Lee ONY, Tan KV, Tripathi V, Yuan H, Chan WW, Chiu KWH. The Role of 68 Ga-DOTA-SSA PET/CT in the Management and Prediction of Peptide Receptor Radionuclide Therapy Response for Patients With Neuroendocrine Tumors : A Systematic Review and Meta-analysis. Clin Nucl Med. 2022;47(9):781-93.

150. Eisenhauer EA, Therasse P, Bogaerts J, Schwartz LH, Sargent D, Ford R, et al. New response evaluation criteria in solid tumours: revised RECIST guideline (version 1.1). Eur J Cancer. 2009;45(2):228-47.

151. Brabander T, van der Zwan WA, Teunissen JJM, Kam BLR, de Herder WW, Feelders RA, et al. Pitfalls in the response evaluation after peptide receptor radionuclide therapy with [(177)Lu-DOTA(0),Tyr(3)]octreotate. Endocrine-related cancer. 2017;24(5):243-51.

152. Jayaprakasam VS, Bodei L. Neuroendocrine Tumor Therapy Response Assessment. PET Clin. 2023;18(2):267-86.

153. Choi H, Charnsangavej C, Faria SC, Macapinlac HA, Burgess MA, Patel SR, et al. Correlation of computed tomography and positron emission tomography in patients with metastatic gastrointestinal stromal tumor treated at a single institution with imatinib mesylate: proposal of new computed tomography response criteria. Journal of clinical oncology : official journal of the American Society of Clinical Oncology. 2007;25(13):1753-9.

154. van Treijen MJC, Schoevers JMH, Heeres BC, van der Zee D, Maas M, Valk GD, Tesselaar MET. Defining disease status in gastroenteropancreatic neuroendocrine tumors: Choi-criteria or RECIST? Abdom Radiol (NY). 2022;47(3):1071-81.

155. Parihar AS, Dehdashti F, Wahl RL. FDG PET/CT–based Response Assessment in Malignancies. RadioGraphics. 2023;43(4):e220122.

156. Young H, Baum R, Cremerius U, Herholz K, Hoekstra O, Lammertsma AA, et al. Measurement of clinical and subclinical tumour response using [18F]-fluorodeoxyglucose and positron emission tomography: review and 1999 EORTC recommendations. European Organization for Research and Treatment of Cancer (EORTC) PET Study Group. Eur J Cancer. 1999;35(13):1773-82.

157. Skougaard K, Nielsen D, Jensen BV, Hendel HW. Comparison of EORTC Criteria and PERCIST for PET/CT Response Evaluation of Patients with Metastatic Colorectal Cancer Treated with Irinotecan and Cetuximab. Journal of Nuclear Medicine. 2013;54(7):1026-31.

158. Hope TA, Bergsland EK, Bozkurt MF, Graham M, Heaney AP, Herrmann K, et al. Appropriate Use Criteria for Somatostatin Receptor PET Imaging in Neuroendocrine Tumors. Journal of Nuclear Medicine. 2018;59(1):66-74.

159. Aaronson NK, Ahmedzai S, Bergman B, Bullinger M, Cull A, Duez NJ, et al. The European Organization for Research and Treatment of Cancer QLQ-C30: a quality-of-life instrument for use in international clinical trials in oncology. J Natl Cancer Inst. 1993;85(5):365-76.

160. Giesinger JM, Kieffer JM, Fayers PM, Groenvold M, Petersen MA, Scott NW, et al. Replication and validation of higher order models demonstrated that a summary score for the EORTC QLQ-C30 is robust. Journal of Clinical Epidemiology. 2016;69:79-88.

161. Husson O, de Rooij BH, Kieffer J, Oerlemans S, Mols F, Aaronson NK, et al. The EORTC QLQ-C30 Summary Score as Prognostic Factor for Survival of Patients with Cancer in the "Real-World": Results from the Population-Based PROFILES Registry. Oncologist. 2020;25(4):e722-e32.

162. Davies AH, Larsson G, Ardill J, Friend E, Jones L, Falconi M, et al. Development of a disease-specific Quality of Life questionnaire module for patients with gastrointestinal neuroendocrine tumours. Eur J Cancer. 2006;42(4):477-84.

163. Yadegarfar G, Friend L, Jones L, Plum LM, Ardill J, Taal B, et al. Validation of the EORTC QLQ-GINET21 questionnaire for assessing quality of life of patients with gastrointestinal neuroendocrine tumours. Br J Cancer. 2013;108(2):301-10.

164. Oken MM, Creech RH, Tormey DC, Horton J, Davis TE, McFadden ET, Carbone PP. Toxicity and response criteria of the Eastern Cooperative Oncology Group. Am J Clin Oncol. 1982;5(6):649-55.

165. Singh S, Granberg D, Wolin E, Warner R, Sissons M, Kolarova T, et al. Patient-Reported Burden of a Neuroendocrine Tumor (NET) Diagnosis: Results From the First Global Survey of Patients With NETs. J Glob Oncol. 2017;3(1):43-53.

166. Ohlsson H, Wahlberg G, Malmström M, Gustafsson R, Sundlöv A, Nordenström E, Almquist M. Impact of Specific Bowel Symptoms on Quality of Life in Patients with Midgut Neuroendocrine Tumours. World Journal of Surgery. 2021;45(9):1.

167. Ohlsson H, Gålne A, Trägårdh E, Malmström M, Sundlöv A, Almquist M. Relationship between somatostatin receptor expressing tumour volume and health-related quality of life in patients with metastatic GEP-NET. J Neuroendocrinol. 2022;34(6):e13139.

168. Vinik E, Silva MP, Vinik AI. Measuring the relationship of quality of life and health status, including tumor burden, symptoms, and biochemical measures in patients with neuroendocrine tumors. Endocrinol Metab Clin North Am. 2011;40(1):97-109, viii.

169. Dermine S, Palmieri LJ, Lavolé J, Barré A, Dohan A, Abou Ali E, et al. Non-Pharmacological Therapeutic Options for Liver Metastases in Advanced Neuroendocrine Tumors. J Clin Med. 2019;8(11).

170. Watzka FM, Fottner C, Miederer M, Schad A, Weber MM, Otto G, et al. Surgical therapy of neuroendocrine neoplasm with hepatic metastasis: patient selection and prognosis. Langenbecks Arch Surg. 2015;400(3):349-58.

171. Zandee WT, Brabander T, Blažević A, Kam BLR, Teunissen JJM, Feelders RA, et al. Symptomatic and Radiological Response to 177Lu-DOTATATE for the Treatment of Functioning Pancreatic Neuroendocrine Tumors. J Clin Endocrinol Metab. 2019;104(4):1336-44.

172. Marinova M, Mücke M, Fischer F, Essler M, Cuhls H, Radbruch L, et al. Quality of life in patients with midgut NET following peptide receptor radionuclide therapy. European journal of nuclear medicine and molecular imaging. 2019;46(11):2252-9.

173. Strosberg J, Wolin EM, Chasen B, Kulke MH, Bushnell D, Caplin M, et al. Improved time to quality of life deterioration in patients with progressive midgut neuroendocrine tumors treated with 177Lu-DOTATATE: The NETTER-1 phase III trial. Annals of Oncology. 2017;28:v146.

174.    Lång K, Josefsson V, Larsson AM, Larsson S, Högberg C, Sartor H, et al. Artificial intelligence-supported screen reading versus standard double reading in the Mammography Screening with Artificial Intelligence trial (MASAI): a clinical safety analysis of a randomised, controlled, non-inferiority, single-blinded, screening accuracy study. Lancet Oncol. 2023;24(8):936-44.

175.    Goodfellow I BY, Courville A. Deep learning: MIT Press; 2016.

176.    Murray C, Hoane AJ, Feng-hsiung H. Deep Blue. Artificial Intelligence. 2002;134(1):57-83.

177.    Saba L, Biswas M, Kuppili V, Cuadrado Godia E, Suri HS, Edla DR, et al. The present and future of deep learning in radiology. Eur J Radiol. 2019;114:14-24.

178.    Yamashita R, Nishio M, Do RKG, Togashi K. Convolutional neural networks: an overview and application in radiology. Insights into Imaging. 2018;9(4):611-29.

179.    Michael E, Alexandre G, Gaël V, Bertrand T. Seeing it all: Convolutional network layers map the function of the human visual system. NeuroImage. 2017;152:184-94.

180.    Valliani AA, Ranti D, Oermann EK. Deep Learning and Neurology: A Systematic Review. Neurol Ther. 2019;8(2):351-65.

181.    Mazurowski MA, Buda M, Saha A, Bashir MR. Deep learning in radiology: An overview of the concepts and a survey of the state of the art with focus on MRI. J Magn Reson Imaging. 2019;49(4):939-54.

182.    Krig S. Ground Truth Data, Content, Metrics, and Analysis.  Computer Vision Metrics: Survey, Taxonomy, and Analysis. Berkeley, CA: Apress; 2014. p. 283-311.

183.    Hosny A, Parmar C, Quackenbush J, Schwartz LH, Aerts H. Artificial intelligence in radiology. Nat Rev Cancer. 2018;18(8):500-10.

184.    Najjar R. Redefining Radiology: A Review of Artificial Intelligence Integration in Medical Imaging. Diagnostics. 2023;13(17):2760.

185.    Chilamkurthy S, Ghosh R, Tanamala S, Biviji M, Campeau NG, Venugopal VK, et al. Deep learning algorithms for detection of critical findings in head CT scans: a retrospective study. Lancet. 2018;392(10162):2388-96.

186.    de Margerie-Mellon C, Chassagnon G. Artificial intelligence: A critical review of applications for lung nodule and lung cancer. Diagnostic and Interventional Imaging. 2023;104(1):11-7.

187.    Gålne A, Enqvist O, Sundlöv A, Valind K, Minarik D, Trägårdh E. AI-based quantification of whole-body tumour burden on somatostatin receptor PET/CT. Eur J Hybrid Imaging. 2023;7(1):14.

188.    Kawamura M, Kamomae T, Yanagawa M, Kamagata K, Fujita S, Ueda D, et al. Revolutionizing radiation therapy: the role of AI in clinical practice. Journal of Radiation Research. 2023;65(1):1-9.

189.    Bhattacharya I, Khandwala YS, Vesal S, Shao W, Yang Q, Soerensen SJC, et al. A review of artificial intelligence in prostate cancer detection on imaging. Ther Adv Urol. 2022;14:17562872221128791.

190.    European Medicines Agency, Medical devices Internet: European Medicines Agency; 2024 [cited 2024 6th June]. Human regulatory: overview:[Available from: https://www.ema.europa.eu/en/human-regulatory-overview/medical-devices.

191. The AI Act, European Union Internet: European Parliament; 2024 [cited 2024 12 June]. Available from: https://www.europarl.europa.eu/topics/en/article/20230601STO93804/eu-ai-act-first-regulation-on-artificial-intelligence.

192. Health AI Register Internet: Health AI Register, Romion Health; 2024 [2024-06-12]. Available from: https://radiology.healthairegister.com/.

193. Fryback DG, Thornbury JR. The efficacy of diagnostic imaging. Med Decis Making. 1991;11(2):88-94.

194. van Leeuwen KG, Schalekamp S, Rutten M, van Ginneken B, de Rooij M. Artificial intelligence in radiology: 100 commercially available products and their scientific evidence. Eur Radiol. 2021;31(6):3797-804.

195. van Leeuwen KG, de Rooij M, Schalekamp S, van Ginneken B, Rutten M. How does artificial intelligence in radiology improve efficiency and health outcomes? Pediatr Radiol. 2022;52(11):2087-93.

196. Zhernosekov KP, Filosofov DV, Baum RP, Aschoff P, Bihl H, Razbash AA, et al. Processing of generator-produced 68Ga for medical application. Journal of nuclear medicine : official publication, Society of Nuclear Medicine. 2007;48(10):1741-8.

197. Mueller D, Klette I, Baum RP, Gottschaldt M, Schultz MK, Breeman WA. Simplified NaCl based (68)Ga concentration and labeling procedure for rapid synthesis of (68)Ga radiopharmaceuticals in high radiochemical purity. Bioconjugate chemistry. 2012;23(8):1712-7.

198. Fayers P AN, Bjordal K, Groenvold M, Curran D, Bottomley A. EORTC QLQ-C30 Scoring Manual. 3rd ed. Brussels: European Organisation for Research and Treatment of Cancer; 2001.

199. Akoglu H. User's guide to correlation coefficients. Turk J Emerg Med. 2018;18(3):91-3.

200. Gålne A, Almquist H, Almquist M, Hindorf C, Ohlsson T, Nordenström E, et al. A Prospective Observational Study to Evaluate the Effects of Long-Acting Somatostatin Analogs on 68Ga-DOTATATE Uptake in Patients with Neuroendocrine Tumors. Journal of Nuclear Medicine. 2019;60(12):1717-23.

201. Cherk MH, Kong G, Hicks RJ, Hofman MS. Changes in biodistribution on (68)Ga-DOTA-Octreotate PET/CT after long acting somatostatin analogue therapy in neuroendocrine tumour patients may result in pseudoprogression. Cancer imaging : the official publication of the International Cancer Imaging Society. 2018;18(1):3.

202. Ayati N, Lee ST, Zakavi R, Pathmaraj K, Al-Qatawna L, Poon A, Scott AM. Long-acting somatostatin analog therapy differentially alters (68)Ga-DOTATATE uptake in normal tissues compared with primary tumors and metastatic lesions. Journal of nuclear medicine : official publication, Society of Nuclear Medicine. 2018;59(2):223-7.

203. Haug AR, Rominger A, Mustafa M, Auernhammer C, Goke B, Schmidt GP, et al. Treatment with octreotide does not reduce tumor uptake of (68)Ga-DOTATATE as measured by PET/CT in patients with neuroendocrine tumors. Journal of nuclear medicine : official publication, Society of Nuclear Medicine. 2011;52(11):1679-83.

204. Chahid Y, Hashimi K, van de Garde EMW, Klümpen HJ, Hendrikse NH, Booij J, Verberne HJ. The Influence of Long-Acting Somatostatin Analogs on 68 Ga-DOTATATE Uptake in Patients With Neuroendocrine Tumors. Clin Nucl Med. 2023;48(9):757-62.

205. van de Weijer T, Bemer F, de Vos-Geelen J, Hermans B, Mitea C, van der Pol JAJ, et al. Altered biodistribution of [68Ga]Ga-DOTA-TOC during somatostatin analogue treatment. European journal of nuclear medicine and molecular imaging. 2024.

206. Aalbersberg EA, de Wit-van der Veen BJ, Versleijen MWJ, Saveur LJ, Valk GD, Tesselaar MET, Stokkel MPM. Influence of lanreotide on uptake of (68)Ga-DOTATATE in patients with neuroendocrine tumours: a prospective intra-patient evaluation. European journal of nuclear medicine and molecular imaging. 2019;46(3):696-703.

207. Reubi JC, Schonbrunn A. Illuminating somatostatin analog action at neuroendocrine tumor receptors. Trends in pharmacological sciences. 2013;34(12):676-88.

208. Reubi JC, Waser B, Cescato R, Gloor B, Stettler C, Christ E. Internalized somatostatin receptor subtype 2 in neuroendocrine tumors of octreotide-treated patients. J Clin Endocrinol Metab. 2010;95(5):2343-50.

209. Velikyan I, Sundin A, Eriksson B, Lundqvist H, Sorensen J, Bergstrom M, Langstrom B. In vivo binding of [68Ga]-DOTATOC to somatostatin receptors in neuroendocrine tumours--impact of peptide mass. Nuclear medicine and biology. 2010;37(3):265-75.

210. Jahn U, Ilan E, Velikyan I, Fröss-Baron K, Lubberink M, Sundin A. Receptor depletion and recovery in small-intestinal neuroendocrine tumors and normal tissues after administration of a single intravenous dose of octreotide measured by (68)Ga-DOTATOC PET/CT. EJNMMI Res. 2021;11(1):118.

211. Yordanova A, Wicharz MM, Mayer K, Brossart P, Gonzalez-Carmona MA, Strassburg CP, et al. The Role of Adding Somatostatin Analogues to Peptide Receptor Radionuclide Therapy as a Combination and Maintenance Therapy. Clinical cancer research : an official journal of the American Association for Cancer Research. 2018;24(19):4672-9.

212. Syguła A, Ledwon A, Hasse-Lazar K, Jurecka-Lubieniecka B, Michalik B, Paliczka-Cieślik E, et al. In patients with well-differentiated neuroendocrine tumours, there is no apparent benefit of somatostatin analogues after disease control by peptide receptor radionuclide therapy. European journal of nuclear medicine and molecular imaging. 2022;49(11):3841-51.

213. Derogar M, van der Schaaf M, Lagergren P. Reference values for the EORTC QLQ-C30 quality of life questionnaire in a random sample of the Swedish population. Acta Oncologica. 2012;51(1):10-6.

214. Khan S, Krenning EP, van Essen M, Kam BL, Teunissen JJ, Kwekkeboom DJ. Quality of life in 265 patients with gastroenteropancreatic or bronchial neuroendocrine tumors treated with [177Lu-DOTA0,Tyr3]octreotate. Journal of nuclear medicine : official publication, Society of Nuclear Medicine. 2011;52(9):1361-8.

215. Fanakidou I, Zyga S, Alikari V, Tsironi M, Stathoulis J, Theofilou P. Mental health, loneliness, and illness perception outcomes in quality of life among young breast cancer patients after mastectomy: the role of breast reconstruction. Qual Life Res. 2018;27(2):539-43.

216. Dinkel J, Khalilzadeh O, Hintze C, Fabel M, Puderbach M, Eichinger M, et al. Inter-observer reproducibility of semi-automatic tumor diameter measurement and volumetric analysis in patients with lung cancer. Lung Cancer. 2013;82(1):76-82.

217. Yoon SH, Kim KW, Goo JM, Kim D-W, Hahn S. Observer variability in RECIST-based tumour burden measurements: a meta-analysis. European Journal of Cancer. 2016;53:5-15.

218. Pfaehler E, Mesotten L, Kramer G, Thomeer M, Vanhove K, de Jong J, et al. Repeatability of two semi-automatic artificial intelligence approaches for tumor segmentation in PET. EJNMMI Research. 2021;11(1):4.

219. Cottereau AS, Hapdey S, Chartier L, Modzelewski R, Casasnovas O, Itti E, et al. Baseline Total Metabolic Tumor Volume Measured with Fixed or Different Adaptive Thresholding Methods Equally Predicts Outcome in Peripheral T Cell Lymphoma. Journal of nuclear medicine : official publication, Society of Nuclear Medicine. 2017;58(2):276-81.

220. Ilyas H, Mikhaeel NG, Dunn JT, Rahman F, Møller H, Smith D, Barrington SF. Defining the optimal method for measuring baseline metabolic tumour volume in diffuse large B cell lymphoma. European journal of nuclear medicine and molecular imaging. 2018;45(7):1142-54.

221. Tirosh A, Papadakis GZ, Millo C, Hammoud D, Sadowski SM, Herscovitch P, et al. Prognostic Utility of Total (68)Ga-DOTATATE-Avid Tumor Volume in Patients With Neuroendocrine Tumors. Gastroenterology. 2018;154(4):998-1008.e1.

222. Pauwels E, Van Binnebeek S, Vandecaveye V, Baete K, Vanbilloen H, Koole M, et al. Inflammation-Based Index and (68)Ga-DOTATOC PET-Derived Uptake and Volumetric Parameters Predict Outcome in Neuroendocrine Tumor Patients Treated with (90)Y-DOTATOC. Journal of nuclear medicine : official publication, Society of Nuclear Medicine. 2020;61(7):1014-20.

223. Ortega C, Wong RK, Schaefferkoetter J, Veit-Haibach P, Myrehaug S, Juergens R, et al. Quantitative ^{68}Ga-DOTATATE PET/CT parameters for the prediction of therapy response in patients with progressive metastatic neuroendocrine tumors treated with ^{177}Lu-DOTATATE. Journal of Nuclear Medicine. 2021:jnumed.120.256727.

224. Lee H, Kipnis ST, Niman R, O'Brien SR, Eads JR, Katona BW, Pryma DA. Prediction of 177Lu-DOTATATE Therapy Outcomes in Neuroendocrine Tumor Patients Using Semi-Automatic Tumor Delineation on 68Ga-DOTATATE PET/CT. Cancers. 2024;16(1):200.

225. Carlsen EA, Lindholm K, Hindsholm A, Gæde M, Ladefoged CN, Loft M, et al. A convolutional neural network for total tumor segmentation in [(64)Cu]Cu-DOTATATE PET/CT of patients with neuroendocrine neoplasms. EJNMMI Res. 2022;12(1):30.

226. European Cancer Imaging Initiative Internet: European Commission, An official website of the European Union; 2024 [cited 2024 21 May]. Shaping Europe's digital future:[Available from: https://digital-strategy.ec.europa.eu/en/policies/cancer-imaging.

227. Haug AR, Auernhammer CJ, Wangler B, Schmidt GP, Uebleis C, Goke B, et al. 68Ga-DOTATATE PET/CT for the early prediction of response to somatostatin receptor-mediated radionuclide therapy in patients with well-differentiated neuroendocrine tumors. Journal of nuclear medicine : official publication, Society of Nuclear Medicine. 2010;51(9):1349-56.

228. Opalińska M, Morawiec-Sławek K, Kania-Kuc A, Al Maraih I, Sowa-Staszczak A, Hubalewska-Dydejczyk A. Potential value of pre- and post-therapy [68Ga]Ga-DOTA-TATE PET/CT in the prognosis of response to PRRT in disseminated neuroendocrine tumors. Front Endocrinol (Lausanne). 2022;13:929391.

229. Albertelli M, Dotto A, Di Dato C, Malandrino P, Modica R, Versari A, et al. PRRT: identikit of the perfect patient. Reviews in Endocrine and Metabolic Disorders. 2021;22(3):563-79.

230. Ezziddin S, Attassi M, Yong-Hing CJ, Ahmadzadehfar H, Willinek W, Grünwald F, et al. Predictors of long-term outcome in patients with well-differentiated gastroenteropancreatic neuroendocrine tumors after peptide receptor radionuclide therapy with 177Lu-octreotate. Journal of nuclear medicine : official publication, Society of Nuclear Medicine. 2014;55(2):183-90.

231. Mileva M, Marin G, Levillain H, Artigas C, Van Bogaert C, Marin C, et al. Prediction of (177)Lu-DOTATATE PRRT Outcome Using Multimodality Imaging in Patients with Gastroenteropancreatic Neuroendocrine Tumors: Results from a Prospective Phase II LUMEN Study. Journal of nuclear medicine : official publication, Society of Nuclear Medicine. 2024;65(2):236-44.

232. Hebert K, Santoro L, Monnier M, Castan F, Berkane I, Assénat E, et al. Absorbed Dose–Response Relationship in Patients with Gastroenteropancreatic Neuroendocrine Tumors Treated with [177Lu]Lu-DOTATATE: One Step Closer to Personalized Medicine. Journal of Nuclear Medicine. 2024;65(6):923-30.

233. Soret M, Bacharach SL, Buvat I. Partial-Volume Effect in PET Tumor Imaging. Journal of Nuclear Medicine. 2007;48(6):932-45.

234. Sadek AN, Yusuf EE. Respiratory Motion in Positron Emission Tomography/Computed Tomography: A Review. Seminars in Nuclear Medicine. 2008;38(3):167-76.

235. Becx MN, Minczeles NS, Brabander T, de Herder WW, Nonnekens J, Hofland J. A Clinical Guide to Peptide Receptor Radionuclide Therapy with (177)Lu-DOTATATE in Neuroendocrine Tumor Patients. Cancers (Basel). 2022;14(23).

# About the author

ANNI GÅLNE, MD., is currently working as a radiologist and completing a residency in Nuclear Medicine at the Department of Medical Imaging and Physiology, Skåne University Hospital, Sweden.

This thesis explores various aspects of somatostatin receptor PET-CT imaging of neuroendocrine tumours. The studies investigate how treatment affects tumour imaging, the correlation between tumour burden and quality of life, the development of an AI model for automated tumour segmentation, and whether tumour burden can predict treatment outcomes in patients receiving $^{177}$Lu-DOTATATE therapy. By extending beyond the basic diagnostic capabilities of PET-CT, this thesis contributes to advancements in both diagnostic and therapeutic approaches for patients with neuroendocrine tumours.

## FACULTY OF MEDICINE